

DISSERTATION

TRANSLATION-DEPENDENT MRNA LOCALIZATION IN THE *CAENORHABDITIS*
ELEGANS EMBRYO

Submitted by

Lindsay P. Winkenbach

Department of Biochemistry and Molecular Biology

In partial fulfillment of the requirements

For the Degree of Doctor of Philosophy

Colorado State University

Fort Collins, Colorado

Fall 2022

Doctoral Committee:

Advisor: Erin Osborne Nishimura

Carol Wilusz

Tim Stasevich

Santiago Di Pietro

Copyright by Lindsay P. Winkenbach 2022

All Rights Reserved

ABSTRACT

TRANSLATION-DEPENDENT MRNA LOCALIZATION IN THE *CAENORHABDITIS* *ELEGANS* EMBRYO

Though each animal cell contains the same genetic information, cell-specific gene expression is required for embryos to develop into mature organisms. Embryos rely on maternally inherited components during early development to guide cell fate specification. In animals, *de novo* transcription is paused after fertilization until zygotic genome activation. Consequently, early embryos rely on post-transcriptional regulation of maternal mRNA to spatially and temporally regulate protein production.

Caenorhabditis elegans has emerged as a powerful developmental model for studying mRNA localization of maternally-inherited transcripts. We have identified subsets of maternal mRNAs with cell-specific and subcellular patterning in the early *C. elegans* embryo. Previous RNA localization studies in *C. elegans* focused on maternal transcripts that cluster in the posterior lineage and showed mRNA localization occurs in a translation-independent manner through localization sequence elements in the 3'UTR. However, little is known about the mechanisms directing RNA localization to other subcellular locales in early embryos. Therefore, we sought to understand the localization of maternal transcripts found enriched at the plasma membrane and nuclear periphery, *erm-1* (*Ezrin/Radixin/Moesin*) and *imb-2* (*Importin Beta*), respectively.

In this thesis, I characterize two different translation-dependent pathways for mRNA localization of maternal transcripts at the plasma membrane and nuclear periphery. I identified the PIP₂-membrane binding region of the ERM-1 proteins is necessary for *erm-1* mRNA localization while identifying additional membrane localized maternal transcripts through the presence of encoded PIP₂-membrane binding domains. Additionally, I observed that mRNA localization patterns can change over developmental time corresponding to changes in translation status. For *imb-2* mRNA localization, I found localization to the nuclear periphery is also translation-dependent. Through recoding the *imb-2* mRNA sequence while maintaining the translated peptide sequence using alternative codons, I found both localization and transcript stability additionally depends on mRNA sequence context. These findings represent the first report of a translation-dependent localization pathway for two maternally-inherited transcripts in *C. elegans* and demonstrate the utility of *C. elegans* as a model for studying translation-dependent mRNA localization during development.

ACKNOWLEDGEMENTS

There are more people than I can count who have helped me get to this point. I deeply apologize for anyone I leave out.

First, I would like to thank my PhD advisor, Erin Osborne Nishimura. She is truly exemplary in fostering an environment that allows the people in her lab to show up as their whole selves. If it weren't for her continued patience and compassion, I likely would have quit the program. I am also very grateful for the flexibility Erin gave me to both explore the research questions I was interested in as well as develop skills outside of the lab.

I would also like to thank all members of the Nishimura lab. Dylan Parker, Robert Williams, and I are the first three graduate students out of Erin's lab and it has forged a deep bond. I would not have developed as a scientist without Dylan constantly telling me to do better and Robert always being my cheerleader. You two were excellent mentors in the lab and incredible friends outside. I miss our sunset trips to the reservoir after lab on hot summer days. Thanks to David King for keeping the technology in the lab alive and keeping my data from not disappearing. But also, I will always cherish the Friday afternoon diversions. I never knew what was coming but I knew my face would hurt from laughing. Good, strange times. Thanks to my undergraduates Lauren Billow and Emily Miner for taking a chance on me being your mentor. You were both so wonderful to train and work with and we missed you when you had to move on. I am also grateful for the newer members of our lab, Jessica Hill and Naly Torres. It is so wonderful having other women in the lab to grow and share with. Jess, you're a legend. Naly, thanks for continuing on with team RNA localization (the best team), and for always bringing sass and smiles to lab.

I would also like to thank the *C. elegans* community at large for being such an amazing, welcoming, and collaborative group of scientists. My first worm conference was in person and I got science whiplash from the breadth of amazing work done in our favorite model and it was such a rewarding experience. It was an absolute honor to present at another conference (even though it was virtual and should have been in Scotland) and be able to share out my work. Collaborating and sharing ideas with Dustin Updike, Mike Boxem, Susan Mango, and many others greatly enriched my experience and helped me to think differently and give insight into my research. I am also grateful to all the worm labs in the Front Range and for getting to share and develop ideas over the years as well as for the chance to develop local community.

For folks at CSU, I am particularly grateful to the Montgomery and Stasevich labs. Tai and Brooke have been excellent resources and have generously provided me with materials for my research. I'm also so grateful to Tai for inviting me to attend a small RNA conference he organized in Todos Santos, Mexico. It was my first small conference, and it was so amazing to see the sharing of ideas and watch collaborations develop over a weekend. It also gave me the opportunity to know other people in the field who I would continue contact with (Dustin Updike, Shawn Ahmed, Swathi Arur). Additionally, this conference resulted in my first publication, a co-first authored review with two of my favorite worm gals (Rachel Doser and Kailee Reed) and truly the least painful publishing experience yet. Tai has also always been willing to engage with me both in research as well as general mentor/mentee philosophy, which I appreciate. The Montgomery students were also an absolute kick and I'm so grateful to have met Kailee and all the ridiculous memories we've made together at CSU, conferences, and just life. Wooorrrrrm! As for the Stasevich lab, Tim Stasevich has been an excellent committee member and mentor and I always leave a conversation with him excited about some new aspect of my project or just

science generally. The Stas lab has been a place of learning as well as a source for some of the best friends I have made at CSU.

There are many thanks I owe to the Biochemistry and Molecular Department. First, a huge thank you to the office staff who keep our department afloat and put up with my constant questions. And thank you, Laurie Stargell, for heading the department and steering us through a pandemic and being receptive to my many thoughts and ideas on how to make the world a better place for students. I also owe many thanks to my committee members Santiago DiPietro, Tim Stasevich, and Carol Wilusz (who is not BMB but has a lot of overlap). You all made me a much, much better scientist. I am grateful to Santiago for providing directions and motivation for next steps in my project and also for being a very patient mentor to me during my first rotation. I owe thanks to Tim for his absolute enthusiasm for my project and teaching me everything I know about microscopy. And I am so thankful for Carol for many things. First, I am grateful that she agreed to be on my committee. When I first met with her she managed to give me insightful advice on my project, introduce me to other graduate women on campus, as well as encourage me to apply for the GAUSSI training grant. All three of you have been integral contributors in your own unique ways.

I have met so many wonderful folks at CSU and there simply is not enough space to write as much as I would like to about all the people who have made my experience in Colorado what it's been. Grace Campagnola, thanks for being my friend from the start. I am grateful for the opportunity to participate in the incredible organization Graduate Women in Science, Science in Action, and Graduate Student Council. GWIS provided me with my first community of women in science since I am the only woman in my cohort. Science in Action completely shifted my ideas of what I wanted to do with my degree and introduced me to some of my absolutely most

dear friends Clara Tibbetts, Amanda Koch and Matt Saxton. By the time I joined GSC I learned that there is a lot of overlap in graduate students who participate in extra service on campus and I am so grateful I had the chance to work with Ryan Czarny, Dylan Parker, Amanda Koch, Matt Saxton, Juli Scamardo, and so many more. We improved graduate students' experience at CSU. Also as part of work with the GSC, I am grateful to have formed such amazing relationships with the Graduate School, particularly Mary Stromberger and Colleen Webb.

I absolutely owe thanks to other graduate students in the department, past and present. Starting with my cohort, I would not have made it through my first year without you. In particular, so much appreciation goes to Ryan Czarny, Craig Marshall, and Wyatt Beyers. Your friendship and support have meant so much to me. Julie Sun, you aren't actually in our cohort or department but I'm counting you. Ryan and Julie, I love and appreciate you. Lindsay Lammers graduated my second year, but she absolutely paved the way for other graduate students in our department and beyond to explore and make impacts beyond the lab. Thank you to all of the grads who have been willing to work with me to make our department a more welcoming and inclusive place.

Outside of CSU, but closely affiliated, thank you Larry Hsu, Katie Bonack, Jenna Kresack, and the whole Parker family. You have become my Colorado family.

From my time before CSU, thank you to those who have encouraged me academically and to pursue science. Kevin Ahern and Indira Rajogopal, I never would have pursued Biochemistry and Biophysics if I hadn't randomly met you during my senior year of high school. That was an absolute turning point in my life. Kevin, Indira, and Kari Van Zee, you were the most incredible undergraduate advisors I could ask for and are absolutely the reason I attended

graduate school. Thank you to my friends from undergrad as well, particularly Hayati Wolfenden and Madison Thompson.

I would like to thank my family. To my parents, Carla and Bill, my bonus parents, David and Jody, and my sister Caitlin, I would have never made it to this point without you. Dylan Parker, partner in science and soon to be husband (wow!). You all are my life. And we've been through a lot of life, especially in the last few years.

DEDICATION

I would like to dedicate this dissertation to my incredible mother, Carla Garner, who passed away earlier this year after an impressive battle with pancreatic cancer. She gave me my first informal lessons on developmental biology with stories of how she grew me in her belly and “bornded” me. Little did she know that 20 some odd years later I would come home to tell her stories about how I’m spending five years extensively studying how worm babies are made.

TABLE OF CONTENTS

ABSTRACT.....	ii
ACKNOWLEDGEMENTS.....	iv
DEDICATION.....	ix
Chapter 1 Introduction: A review of mRNA localization and local translation.....	1
1.1 Introduction.....	1
1.1.1 A historical perspective of mRNA localization.....	2
1.1.2 Functions of mRNA localization.....	3
1.2.1 mRNA localization and translation repression.....	4
1.3.1 mRNA localization and local translation.....	6
1.3.2 Local translation by translation-independent mRNA localization.....	7
1.3.2.1 Classical examples of translation-independent mRNA localization and local translation.....	7
1.3.2.2 Emerging examples of translation-independent mRNA localization and local translation.....	10
1.3.3 Local translation by translation-dependent mRNA localization.....	13
1.3.3.1 Classical examples of translation-dependent mRNA localization and local translation.....	13
1.3.3.2 Emerging examples of translation-dependent mRNA localization and local translation.....	15
1.4.1 Future perspectives.....	18
Chapter 2 Translation of the ERM-1 membrane-binding domain directs <i>erm-1</i> mRNA localization to the plasma membrane in the <i>C. elegans</i> embryo.....	20
2.1 Introduction.....	20
2.2 Results.....	23
2.2.1 <i>erm-1</i> mRNA localization to the plasma membrane requires translation initiation.....	23
2.2.2 The ERM-1 nascent peptide is required for <i>erm-1</i> mRNA enrichment at plasma membranes.....	27
2.2.3 <i>erm-1</i> mRNA localization to the plasma membrane does not depend on nucleic acid sequences.....	33
2.2.4 <i>erm-1</i> mRNA and ERM-1 protein localization require the ERM-1 PIP ₂ membrane-binding region.....	34
2.2.5 Genes encoding FERM and PH-like domains are conducive for mRNAs with localization at the plasma membrane.....	39
2.3 Discussion.....	48
2.4 Materials and Methods.....	52
2.4.1 Worm husbandry.....	52
2.4.2 Heat Shock Experiments.....	52
2.4.3 RNAi Feeding for smFISH Microscopy.....	53
2.4.4 Permeabilization and drug delivery.....	54
2.4.5 smFISH.....	55
2.4.6 smiFISH.....	56

2.4.7 Quantification of plasma membrane RNA localization.....	57
2.4.8 Quantification of total mRNA.....	57
2.4.9 Domain search.....	58
2.5 Acknowledgements.....	59
2.6 Competing Interests.....	59
2.7 Funding.....	59
Chapter 3 Translation-dependent localization of <i>imb-2</i> mRNA to the nuclear periphery.....	60
3.1 Introduction.....	60
3.2 Results.....	63
3.2.1 <i>imb-2</i> mRNA localization to the nuclear periphery requires translation initiation.....	63
3.2.2 IMB-2 localization requires the intact ribosome-nascent chain complex.....	64
3.2.3 <i>imb-2</i> mRNA localization is susceptible to heat stress.....	66
3.2.4 <i>imb-2</i> mRNA stability depends on nucleic acid sequence context.....	69
3.3 Discussion.....	74
3.4 Materials and Methods.....	77
3.4.1 Worm husbandry.....	78
3.4.2 Heat Shock Experiments.....	79
3.4.3 RNAi Feeding for smFISH Microscopy.....	79
3.4.4 Permeabilization and drug delivery.....	79
3.4.5 smFISH.....	79
3.4.6 smiFISH.....	79
Chapter 4 Discussion and future perspectives.....	80
4.1 <i>C. elegans</i> as a model for studying mRNA localization in the context of development.....	80
4.2 Contributions of mRNA localization to the maternal-to-zygotic transition.....	83
4.3 Advancing techniques pair mRNA localization with translation dynamics, lending insight into function.....	85
4.4 Perspectives and future directions.....	87
Bibliography	89
Appendix A	109
Appendix B	126

Chapter 1

Introduction: A review of mRNA localization and local translation

1.1 Introduction

The work described in this thesis primarily focuses on understanding the relationship between translation status and subcellular localization patterning for two uncharacterized maternal transcripts, *erm-1* and *imb-2*. Previously in *C. elegans*, RNA localization has only been described for maternal transcripts that cluster in the posterior lineage by translation-independent localization mechanisms. This project expands RNA localization studies to the plasma membrane and nuclear periphery. Additionally, this work proposes a different translation-dependent localization pathway for either locale during early development. This introduction begins with a historical perspective of mRNA localization followed by a description of both classical and novel translation-independent and translation-dependent localization pathways. Where applicable, I will detail the potential functions of mRNA localization, often through the benefits of local translation. Finally, I will posit potential hypotheses guiding the localization of *erm-1* mRNA to the plasma membrane and *imb-2* to the nuclear periphery based on what is known in the RNA localization field and specifically in *C. elegans* embryogenesis.

1.1.1 A historical perspective of mRNA localization

The asymmetric distribution of mRNA was first documented in sea squirt embryos (*Styela plicata*) in 1983 when Jeffries et al. detected β -actin mRNA concentrating within myoplasm (progenitor muscle tissue) by *in situ* hybridization [1]. Later, β -actin mRNA was found polarizing to the leading edge of motile cells within chicken embryonic fibroblasts [2]. A conserved RNA sequence in the β -actin 3'UTR, termed “zip code”, was later recognized as required for β -actin localization [3]. Subsequent studies identified that the RNA binding protein (RBP) ZBP1 was also necessary for β -actin mRNA localization while maintaining a translationally repressed state during transit [4,5]. Since these seminal studies, β -actin has continued to serve as a foundational example of the close relationship between mRNA localization and regulatory control [6–9].

mRNA partitioning was soon observed in other developmental models. In the mid-1980s, studies first in *Xenopus* and later *Drosophila* reported asymmetric distribution of maternally-deposited transcripts in early embryos, leading to the hypothesis that partitioned pools of mRNA could determine morphogen gradients that establish cell fate [10,11]. After the advent of *in situ* visualization, mRNA localization was reported in diverse organisms including rice endosperm cells, yeast (*Saccharomyces cerevisiae*), mammalian neurons, and bacteria (*Escherichia coli*), among others [12–15].

As visualization techniques and genomics assays have advanced, mRNA localization has been recognized as a prevalent feature of biology across domains and kingdoms, sometimes representing a surprising percentage of the transcriptome. In an ambitious study in *Drosophila* embryos, researchers surveyed the localization of 8000 mRNA transcripts by *in situ* hybridization. They found that, depending on the developmental stage, up to 90 % of the surveyed transcripts were spatially restricted [16,17]. Through combining genomics assays with

subcellular dissection, proximity labeling (APEX-seq), or fractionation (subRNA-seq), an expanding catalog of subcellular transcriptomes has led to the identification of many localized mRNAs [18–22]. The RNALocate database was created to organize this new data and manually curated 210,000 RNAs with 171 subcellular localizations in 104 species so far [23]. These studies indicate that mRNA localization is a widespread feature of biology and is a rich area for study. Many questions remain, though recent insights on mechanism and function describe how RNA localization post-transcriptionally fine-tunes gene expression regulation.

1.1.2 Functions of mRNA localization

What is the purpose of concentrating mRNAs in distinct regions of the cell? During production, mRNA concentrates within active transcription sites or at processing centers. Post-transcriptionally, mRNA localization is often linked to translational control, but with diverse relationships. mRNA localization can be associated with translational repression, as in stress granules that coalesce repressed transcripts under stress conditions [21,24,25]. Alternatively, mRNA enrichment to certain locales is also associated with local translation (**Figure 1.1**). At the synapse in neurons, mRNA localization facilitates rapid protein synthesis in response to local stimuli [26–28]. mRNA localization can also direct translation to occur in an environment that fosters proper protein processing, folding, or assembly while preventing deleterious interactions [29,30]. Further, mRNA localization can create high local concentrations or gradients of proteins at subcellular locales leading to asymmetric inheritance in daughter cells [31,32]. mRNAs can also perform diverse functions independent of protein expression. Similar to long non-coding RNAs (lncRNAs) that can have structural roles in the cell, mRNAs too have been shown to act as scaffolds for biomolecular condensate formation [33]. In many instances, the functions and

consequences are just beginning to be understood. It is tempting to hypothesize that RNA localization always occurs for some purpose or to promote a given expression outcome. mRNA localization may also occur as the downstream result of regulatory processes such as translational repression, RNA interference, processing, or decay. However, the link between mRNA localization and local translation is growing stronger with recent evidence spanning diverse systems and cell types.

1.2.1 mRNA localization and translation repression

Historically, mRNA localization patterning has been associated with translation repression. The earliest mRNA localization patterns observed was accumulation, or clustering, within cell structures now known as germ granules [34,35]. Germ granules are membraneless organelles comprised of RNAs and proteins linked to fertility and are one of the major cytoplasmic condensates known to accumulate RNA [35]. Two other major cytoplasmic condensates concentrate RNA and proteins, stress granules and P-bodies.

mRNA localization associated with translation repression has been extensively studied in germ granules due to their conservation across sexually reproducing organisms and being one of the earliest observed membraneless organelles. The culmination of seminal studies informed a model where germ granules promote germline specification in early development through repression of non-germ cell gene expression profiles, maintenance of small RNA surveillance, and other mechanisms [35–37]. The *Caenorhabditis elegans* germ granule, termed P granule for their persistence in the posterior (P) lineage, has served as a tractable model for understanding germ granule function and RNA accumulation. P granules contain proteins associated with translational control and RNA metabolism [38–44]. In recent years the number of known P granule-enriched mRNAs has grown from six transcripts to thousands [45–48]. *nos-2* (homolog

of *Drosophila nanos*) has emerged as a model transcript illustrating that translation repression precedes accumulation in P granules. The accumulation of maternal mRNA in P granules is posited to function in sequestering and storing mRNA for germline-specific translation upon zygotic genome activation (ZGA) [49,50].

Stress granules, first observed by microscopy and cell fractionation, form under conditions that inhibit translation initiation in eukaryotes [51–53]. Stalled 48s pre-initiation complex-associated RNAs, translation regulatory RNA binding proteins (RBPs), and various other metabolic enzymes comprise stress granules [21,53,54]. Nucleocytoplasmic transport is disrupted upon stress induction as stress granules sequester key transport components [55]. The leading “triage” model for stress granule function suggests stress induces coalescence of translationally repressed mRNA and stress granules proteins leading to remodeling, modification, and in some instances the handoff of RNA to decay machinery [55–59]. Ultimately, this is thought to promote gene expression reprogramming to facilitate stress recovery and the process is reversible.

Processing bodies, or P-bodies, were first observed in 1997 as foci of the mouse exonuclease XRN-1 [60]. The identification of additional RNA decay factors within P-bodies, including decapping and Lsm proteins, led to the model that these foci are RNA decay factories [61]. While this simple model is complicated by the presence of cell signaling components and nonsense-mediated decay inhibitors, P-bodies are still known to be associated with translationally repressed mRNA, mRNA metabolism, and decay [55,62,63].

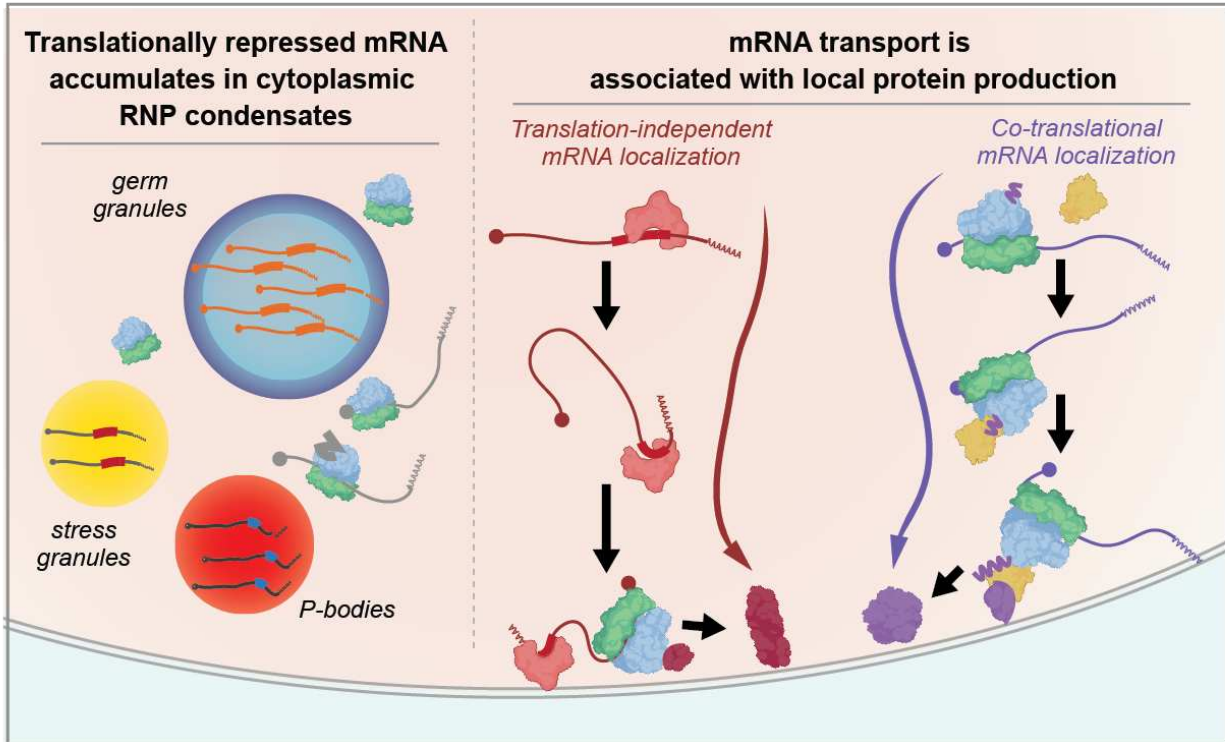


Figure 1.1: Graphical depiction of RNA localization pathways in relation to translation status. Translationally repressed transcripts often accumulate in cytoplasmic condensates (left). Local translation is achieved through translation-dependent or translation-independent mRNA localization pathways (right).

1.3.1 mRNA localization and local translation

While RNA can be localized or accumulated within specific biomolecular condensates for the purposes of decay and metabolism, RNA localization is also linked to facilitating localized translation. Localized translation can be achieved through two primary pathways; translation-independent mRNA localization and translation-dependent mRNA localization (**Figure 1.1**). In the translation-independent pathway, localization is commonly directed by a cis-acting RNA “zipcode”, often located in the 3’UTR and recognized by trans-acting factors [29,64]. In contrast, the translation-dependent pathway requires a nascent polypeptide or protein domain first be synthesized for the localization of the associated mRNA. This can occur either co-translationally with translation actively occurring during transit, or localization can occur during a pause in translation after the initiation of elongation with translation resuming only

upon arrival at the final destination [65,66]. In both scenarios, mRNA transport often precedes complete synthesis of the protein, can involve different stages of translational repression and activation, and can be followed by further rounds of translation at the destination. Whether the information directing localization is carried in the protein, mRNA, or both, local enrichment of mRNA can be mechanistically achieved through directed transport, diffusion and anchoring, and localized protection from degradation [67,68].

1.3.2 Local translation by translation-independent mRNA localization

1.3.2.1 Classical examples of translation-independent mRNA localization and local translation

Many classical examples of local translation are achieved by translation-independent mRNA localization. β -actin mRNA enriches in cell projections to facilitate mobility, *MAP2* mRNA is transported to dendrites to enhance synaptic activity, morphogenic transcripts in *Drosophila* (*bicoid*, *oskar*, and *nanos*) polarize to orchestrate early embryonic development, and *Ash1* mRNA in budding yeast goes to the daughter to determine mating type switching [69]. Many of these examples have contributed to a common theme that RNA sequences embedded in the transcript recruit RBPs capable of moving mRNA to a subcellular destination. These RNP complexes typically use cytoskeletal networks and ATP-dependent motors for transport often in a translationally repressed state [31,70]. As each of these foundational examples continues to inform our understanding of the breadth and diversity of these processes, recent studies are uncovering new complexities and nuances to the models these formative studies revealed.

Since its discovery, studies of the β -actin mRNA localization have advanced our understanding of translation-independent RNA localization [4,71]. We now know that the ZBP1/ β -actin mRNA complex interacts with kinesin motor proteins to bring the mRNA near the leading edge of the cell, resulting in enrichment at the motile region of the cell [6,8,71]. At the leading edge, phosphorylation of ZBP1 by Src kinase dissolves the complex allowing translation to initiate [5]. . Recent characterization of the β -actin interactome identified over 60 new RBPs, including FUBP3, that bind downstream of the known 3'UTR zipcode bound by ZBP1. Interestingly, loss of FUBP3 results in mislocalization of β -actin mRNA and inappropriate translation, similar to the loss of ZBP1. This mislocalization phenotype indicates there are several layers of regulation occurring on this transcript with more potentially to be discovered [5,71]. Ultimately, this carefully orchestrated regulation of local translation stimulated by guidance cues results in local actin production at protrusions facilitating cell motility and migration.

The long, polarized structures of neurons present some of the most striking examples of translation-independent mRNA localization followed local translation and its impact on gene expression. Neurons are highly polarized cells, with extensions up to a meter away from the cell body, and they must be able to respond rapidly to incoming stimuli by regulating their local proteome. An early study in dendritic spines identified a pool of ribosomes, suggesting local translation occurs in these distal projections [72]. The first evidence of locally translated RNA arrived with the identification of MAP2 (microtubule-associated protein 2) mRNA, encoding the MAP2 protein instrumental in synapse formation, in rat hippocampal dendrites [73]. Since the discovery of MAP2 local translation, numerous examples of mRNAs localizing within neurons have been identified, placing them within dendrites, in axons, in neuroblasts, and at synapses.

Translation-independent mRNA localization and local translation in neurons can provide multiple functions during their life cycle. Mature neurons may rely on local translation for response to physiological processes while developing neurons rely on local translation for synaptogenesis and axon pathfinding [28]. Mislocalization has been linked to a growing number of neuronal diseases such as fragile X syndrome (and Fragile X-linked mental retardation), spinal muscular atrophy (SMA), myotonic dystrophy (MD), and amyotrophic lateral sclerosis (ALS) emphasizing the importance of mRNA localization on human health [74–76].

In parallel with the discoveries in highly structured and polarized neurons, translation-independent mRNA localization followed by local translation was observed in *Drosophila* embryos. The maternally-deposited morphogenic transcript *bicoid* is localized in a translationally repressed state to the anterior pole through active transport along the microtubule network [77]. The localizing RNA element is a series of stem-loops in the 3'UTR that facilitates binding by the RBP Vps36 (a subunit of the ESCRT-II complex). Upon enrichment at the anterior pole, Bicoid protein is locally translated and contributes to body axis determination. Mislocalization of maternal *bicoid* mRNA to the posterior pole of the embryo results in dramatic developmental defects, linking the mislocalization of mRNA to a functional outcome during embryogenesis [78,79]. At the posterior of the embryo, translation of another maternal morphogen, *nanos*, is required for proper patterning of the anterior-posterior axis [80,81]. Prior to zygotic genome activation, *nanos* mRNA is localized and maintained in a translationally repressed state through a hand-off of RBPs via zip codes in the 3'UTR and sequestered in germ granules until ZGA. mRNA transport, tethering, and protection from degradation all contribute to the spatial patterning of morphogens that ultimately direct body patterning through local translation [32,82,83].

mRNA localization has also been extensively studied in *Saccharomyces cerevisiae*. While many mRNAs have now been identified as localized and locally translated, the best characterized is the *ASH1* mRNA encoding the transcription factor Ash1 [84–86]. *ASH1* mRNA accumulates at the emergent mother bud tip during anaphase, where its localized protein production represses mating type switching in the bud cell and ensures adequate populations of both **a** and **α** mating types within homothallic populations [14,87]. This is achieved through transport along actin filaments while maintained in a translationally repressed state [88,89]. Local translation of *ASH1* requires phosphorylation of the repressive complexes at the bud tip [89]. This discovery provided further evidence that spatially specified translation can diversify gene expression between mother and daughter cells even as their genotypes remain the same.

1.3.2.2 Emerging examples of translation-independent mRNA localization and local translation

While most cytoplasmic condensates are associated with translation repression (section 1.2), a novel condensate called the TIS granule facilitates local translation at the endoplasmic reticulum (ER) [90]. TIS granules are non-spherical, membraneless organelles formed by the RBP TIS11B and its RNA targets. The CD47 mRNA serves as a model for TIS granule function. TIS11B binds AU-rich elements present only in the longer 3'UTR of two alternatively-spliced CD47 isoforms. TIS11B ushers the long CD47 mRNA to the TIGER (TIs Granule ER) domain, an extraluminal space formed from TIS granules interleaved with the ER. This distinct environment promotes CD47 complex formation with its effector protein, SET, in a splice-variant-specific manner. The TIS granule environment is distinct from other condensates as it creates a translation permissive microenvironment where CD47 RNA interacts with SET protein

co-translationally (**Figure 1.2A**). TIS granules represent a growing list of condensates that are now associated with local translation [91–94].

β -actin mRNA localization was the first model transcript for RNA localization distal projections in neurons and leading edges in embryonic cells, RNAs locally translate to cell peripheries in a diversity of cell types [95–97]. A subset of these transcripts, primarily comprised of mRNAs encoding signaling and cytoskeleton regulators, require the APC tumor suppressor protein for localization [98]. These are classified as APC-dependent, and the 3'UTRs of these transcripts are necessary and sufficient to direct localization to cell projections and require the cytoskeletal network [97,98]. The kinesin motor KIF1C directs APC-dependent mRNAs towards the periphery in HeLa cells while also binding its own mRNA, suggesting a potential feedback model to maintain peripheral localization [99]. Intriguingly, these APC-dependent mRNAs accumulate in clusters at cell peripheries. KIF1C facilitates this clustering upon suppression of local translation, but the exact mechanism is unknown [97,99]. This further supports the model that translationally repressed transcripts coalesce upon translation inhibition as observed for mRNAs in stress granules, P-bodies, and germ granules. However, it remains unclear whether these repressed APC-dependent mRNAs are accumulating in known cytosolic condensates or a novel condensate.

Translation-independent localization of another APC-dependent mRNA, RAB13, expands upon the canonical β -actin model of local translation. RAB13 mRNA encodes a GTPase important for vesicle-mediated membrane trafficking. RAB13 mRNA is enriched at peripheral protrusions while, in contrast, RAB13 protein is perinuclear localized. The RAB13 mRNA 3'UTR is sufficient to direct localization to protrusions, but peripheral translation of the RAB13 mRNA is required for full activation of the encoded GTPase [97]. The peripheral localization is

important for co-translationally associating the nascent RAB13 protein with the exchange factor RABIF. The RAB13-RABIF association at the cell periphery is necessary for RAB13 GTPase activity to promote its function in cell migration. Mislocalization of RAB13 mRNA to the nuclear periphery phenocopies the effect of the loss of RAB13 protein, indicating co-translational association with the effector protein RABIF at the nuclear periphery is necessary for function [97].

As mRNA localization mechanisms are identified in different cell types across kingdoms of life, little is known about which sequencing elements are shared and conserved. RNA proximity labeling identified the basal enriched transcriptome in human intestinal epithelial cells. mRNAs encoding ribosomal proteins contain a localization sequence element in the 5'UTR, the 5'TOP motif, which is bound by the TOP-binding protein LARP1. While initial studies were conducted in human intestinal epithelial cells, this same localization pattern and localization elements persists in mouse neuronal cells. The conserved 5'TOP motif/LARP interaction is sufficient to drive basal RNA localization in both neuronal and epithelial cells [100]. Depleting Larp1 in neuronal cells and epithelial cells causes defective phenotypes, indicating localization of 5'UTR TOP motif transcripts is important for the health of multiple cell types. These findings demonstrate that localization mechanisms can extend across different cell morphologies while also identifying LARP1 as a localization regulator across the apicobasal axis in epithelial cells.

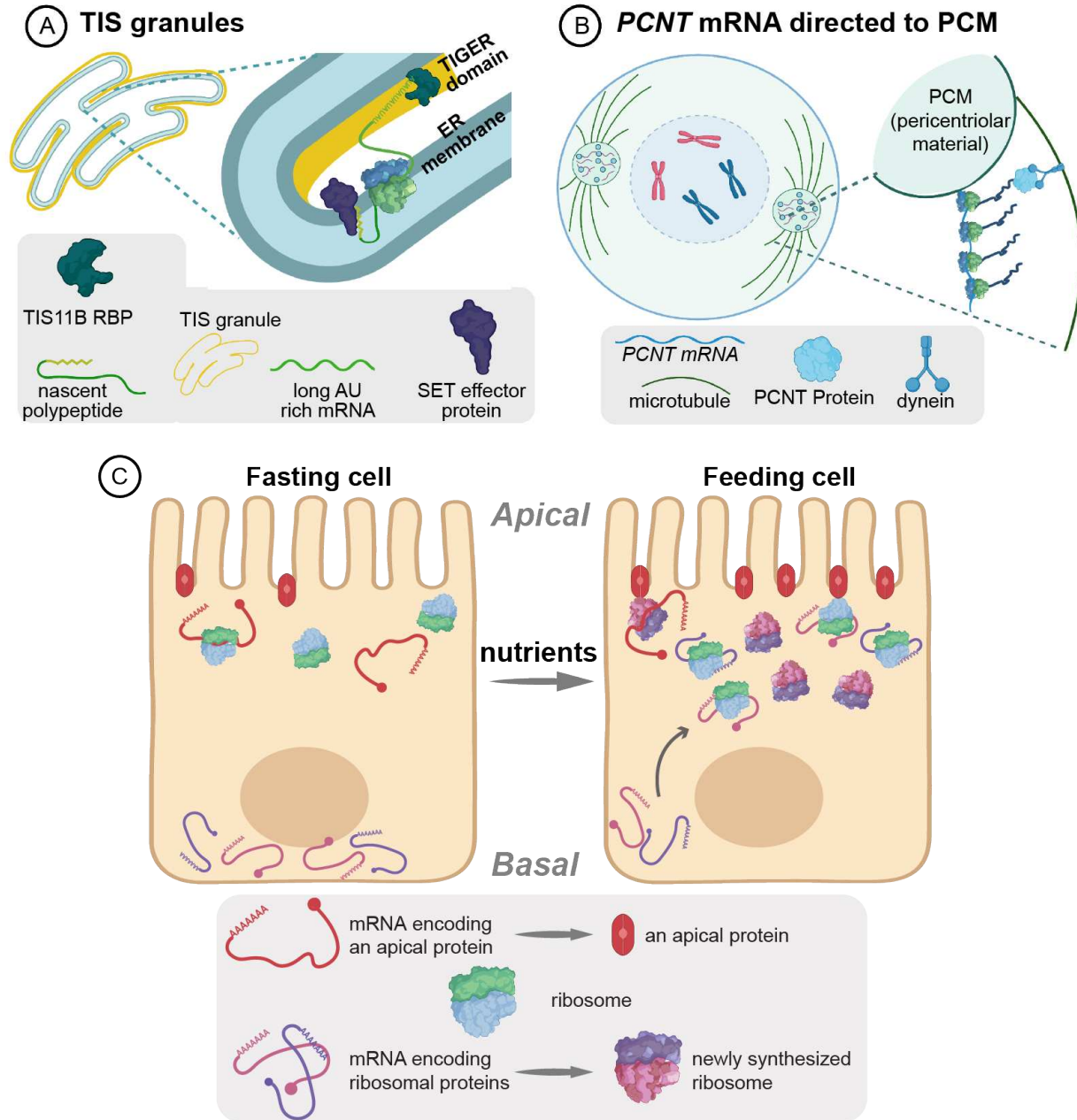


Figure 1.2: Examples of local translation achieved through translation-independent and translation-dependent mRNA localization pathways. (A) TIS granules in human cell lines are mesh-like condensates interweaved with the ER. In these condensates, TIS11B associates with the AU rich elements present in the long 3'UTR isoform of *CD47* mRNA to facilitate interaction with its effector protein, SET, upon translation. (B) In human cells, the *PCNT* mRNA is actively transported towards the centrosome to facilitate rapid incorporation into the transient pericentriolar material (PCM). (C) In fasting mouse enterocytes, mRNA encoding ribosomal proteins is basally enriched. Upon feeding, ribosomal encoding mRNA is localized to the apical side in a translation-dependent manner.

1.3.3 Local translation by translation-dependent mRNA

localization

1.3.3.1 Classical examples of translation-dependent mRNA localization and local translation

In contrast to translation-independent mRNA localization followed by local translation, translation-dependent mRNA localization requires a nascent peptide chain to direct localization to subcellular destinations, and consequently, transport occurs in conjunction with translation. Targeted translation in stable, polarized cells such as neurons can offer advantages of locally producing multiple protein molecules and rapid response to stimulus. Additionally, transporting mRNA in a translationally repressed state can prevent premature or inappropriate interactions, making use of the cytoskeletal network for trafficking across large distances. Therefore, it has been surprising as new studies reveal translation-dependent pathways for mRNA localization in a multitude of cell types and organisms. While the mechanisms and functions of this type of localization remain largely unknown, recent studies are providing insight.

The best characterized example of translation-dependent localization is the secreted, or membrane protein-encoding mRNA population at the ER. In the classic ER localization pathway, mRNAs targeted to the ER are recognized by a signal recognition particle (SRP) binding a nascent signal peptide [101,102]. In eukaryotes, an estimated 30% of proteins are synthesized at the ER (Stevens and Arkin 200). Of these, roughly 57% of the corresponding mRNAs localize in a co-translational, SRP-dependent manner in yeast [103,104]. In this transport pathway, a nascent signal peptide is recognized by the SRP which binds and ushers the entire ribosome-nascent-chain complex (RNC) to the ER [101,102]. SRP binding stalls translation elongation,

indicating SRP-mediated mRNA transport not only depends on translation initiation and initial elongation but can also involve temporary translational repression [105]. This translation-dependent mechanism has served as a model for understanding how nascent peptides can be instructive for localizing the peptide, its translational machinery, and its associated mRNA [104].

Recent studies have unveiled novel aspects of the co-translational SRP-mediated pathway. Translation-independent mechanisms of localizing mRNA to the ER also exist [90,106]. Ribosome profiling has revealed that SRP molecules can pre-associate with most target transcripts prior to translational initiation through 3'UTR sequences, supporting SRP recruitment prior to protein synthesis [107]. Additionally, many ER integral membrane proteins are posited to undergo multiple rounds of translation [108]. This pioneering round of targeting followed by successive rounds of translation at the ER was also observed using single-molecule imaging of nascent peptides (SINAPS) [109]. Together, these findings illustrate how SRP-directed mRNA localization is co-translational but can include a mix of RNA-dependent and peptide-dependent targeting. ER-associated mRNAs are underrepresented in stress granule transcriptomes, suggesting they are not translationally repressed and instead are locally translated to facilitate a regulatory role of the ER during stress response. In this way, proteins can be produced at their site of action, allowing for proper folding, efficient incorporation into complexes and membranes, and rapid, local protein production.

1.3.3.2 Emerging examples of translation-dependent mRNA localization and local translation

mRNA targeting to the outer mitochondrial membrane by translation-dependent mechanisms has been recently observed. mRNA accumulation and translation at the mitochondrial membrane appear to be a combination of translation-dependent and translation-

independent pathways [19,110,111]. The outer membrane protein (OM14) functions as a reception for ribosome-nascent chain complexes (RNC) and translocase of the outer membrane (TOM) complex both facilitate recruitment of cytosolic ribosomes and local translation on mitochondrial membranes [112,113]. This local translation through translation-dependent mechanisms can ensure proper protein targeting, coordinate mitochondrial growth and function, and efficiency of the mitochondria [114].

In addition to the ER and mitochondrial outer membrane, translation-dependent mRNA localization is now recorded at the plasma membrane as well. In *Drosophila*, the *anillin* mRNA encodes the Anillin protein, which separates nuclei within the embryonic syncytium and is critical for the structural integrity of the pseudo cleavage furrow [115]. In early embryogenesis, *anillin* mRNA colocalizes in a distinct hexagonal pattern with the Anillin protein by a translation-dependent mechanism [17,116]. Independent of its 5'UTR or 3'UTR, *anillin* mRNA localization requires translation of the pleckstrin homology (PH) and actin-binding domains, suggesting that mRNA localization can be directed by membrane-associated protein domains. This has since also been observed in *C. elegans* embryos in developing epithelial tissues [117].

During mitosis, cells rely on centrosomes to coordinate microtubule dynamics and ensure proper segregation of genetic material into each daughter cell [118]. Centrosomes are the primary microtubule organizer in most animal cells comprised of a central pair of centrioles surrounded by the pericentriolar material (PCM). Several mRNAs have been identified in association with centrosomes in diverse cell types, a subset of which have been identified as having translation-dependent localization [17,20,30,65]. Accumulation of the PCM is largely driven by the protein PCNT [119]. PCNT mRNA localizes to centrosomes in a translation- and dynein-dependent manner during centrosome maturation [65,120] (**Figure 1.2B**). This is

hypothesized to combat the kinetic challenge of transporting and incorporating this large protein during the short period of early mitosis. The microtubule minus-end regulator ASPM similarly localizes co-translationally to the mitotic spindle poles, presumably to combat the same challenges [20].

In the same study that identified ASPM translation-dependent mRNA localization, a screen of 523 human transcripts found 32 that localize to distinct regions of HeLa cells such as the centrosome, spindle poles, cellular protrusions, endosomes, Golgi, mitochondria, ER, nuclear pores, cell cortex, and punctate cytoplasmic granules [20]. These localizations were often shared by the proteins they encode. Of 13 mRNAs tested, 11 depended on active translation to maintain their localization. This work suggests that co-translational mRNA localization is more prevalent and diverse than initially thought and potentially serves a multitude of different functions depending on location and cell cycle stage.

In both the co-translational and translation-independent pathways, mRNA localization is connected to diverse and unique mechanisms of post-transcriptional regulatory control that can modulate gene expression. The spatial organization of localized mRNAs often coincides with the localization of the proteins they encode. However, this relationship is not seen in all cases (dueling localizations of RAB13 mRNA and RAB13 protein in section 1.3.2.2). Highly polarized cells of the mouse gut epithelium can localize their transcripts to either ribosome rich or ribosome poor locales in correlation with different levels of translational output (**Figure 1.2C**) [121]. These intestinal enterocytes absorb nutrients on their apical side and secrete nutrients into the bloodstream on the basal side. 30% of highly expressed transcripts are polarized to the apical or basal sides of these cells [121]. However, their accumulation overlapped poorly with the ultimate localization of their encoded proteins and instead correlated with their level of

translational output, with translationally active transcripts accumulating apically (**Figure 1.2C**). Associated with this increased translational output, a larger pool of ribosomes, ribosomal RNA, and ribosomal protein encoding mRNA was also observed on the apical side upon feeding. Intriguingly, this provides evidence for a rapid positive feedback mechanism able to upregulate translation under fed conditions. That is, when gut epithelial cells are stimulated to high metabolic states through feeding, ribosomal protein-encoding mRNAs re-orient to the apical side where they are translated by the high ribosomal pool there, thus growing the pool of ribosomal components itself. The function of translating ribosomal components away from the primary site of ribosome assembly (the nucleolus), remains unknown. Altogether, this work shows how mRNA localization can dynamically impact translational status.

1.4.1 Future perspectives, rationale, and hypotheses

With the advance in technologies capable of identifying, visualizing, and characterizing RNA transcriptomes and localization patterns, it is becoming apparent that the cellular transcriptome of organisms across kingdoms of life is highly compartmentalized. Local RNA translation can function to regulate a local proteome in response to stimulus, maintain cell polarity, promote interaction with partner proteins, prevent premature interactions, and overcome kinetic challenges of moving large proteins. These functions can serve to post-transcriptionally regulate gene expression.

However, much remains unknown about specific mechanisms and functions of local translation. Additionally, it is unclear how mRNA distributions are modulated in varying physiological settings and stimuli. What mechanisms and localization elements are conserved? Once identified, can these be leveraged to make predictions on local proteome regulation? As

technologies continue to emerge that achieve high resolution, enhanced RNA detection will facilitate understanding the regulatory connections and functional implications, specifically with relation to diseases, disease progression, and possible interventions.

Our lab has identified maternally-inherited mRNAs with cell-specific and subcellular localization patterns in *Caenorhabditis elegans* embryos. Two of these transcripts, *imb-2* (*Importin Beta*) and *erm-1* (*Ezrin/Radixin/Moesin*), are of specific interest because they localize to the same subcellular locales as the proteins they encode – the nuclear periphery and plasma membrane, respectively. How they localize, and whether those mechanisms depend on the translation of the proteins they encode, remains unclear.

As discussed earlier in Chapter 1, mRNAs can localize either independently of translation, or cotranslationally. In the translation-independent localization model, localization is driven by an mRNA sequence feature often found within the 3'UTR. This is the only localization model that has been described in so far for maternally-inherited transcripts in *C. elegans* [47,48]. However, prior studies from our lab have demonstrated that the 3'UTRs of *erm-1* and *imb-2* were not sufficient to direct localization (Parker et al., 2020). Based on this information, we hypothesized that *erm-1* and *imb-2* mRNA localize through translation-dependent pathways. The primary aims of this dissertation were to test this hypothesis by disrupting translation through various means while also identifying elements necessary for the localization of these maternal transcripts to the appropriate subcellular locale.

Chapter 2

Translation of the ERM-1 membrane-binding domain directs *erm-1* mRNA localization to the plasma membrane in the *C. elegans* embryo¹

2.1 Introduction

mRNA localization is a prevalent feature in diverse cell types and organisms [10,14,20,122]. Subcellular localization of mRNA is associated with spatiotemporal control of gene expression. mRNA localization can occur as a cause or consequence of translational regulatory control, can promote mRNA degradation, facilitate interactions with effector proteins, and prevent premature non-specific interactions [10,20,29,30,79,90,123,124]. In *Caenorhabditis elegans* early embryos, mRNA localization is a prominent feature of maternally inherited mRNAs and may contribute to cell-specific patterning prior to the onset of zygotic transcription [47,48,125–127]. Generally, maternal transcripts enriched in the posterior cells of the embryo localize to membraneless biomolecular condensates called P granules [47,48]. Previous work has indicated that transcripts

¹ The work described in Chapter 2 was published as a preprint in March 2022 under the same title. Winkenbach et al., *BioRxiv*. 2022. doi: 10.1101/2022.05.11.491546. The manuscript was accepted at *Development* in October 2022. Lindsay P. Winkenbach, Dylan M. Parker, Robert TP Williams, and Erin Osborne Nishimura The ERM-1 membrane-binding domain directs *erm-1* mRNA localization to the plasma membrane in the *C. elegans* embryo. *Development* 2022. DOI: 10.1242/dev.200930.

localize to P granules following translation repression [47,48]. In contrast, maternal transcripts that concentrate in the anterior cells often localize to the plasma membrane often colocalizing with their encoded proteins membrane [48]. However, the molecular mechanisms that facilitate membrane localization in *C. elegans* are unclear. Here we focus on *erm-1* as a model membrane-associated transcript and characterize the mechanisms underlying its localization to the cell membrane.

mRNA localization can occur via translation-independent or translation-dependent pathways [31,64,68]. Translation-independent pathways typically rely on *cis*-acting elements, RNA sequences or structures that are often located in untranslated regions (UTRs) and recruit *trans*-recognition factors such as RNA Binding Proteins (RBPs). Recognition by RBPs can lead to either passive or directed transport, often in association with other processes such as mRNA protection, mRNA degradation, or translational regulatory control [128]. The result is an enrichment of mRNAs in specific subcellular locales. In *C. elegans*, some posterior-enriched maternal transcripts localize through translation-independent pathways, relying on *cis*-acting elements in their 3'UTRs to direct translational repression that is required for localization into P granules [47,48]. In contrast, translation-dependent pathways of mRNA localization typically rely on peptide signals in the nascent polypeptide. Transcripts that concentrate at the ER often rely on signal peptides to direct translating mRNAs and their encoded proteins to their destinations [129]. However, previously identified transcripts that localize to the plasma membrane in *C. elegans* embryos lack a discernable signal peptide [48]. Recently, several *C. elegans* transcripts that encode members of the apical junction sub-complexes, their additional ancillary proteins, or other cytoskeletal components were found to localize to the plasma membrane during mid-embryogenesis with subcellular localization patterns that did not appear to

overlap with the endoplasmic reticulum. Of these, the *dlg-1* transcript was shown to localize in a translation-dependent fashion [117]. Together, these findings demonstrate the localization of plasma membrane enriched transcripts is occurring in a distinct manner from the canonical, ER signal peptide directed pathway and that local translation may be a general feature of junction and membrane-linker proteins.

erm-1 (*ezrin/radixin/moesin*) mRNA is the most anterior-enriched transcript in the 2-cell *C. elegans* embryo [126,130]. In addition to its high enrichment within anterior cells of the early embryo, *erm-1* mRNA concentrates at plasma membranes within those cells, a pattern coincident with its encoded ERM-1 protein [48,131,132]. Previously, we showed the *erm-1* 3'UTR was insufficient to direct membrane mRNA localization, indicating that the localization element resides elsewhere in the RNA sequence or the encoded protein [133]. In this study, we set out to identify which elements in *erm-1* mRNA or the encoded ERM-1 protein are necessary for membrane localization.

In *C. elegans*, ERM-1 is the sole ortholog of the conserved ERM protein family that serve as membrane-actin linkers [131]. ERM proteins regulate cell morphology and signaling events at the plasma membrane. Therefore, they are prominent in processes such as epithelial junction remodeling, cell migration, promotion of microvilli formation, and interactions with actin at the cell cortex [131,132,134,135]. Proper specialization of the cell cortex and plasma membrane is critical for controlling cell morphology, as evidenced by the fact that in *C. elegans*, loss of the *erm-1* in the intestine results in early embryo lethality due to constrictions and disjunctions in the intestinal lumen [131,136].

Here we demonstrate *erm-1* mRNA accumulation at the plasma membrane is translation-dependent and requires the membrane-binding ability of the FERM domain to enrich at the

plasma membrane. Further, we screened 17 genes encoding similar membrane-binding FERM or PH-like domains. We identified twelve additional plasma membrane localized transcripts and other patterns of subcellular mRNA localization that change over developmental time. Our findings suggest translation of this conserved membrane-binding domain is conducive to subcellular localization of both the mRNA and the encoded protein.

2.2 Results

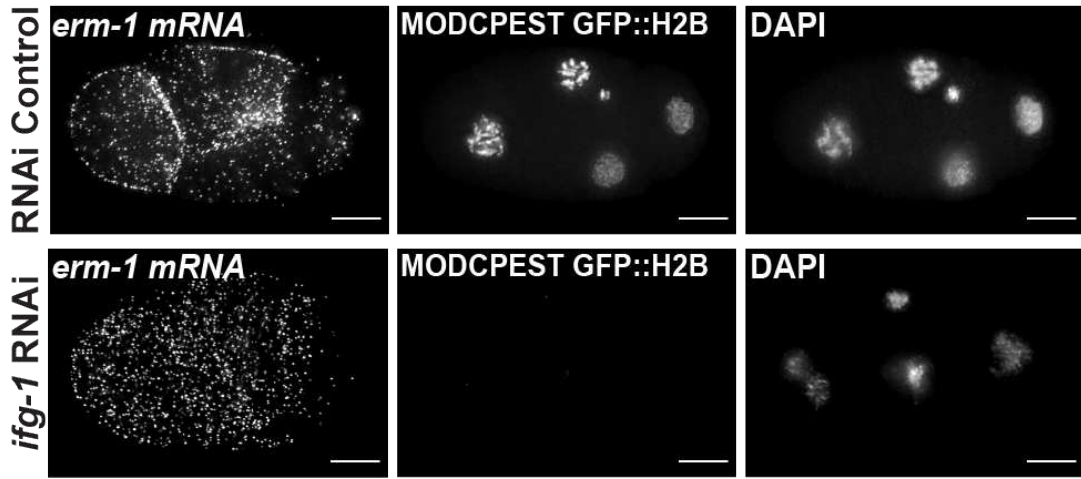
2.2.1 *erm-1* mRNA localization to the plasma membrane requires translation initiation

mRNA localization is directed through either translation-dependent or translation-independent pathways [31,64,68]. To test which pathway was responsible for *erm-1* mRNA localization, we disrupted global translation by two methods and determined whether either perturbed *erm-1* mRNA accumulation at the membrane. We first depleted the translation initiation factor *ifg-1* (*Initiation Factor 4G (eIF4G) family*) by RNA interference (RNAi). IFG-1 is the sole *C. elegans* ortholog of eIF4G, and both cap-dependent and -independent translation initiation require IFG-1 [137–140]. Using a destabilized-GFP as a translation reporter (MODCPEST GFP::H2B), we found that *ifg-1* RNAi decreased translation in a partially penetrant fashion as indicated by a decrease in GFP::H2B fluorescence (**Figure 2.1A, C**) [141–143]. *ifg-1* RNAi introduced in the L2 stage of development led to 46% of 4-cell progeny exhibiting a significant loss of GFP signal and 54% showing no significant change compared to wild type. Importantly, we observed that embryos with impacted translation also experienced a loss of *erm-1* mRNA localization at the

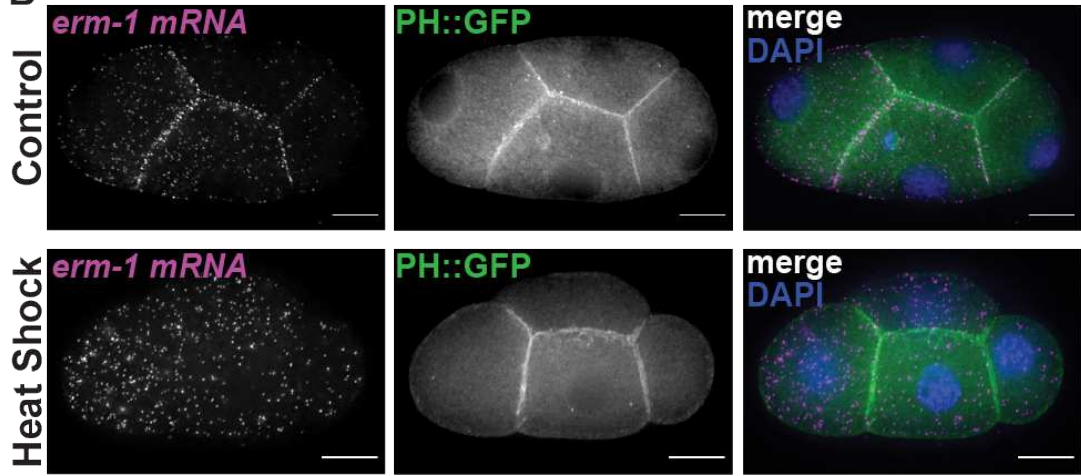
plasma membrane with high concordance (**Figure 2.1A, C**). These results support the model that *erm-1* mRNA localization to the plasma membrane is translation-dependent.

As a complementary approach to disrupting global translation initiation via RNAi, we next disrupted translation through heat shock and quantified the resulting changes in *erm-1* mRNA enrichment at the plasma membrane [48]. Heat shock prevents protein synthesis primarily through changes in phosphorylation states of translation initiation factors followed by their subsequent inactivation [144–147]. Heat shock acts within a shorter time frame than *ifg-1* RNAi (25 minutes heat shock vs. 48 hrs RNAi exposure). In heat treated 4-cell embryos, we observed a 1.6-fold reduction in *erm-1* mRNA enrichment alongside the plasma membrane (at a distance of less than 10% of the normalized radius from the plasma membrane) after only 25 minutes of 30 °C heat exposure compared to controls that were kept at 20 °C for the same duration (**Figure 2.1B, D**). Combined with the *ifg-1* RNAi experiment findings, this illustrated that *erm-1* mRNA localization to the plasma membrane depended on translation-initiation for establishment and maintenance. Together, these results suggest a translation-dependent pathway and imply that the signal to localize *erm-1* mRNA to membranes may be an encoded peptide sequence in the nascent ERM-1 protein. However, these assays do not yield information on whether active translation or an intact ribosome nascent chain complex (RNC), or both, are required for localization.

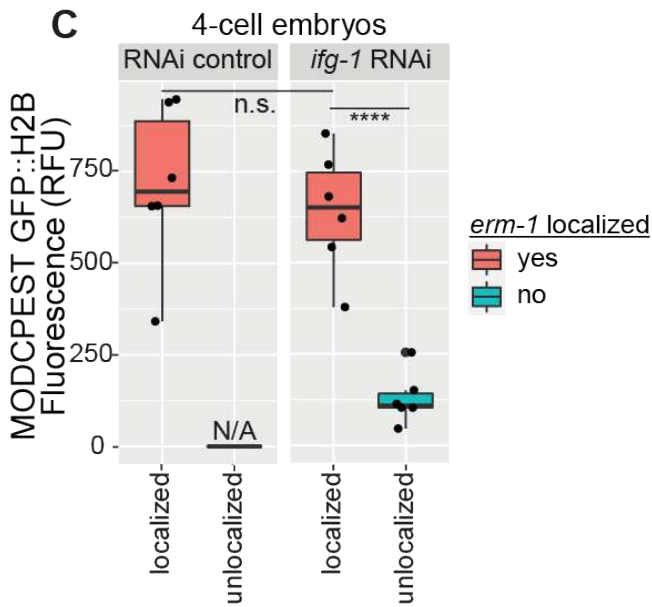
A



B



C



D

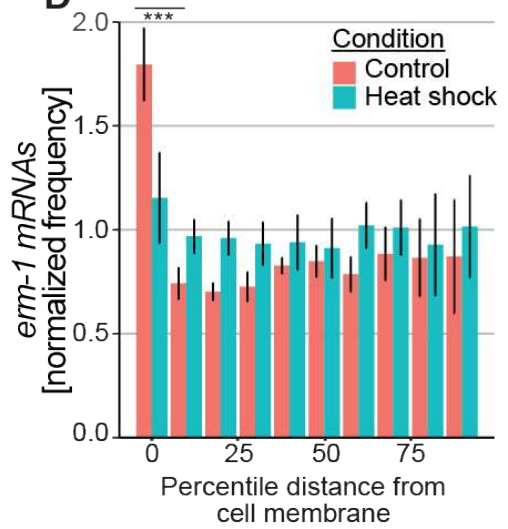


Figure 2.1: Disruption of global translation leads to loss of *erm-1* mRNA localized to the membrane. (A) Fluorescent micrographs of 4-cell stage *C. elegans* embryos. RNAi was performed to deplete the translational initiation factor *ifg-1*, or an empty vector RNAi control was performed. *erm-1* transcripts were imaged by smFISH. In the same embryos, GFP from a translational reporter transgene (MODCPEST-GFP::H2B) and DNA (DAPI) were also imaged. Representative images are shown from a total of 102 4-cell stage embryos surveyed ($n = 23$ RNAi control, $n = 79$ *ifg-1* RNAi [$n = 43$ reporter signal retained, $n = 36$ reporter signal depleted]). Scale bars are 10 μm . (B) 4-cell stage *C. elegans* embryos harboring a membrane marker transgene (PH::GFP, green) were imaged for *erm-1* transcripts by smFISH (magenta) under no heat shock (control 20°C) and heat stress conditions (25 minutes at 30°C heat shock). DNA was also imaged as DAPI staining (blue). Scale bars are 10 μm . (C) Quantification of translation reporter fluorescence under RNAi control ($n = 6$), *ifg-1* RNAi *erm-1* localization retained ($n = 6$), *ifg-1* RNAi *erm-1* localization lost ($n = 6$) conditions. Background subtracted GFP intensities were measured as relative fluorescent units (RFU) using nuclear masks generated using DAPI. *erm-1* mRNA localization was assessed qualitatively as localized or unlocalized in 4-cell embryos. Significance indicates *P*-values derived from Welch Two Sample *t*-tests comparing the RFU values for localized versus unlocalized for the transcript *erm-1* at the given condition. P value legend: 0.00005>****(D) Quantification of *erm-1* mRNA under control (a representative set of $n=5$) and heat shock conditions (a representative set of $n=7$) indicating the normalized frequency of *erm-1* mRNA at increasing, normalized distances from the cell periphery. Significance indicates *P*-values derived from Welch Two Sample *t*-tests comparing the cell membrane localization for heat shock versus control for the transcript *erm-1* at the given stage. *P* value legend: ***>0.00005

2.2.2 The ERM-1 nascent peptide is required for *erm-1* mRNA

enrichment at plasma membranes

We identified that translation is required for *erm-1* mRNA enrichment at plasma membranes.

This suggests a model in which the RNC – comprised of *erm-1* mRNA, the translating ribosome, and the emerging nascent ERM-1 protein – is transported to the plasma membrane together through recognition of amino acid sequences in the nascent ERM-1 protein. We hypothesize that *erm-1* mRNA localization requires intact RNCs, likely at steps that both establish and maintain localization. To test this hypothesis, we inhibited translation elongation using two different drugs, one that preserves RNCs (cycloheximide) and one that disrupts them (puromycin) [148,149].

The eggshell and permeability barrier in the *C. elegans* embryo complicate drug treatment by limiting small molecule penetrance [150–152]. To circumvent this, we disrupted the sugar modifying enzyme and permeability barrier protein PERM-1 by RNAi, thereby allowing

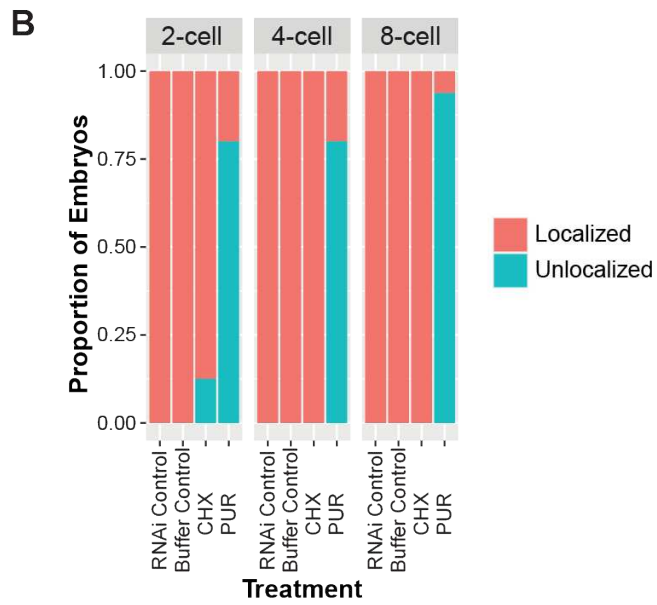
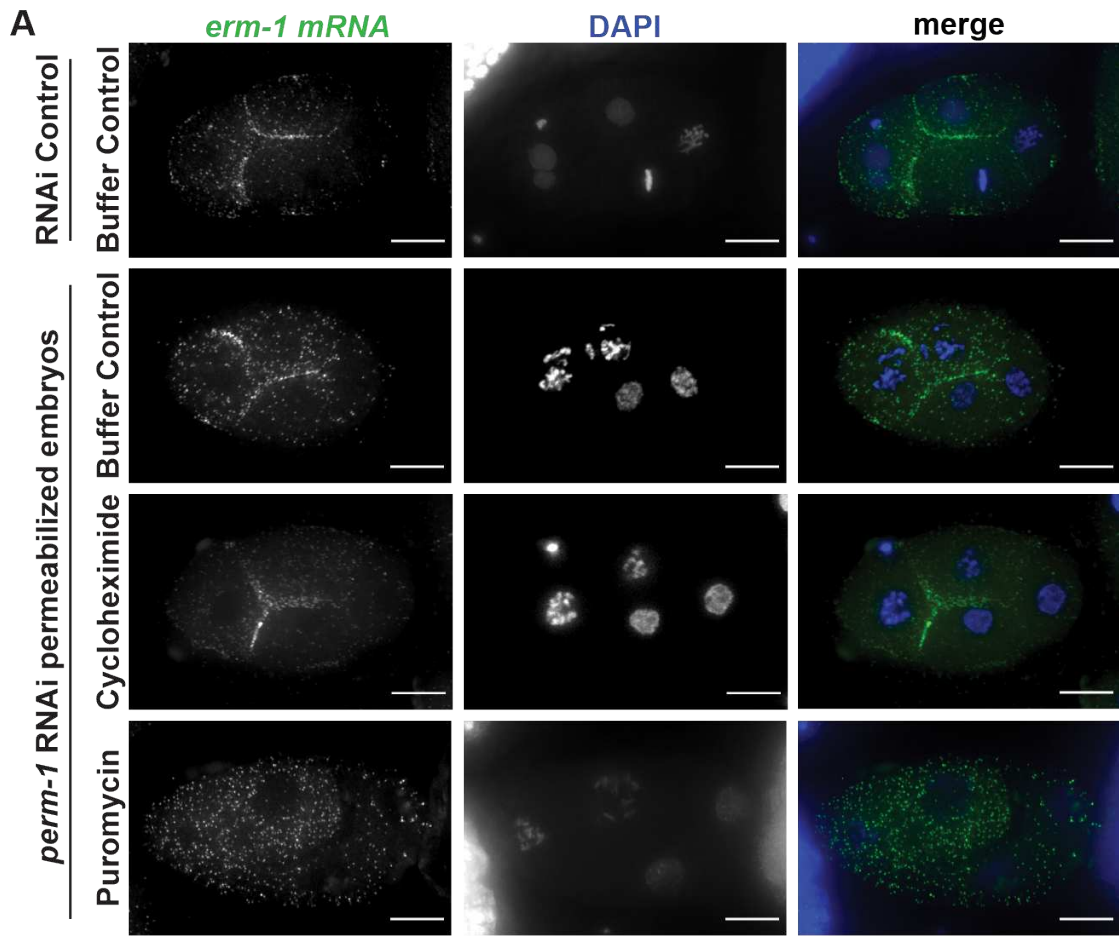


Figure 2.2: The intact ERM-1 ribosome nascent chain complex (RNC) is required for *erm-1* mRNA enrichment at cell membranes. (A) Fluorescent micrographs of 4-cell stage *C. elegans* embryos are shown in which embryos were permeabilized by *perm-1* RNAi and subsequently treated with small molecule translation inhibitors, in comparison to RNAi and drug treatment controls. *erm-1* mRNA (green) was imaged by smFISH, under control, cycloheximide (500 µg/mL, 20min), or puromycin (500 µg/mL, 20min) treatment conditions. Scale bars 10 µm. (B) Bar plot indicating the proportion of embryos displaying *erm-1* mRNA enriched at cell membranes (localized) or homogenously distributed through the cell (unlocalized) for 2-cell, 4-cell, and 8-cell embryos subjected to the indicated treatments.

ingression of small molecules such as cycloheximide and puromycin. Though *perm-1* RNAi eventually leads to lethality in late embryos, development in early embryonic stages proceeds typically [152]. Importantly, *perm-1* RNAi is compatible with both drug treatment and smFISH imaging of *erm-1* mRNA.

We observed that disruption of the RNC via puromycin treatment led to loss of *erm-1* mRNA localization at the membrane in 84% of embryos between the 2-cell and 8-cell stages (**Figure 2.2A, B; Figure 2.3A, B**). In contrast, cycloheximide treatment, which stalls translation during elongation while preserving the RNC only altered *erm-1* mRNA localization in 4% of embryos surveyed (**Figure 2.2A, B; Figure 2.3A, B**). This suggests that the *erm-1* mRNA must maintain association with the ribosome for *erm-1* mRNA molecules to maintain localization to plasma membranes upon translation disruption. Additionally, the maintenance of *erm-1* mRNA localization does not require ongoing translational elongation provided stalled RNCs are preserved intact, as is the case with cycloheximide treatment. These findings further support the translation-dependent model and suggest that *erm-1* mRNA transcripts localize through association with the RNC.

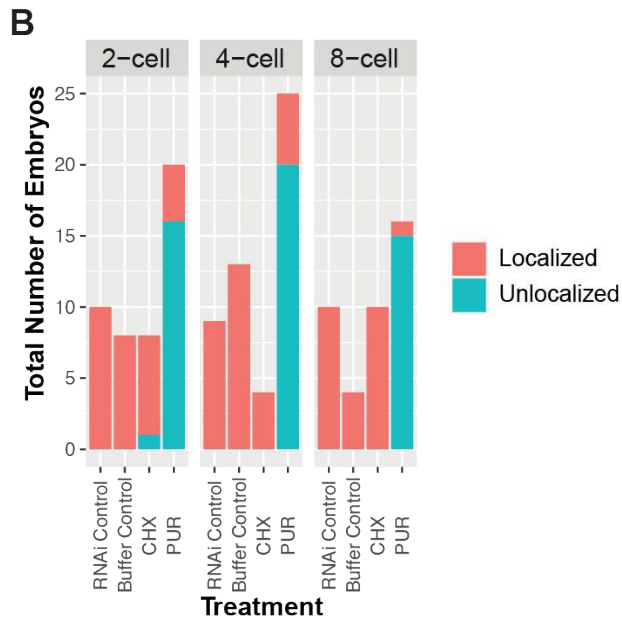
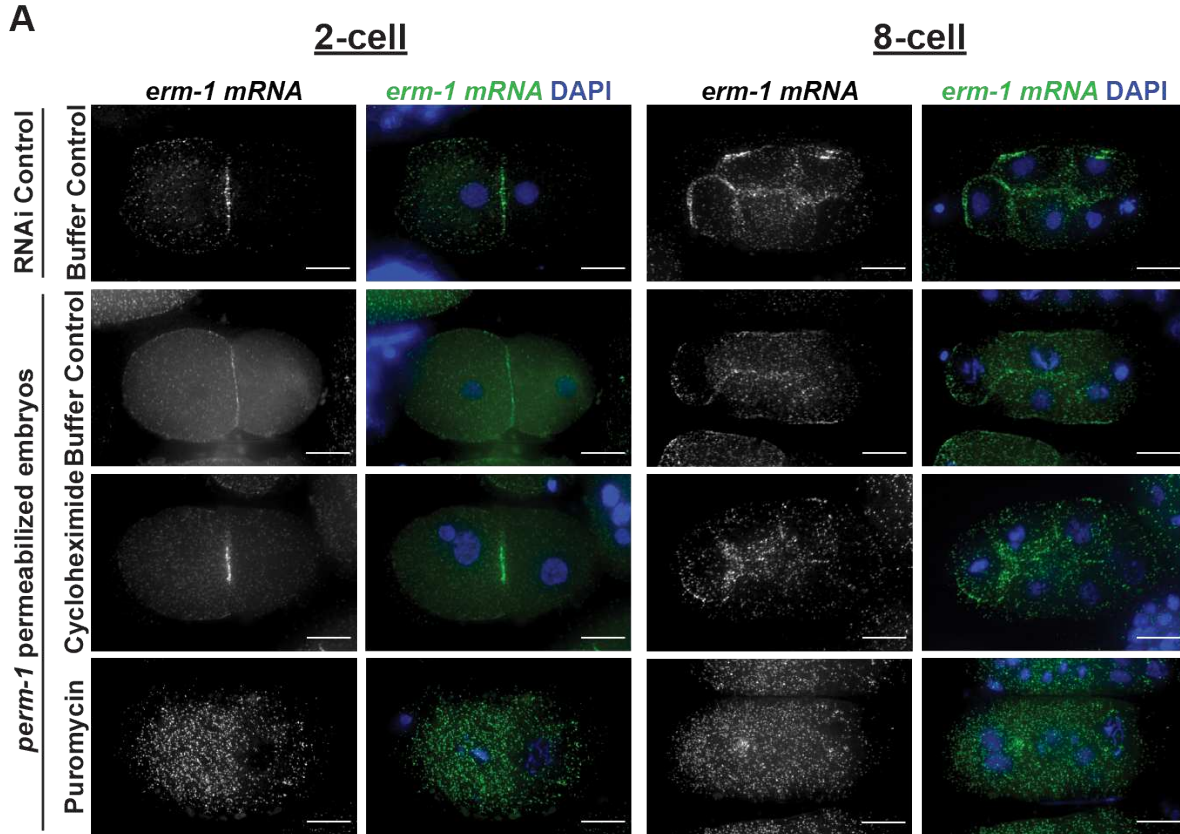


Figure 2.3: The ERM-1 nascent peptide is required for *erm-1* mRNA cell membrane localization. (A) Fluorescent micrographs of 2-cell and 8-cell *C. elegans* embryos are shown in which embryos were permeabilized by *perm-1* RNAi and subsequently treated with small molecule translation inhibitors, in comparison to RNAi and drug treatment controls. *erm-1* mRNA (green) was imaged by smFISH, under control, cycloheximide (500 μ g/mL, 20min), or puromycin (500 μ g/mL, 20min) treatment conditions. Scale bars 10 μ m. (B) Bar plot indicating the number of embryos displaying *erm-1* mRNA enriched at cell membranes (localized) or homogenously distributed through the cell (unlocalized) for 2-cell, 4-cell, and 8-cell embryos subjected to the indicated treatments.

2.2.3 *erm-1* mRNA localization to the plasma membrane does not depend on nucleic acid sequences

We have established that *erm-1* mRNA localizes to plasma membranes in a translation-dependent manner. However, *erm-1* mRNA can persist at membranes if the RNC remains intact when disrupting translation elongation. This suggests that localization is dependent on ERM-1 amino-acid sequence and not *erm-1* mRNA sequence. Supporting this hypothesis, previous evidence has illustrated that the *erm-1* 3'UTR (typically a common site of *cis*-acting localization elements) is insufficient to direct mRNA to the membrane [48]. To test whether other *erm-1* mRNA nucleotide sequences are dispensable for localization, we artificially re-coded the *erm-1* mRNA nucleotide sequence while preserving the amino acid sequence by capitalizing on the redundancy of the genetic code (**Figure 2.5A**). Our nucleotide recoded, yet amino-acid synonymous, *erm-1* sequence (called *erm-1* *synon*) shares 64% identity at the nucleic acid level with the wild-type *erm-1* sequence (called *erm-1*) while maintaining 100% identity of the amino acid sequence (**Figure 2.4A; Figure 2.5B**). We designed single molecule inexpensive FISH (smiFISH) probes that could distinguish between the recoded, synonymous *erm-1* and wild-type sequences (**Figure 2.4B, C**). Using these probes, we found the *erm-1* *synon* transcript retained enrichment at the plasma membrane with no significant difference between it and either the endogenous *erm-1* transcript (**Figure 2.4B D**) or a matched transgenic wild-type *erm-1* sequence inserted at the same transgenic location (**Figure 2.5D, C**). These data imply that RNA sequences within the *erm-1* transcript are dispensable for *erm-1* mRNA localization, and instead, localization elements reside in the translated ERM-1 protein.

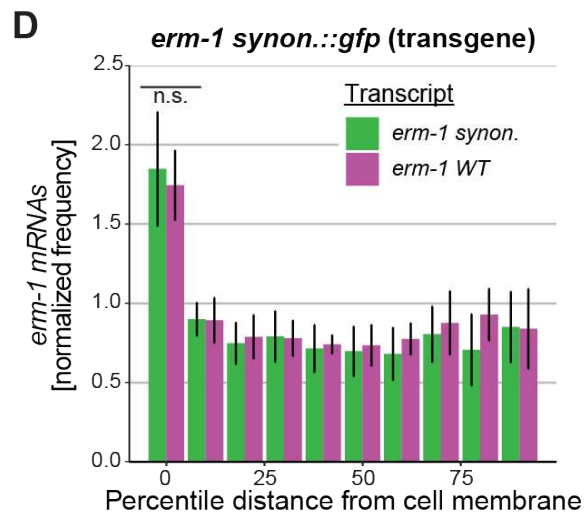
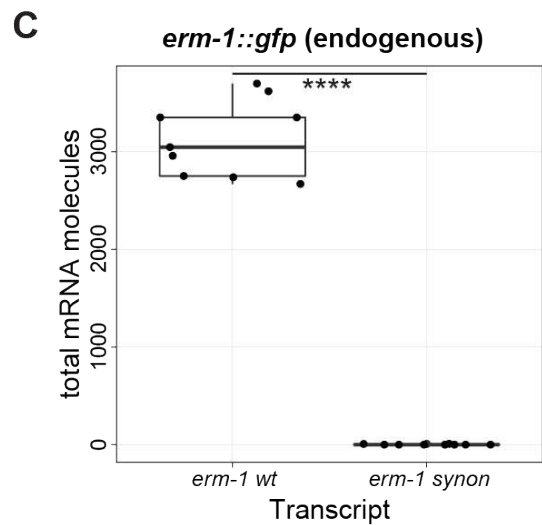
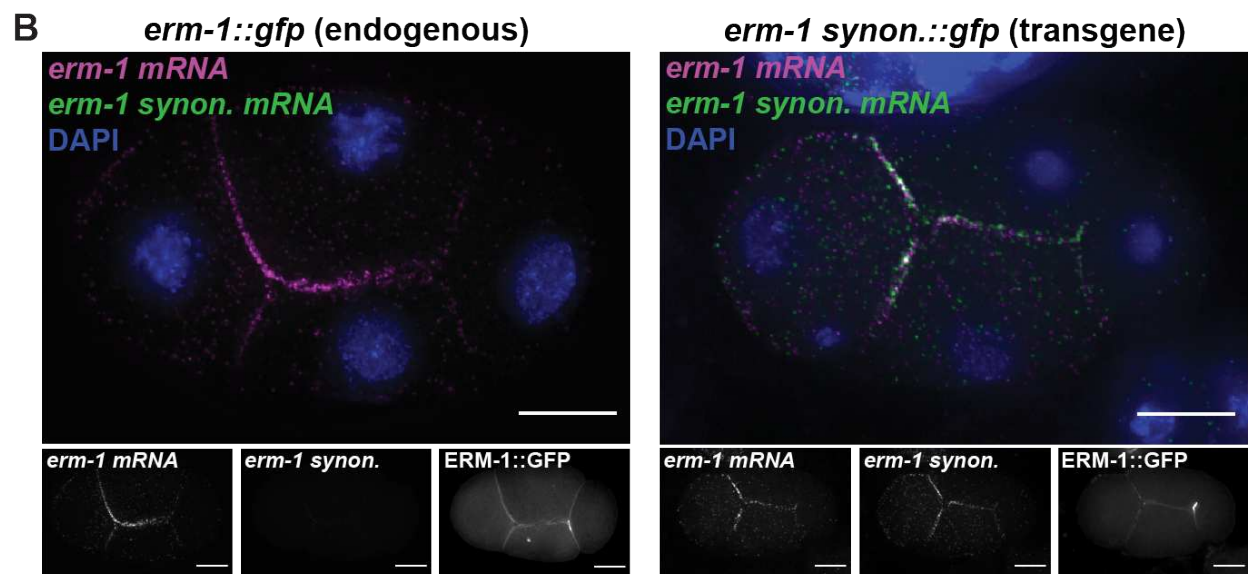


Figure 2.4: *erm-1* mRNA localization to the cell membrane is mRNA coding sequence independent. (A) Schematic depictions comparing wild-type *erm-1* mRNA (magenta) to the re-coded, *synonymous erm-1* mRNA (green). (B) smFISH micrographs of 4-cell staged *C. elegans* embryos imaging wild-type *erm-1* (magenta) and the re-coded, *synonymous erm-1* mRNA (*erm-1* *synon. mRNA*, green). GFP tagged *erm-1* control 4-cell embryo (left) and MosSCI GFP tagged *synonymous erm-1* 4-cell embryo (right). DNA (DAPI, blue) and membranes marked by ERM-1::GFP are also shown. Scale bars 10 μ m. (C) Total number of *erm-1* *wt* and *erm-1* *synonymous* mRNA molecules detected in *erm-1::gfp* (endogenous) ($n = 9$). Significance indicates *P*-values derived from Welch Two Sample *t*-tests comparing the total number of *erm-1* molecules detected by the *erm-1* *wt* probe vs the *erm-1* *synonymous* probe in the endogenously tagged *erm-1::gfp* background. (D) Quantification of endogenous and *synonymous erm-1* mRNA ($n = 6$) indicating the normalized frequency of mRNAs within binned, percentile distances from the cell membrane counted and normalized against the total volume of each cell. Significance indicates *P*-values derived from Welch Two Sample *t*-tests comparing the cell membrane localization of endogenous and *synonymous erm-1* mRNA in the *erm-1* *synon::gfp* transgenic background. *P* value legend: NS>0.05; ***>0.00005

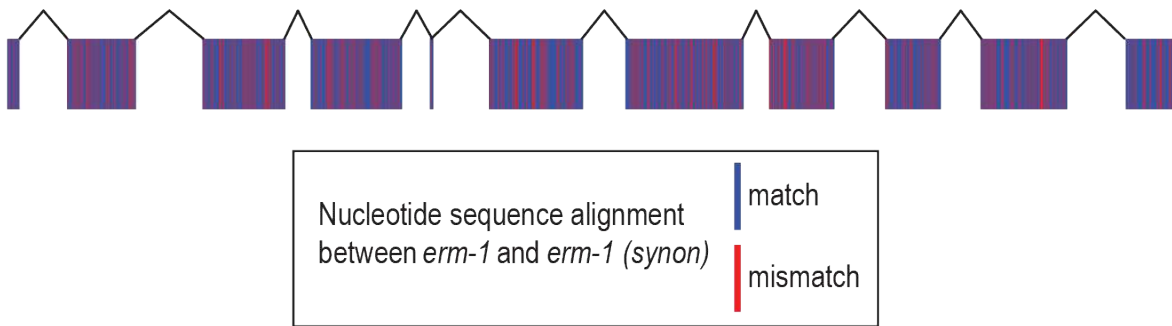
2.2.4 *erm-1* mRNA and ERM-1 protein localization require the ERM-1 PIP₂ membrane-binding region

To identify domains within the ERM-1 protein required to localize translating *erm-1* to plasma membranes, we examined *erm-1* mRNA localization upon mutations in key conserved ERM-1 domains. Generally, ERM proteins are a conserved family defined by domains common to their founding members, Ezrin, Radixin, and Moesin [153–155]. ERM proteins serve as structural linkers between the plasma membrane and the actin cytoskeleton and play central roles in cell morphology and signaling processes that converge on the plasma membrane. Two key domains coordinate their linker function. The N-terminal band 4.1 Ezrin/Radixin/Moesin (FERM) domain houses a PH-like (Pleckstrin Homology-like) domain that associates with the plasma membrane through interactions with PIP₂ (phosphatidylinositol (4,5) bisphosphate) [134,156,157]. In contrast, the C-terminal C-ERMAD domain interacts with the actin cytoskeleton in a phosphorylation-dependent manner [135,136]. The FERM and C-ERMAD domains can also intramolecularly bind to prevent their respective substrate associations. A dephosphorylation event on the C-ERMAD domain increases intramolecular affinity thereby permitting the inactive

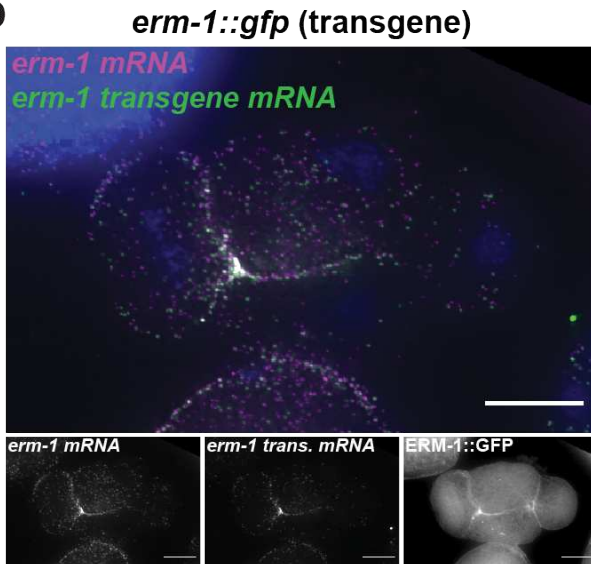
A

Figure 3 worm strains		
<i>erm-1::gfp</i> (endogenous)	<i>erm-1p::erm-1::gfp::erm-1 3'UTR I</i>	<i>gfp</i> knock-in at endogenous <i>erm-1</i> locus on Chr I (Ramalho et al., 2021)
<i>erm-1::gfp</i> (transgene)	<i>erm-1p::erm-1::gfp::erm-1 3'UTR IV</i>	single copy insertion at Chr IV MosSCI locus (this study)
<i>erm-1 synon::gfp</i> (transgene)	<i>erm-1p::erm-1 synon::gfp::erm-1 3'UTR IV</i>	single copy insertion at Chr IV MosSCI locus (this study)

B



D



C

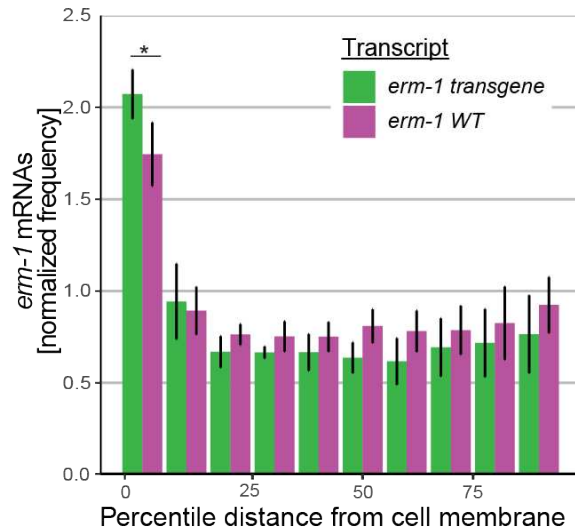


Figure 2.5: *erm-1* mRNA localizes at the cell membrane when expressed from a transgenic MosSCI locus. (A) Description of the three worm strains used in the synonymous *erm-1* assays. (B) smFISH micrographs of 4-cell staged *C. elegans* embryos imaging wild-type *erm-1* probed by *erm-1* (magenta) and the transgenic *erm-1::gfp* mRNA probed by *nemametrix gfp* (*erm-1* transgene mRNA, green). DNA (DAPI, blue) and membranes marked by ERM-1::GFP expressed at the MosSCI locus are also shown. (C) Quantification of endogenous and MosSCI-expressed transgenic *erm-1* mRNA ($n = 6$) indicating the volume normalized frequency of mRNAs within binned, normalized distances from the cell membrane. Welch Two Sample t-test p-value = 0.006 at the cell membrane. Scale bars 10 μ m. P value legend: NS>0.05; 0.05>*>0.005; 0.005>*>0.0005; 0.0005>***>0.00005;

form [157–159]. Therefore, the architecture of ERM-1 connects the plasma membrane and the actin cytoskeleton in a phosphorylation-dependent mechanism.

Mutating four lysines to asparagines abrogates the PIP₂ binding ability of the FERM domain [156,157] (**Figure 2.6A**), termed the ERM-1[4KN] mutant [136]. In *C. elegans*, this leads to intestinal lumen cysts and disjunctions as well as early larval lethality that phenocopy the *erm-1* null [132,136]. In contrast, mutating the conserved, phosphorylatable residue T544 to alanine (ERM-1[T544A]) disrupts the function of the C-ERMAD domain, thereby rendering C-ERMAD non-phosphorylatable [160,161] (Carreno et al., 2008; Zhang et al., 2020). In *C. elegans*, this leads to disrupted cortical actin organization and reduced apical localization of ERM-1 [136]. We assessed *erm-1* mRNA localization in these two previously characterized mutant strains to determine whether *erm-1* mRNA accumulation at the plasma membrane requires the FERM or C-ERMAD domains.

Because the ERM-1[T544A] and ERM[4KN] mutant strains were extensively studied in previous reports during mid-stage embryogenesis for their impacts on intestinal development [136], we examined *erm-1* mRNA localization at both the 4-cell stage we have previously studied and at mid-stage embryogenesis. These assays were performed in ERM-1[T544A] homozygous mutants with no wild-type ERM-1 in the background. In 4-cell stage embryos, both *erm-1*[T544A] mRNA and ERM-1[T544A] protein localized to the plasma membranes similar to wild-type (**Figure 2.6B**). However, the mutants exhibited plasma membranes with “ruffled” or distorted phenotypes, indicating that loss of this phospho-moiety imparts a cellular phenotype through its previously reported reduction in actin organization (**Figure 2.6B**) [136]. In 2.5-fold embryos, *erm-1*[T544A] mRNA also localized at the plasma membrane, similar to wild-type strains. In these embryos, the ERM-1[T544A] protein displayed increased basolateral

localization in the intestinal lumen, as has been previously reported (**Figure 2.6B**) [136]. Therefore, the T544A mutant, though disruptive of ERM-1 phosphorylation and actin association, was not sufficient to disrupt *erm-1* mRNA localization to the plasma membrane at these stages.

Mutations in ERM-1 that disrupt FERM domain/PIP₂ interactions (called ERM-1[4KN]) reduce (in the intestine and excretory canal) or eliminate (in progenitor germ cells and seam cells) ERM-1[4KN] protein localization to apical membranes [136]. We performed smFISH on 4-cell and 2.5-fold stage ERM-1[4KN] homozygous mutant embryos lacking any ERM-1 wild-type copies to assess how this mutation impacted *erm-1* mRNA localization (**Figure 2.6A; Figure 2.7A, B**). At the 4-cell stage, *erm-1[4KN]* mRNA failed to localize to the plasma membrane in 100% of embryos surveyed (**Figure 2.6B**). However, the number of *erm-1* mRNA molecules detected did not significantly change between *erm-1 wt* and *erm-1[4KN]* (**Figure 2.6C**). ERM-1[4KN] protein enrichment at the plasma membrane was also abolished. RNA localization was not observed at the 2.5-fold stage and protein localization was reduced, displaying disjunctions in the lumen as previously reported [136]. Thus, the FERM-domain was required to localize both the *erm-1* mRNA and the ERM-1 protein to the plasma membrane. Combined with our previous findings, this indicates that the peptide signal required to localize the ERM-1 RNC, including its associated *erm-1* mRNA, resides within the FERM domain of the nascent peptide.

2.2.5 Genes encoding FERM and PH-like domains are conducive for mRNAs with localization at the plasma membrane

Given that PIP₂-binding FERM domains have a high affinity for membranes [162], their ability to direct membrane-localized mRNA transcripts may be generalizable. Evidence for this exists in other systems: In early *Drosophila* embryogenesis, the PIP₂-binding PH and actin-binding domains of the Anillin protein are required to localize *anillin* mRNA to pseudocleavage furrow membranes [116]. Based on the findings from the ERM-1[4KN]:GFP mutant strain, we hypothesized that the PIP₂-binding element of the FERM domain could be a general predictor of transcripts that enrich at cell membranes.

To test our hypothesis, we conducted a smiFISH-based screen in *C. elegans* early embryos for membrane localization of other PIP₂-binding FERM or PH-like domain containing transcripts [126,130]. A total of 17 transcripts (9 with FERM domains and 8 with PH-like domains) were selected for visualization based on their expression in early embryos and with preference given to homology in other organisms (**Table 1; Figure 2.8; Figure 2.9; Figure 2.11; Figure 2.12; Materials and Methods**). The set of transcripts selected comprised those that enriched to anterior embryonic cells, posterior embryonic cells, and those with ubiquitous distribution across the early embryo.

Of the 17 screened transcripts, three (*frm-4*, *frm-7*, *ani-1*) displayed clear membrane localization in early embryos at the 4-cell stage (**Figure 1.8A, B; Figure 2.9A-C**). Seven transcripts displayed clustered subcellular patterning in the posterior cell (*Y41E3.7*, *unc-112*, *mrck-1*, *wsp-1*, *ani-2*, *dyn-1*, and *exoc-8*) (**Figure 2.9C**). Four transcripts displayed uniform distribution or other patterns (*F07C6.4*, *efa-6*, *mtm-1*, and *let-502*) (**Figure 2.9A, B**). Three transcripts (*frm-2*, *nfm-1*, and *ptp-1*) yielded RNA abundance too low to determine subcellular enrichment (**Table 2.1; Figure 2.9A, B**).

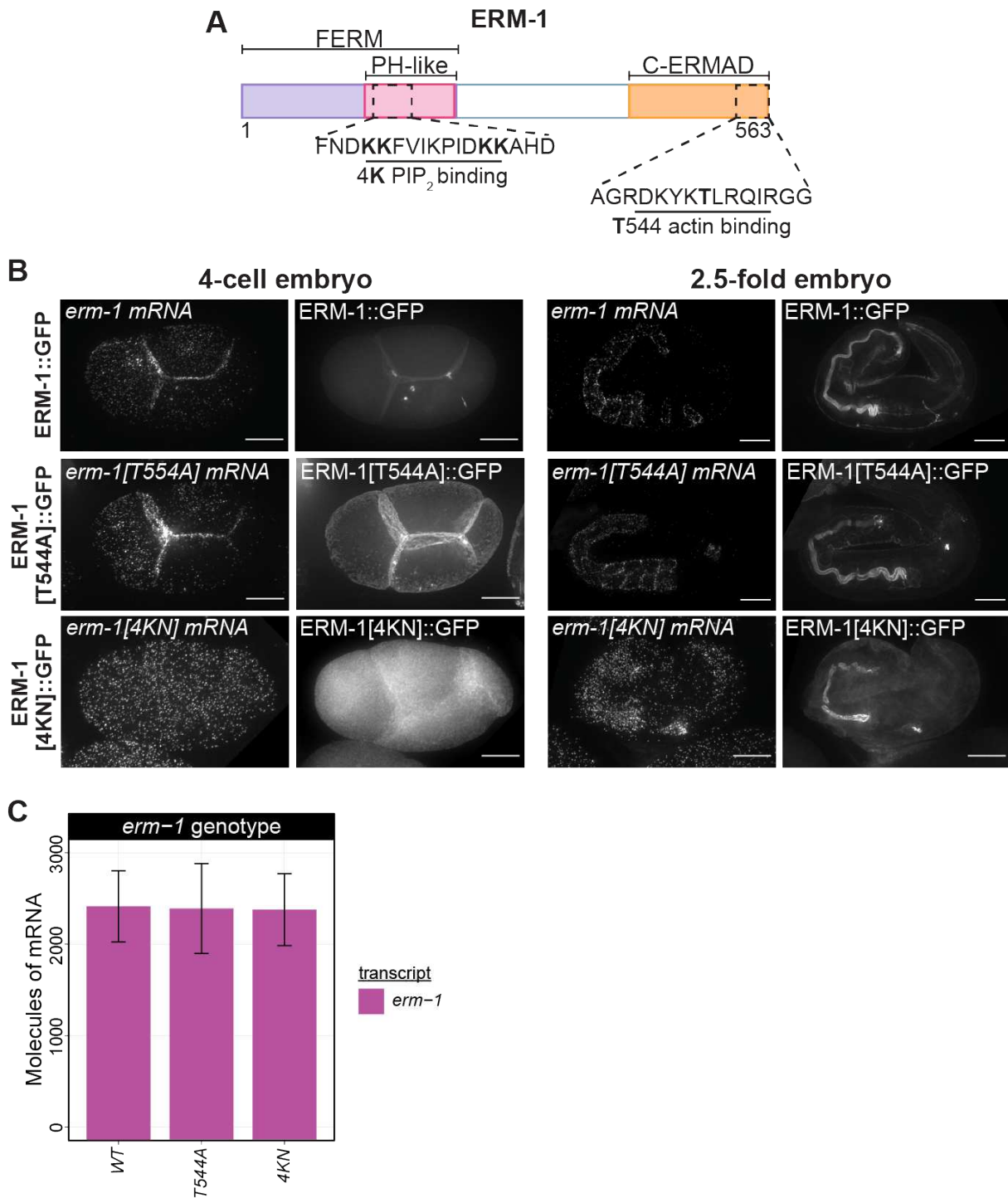


Figure 2.6: PIP₂ binding is required for *erm-1* mRNA and ERM-1 protein localization in early and late embryos. (A) Schematic model of the ERM-1 protein showing the N-terminal FERM domain (purple) containing the conserved PIP₂ – membrane binding region (PH-like, pink) and C-terminal conserved C-ERMAD actin-binding domain (orange). (B) smFISH micrographs of 4-cell and 2.5-fold embryos displaying *erm-1* mRNA and ERM-1 protein localization in *erm-1::gfp*, *erm-1*[T544A]::gfp, and *erm-1*[4KN]::GFP backgrounds. Scale bars 10 μ m. (C) *erm-1* mRNA abundance does not significantly differ between *erm-1::gfp*, *erm-1*[T544A]::gfp, and *erm-1*[4KN]::GFP expressing strains. *P*-values derived from Welch Two Sample *t*-tests comparing the number of *erm-1* mRNA molecules detected in the *erm-1::gfp*, *erm-1*[T544A]::gfp, and *erm-1*[4KN]::GFP expressing strains. *P* value legend: NS>0.05.

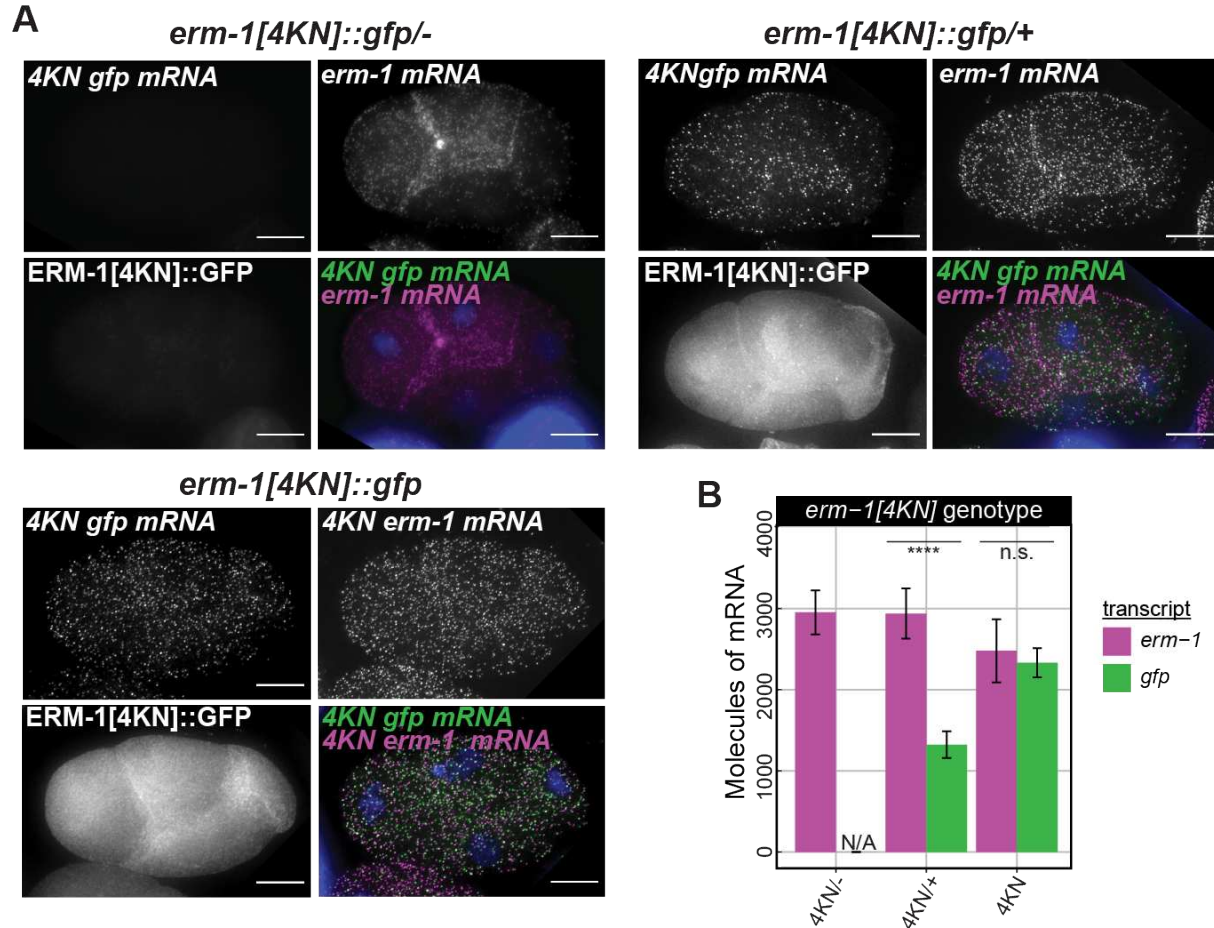


Figure 2.7: ERM-1[4KN]::GFP RNA abundance corresponds to genomic copy-number. (A) 4-cell embryos of the ERM-1[4KN]::GFP mutant probing for *erm-1* mRNA (magenta) and *4KN gfp* (green) are shown. Scale bars 10 μ m. (B) Total number of *erm-1* and *gfp* mRNA molecules in *erm-1[4KN]::gfp/-* (4KN⁻, $n = 9$), *erm-1[4KN]::gfp/+* (4KN^{-/+}, $n = 9$), *erm-1[4KN]::gfp* (4KN, $n = 9$). Scale bars 10 μ m. P -values derived from Welch Two Sample t -tests comparing the number of *gfp* and *erm-1* mRNA molecules detected in the *erm-1[4KN]::GFP* null, heterozygous, and homozygous 4-cell embryos. P value legend: NS>0.05; 0.05>*>0.005; 0.005>***>0.0005; 0.0005>****>0.00005; 0.00005>****

Notably, all transcripts previously reported as posterior-cell enriched [126,130] exhibited clustered patterning in early embryos (Table 2.1; Figure 2.9C). This is consistent with prior visualizations of posterior-enriched transcripts at the 4-cell stage that often concentrate within P granules [48]. Of the transcripts that were uniformly distributed between the anterior and posterior cells (as assayed by RNA-seq), those with posterior-enrichment below the significance cut-off (*Y43E3.7*, *mrck-1*, *wsp-1*) also displayed clustered patterning (Table 2.1; Figure 2.9C).

Overall, these results support previous findings in the early embryo that AB-cell enriched transcripts tend to localize to membranes, whereas P₁-enriched transcripts tend to localize to P granules, membraneless organelles housing lowly translated mRNAs [47,48,127]. To determine whether clustered transcripts were indeed localizing to P granules or membranes, smFISH was conducted in a P granule or membrane marker strain, respectively. Indeed, even in the case of the homologs *ani-1* and *ani-2*, the anterior-enriched *ani-1* mRNA was membrane localized, whereas the posterior-enriched *ani-2* mRNA localized to P granules (**Figure 2.8A**). Importantly, ANI-1 protein is translated in early embryos and concentrates at the plasma membrane while early embryo expression of ANI-2 protein is not detected [163]. Together, these results suggest that translational dependence of plasma membrane mRNA localization is not limited to *erm-1*.

Our visual screen found that subcellular localization patterns of some transcripts changed over developmental time. At the 4-cell stage, *unc-112* mRNA clustered in the P-lineage in P granules (**Figure 2.8A**). However, later in embryonic development, at the 3-fold stage, *unc-112* mRNA localized along the body wall where the encoded UNC-112 protein reportedly functions (**Figure 2.10A**) [164]. At the 4-cell stage, *F07C6.4* mRNA had uniform distribution (**Figure 2.8A**), but at the 100-cell stage it localized to the plasma membranes of a subset of discrete cells (**Figure 2.10B**). Similarly, at the 4-cell stage *let-502* had uniform localization (**Figure 2.9B**), but at the 1.5-fold stage it was localized to adherens junctions where the encoded LET-502 protein localizes and functions (**Figure 2.10C**) [165]. While the *ani-2* transcript clustered in P granules at the 4-cell stage (**Figure 2.8A**), at the bean stage *ani-2* was excluded from P granules and found at the interface of the primordial germ cells where ANI-2 functions in maintaining the structure of the syncytial compartment of germline cytoplasm at the membrane [163] (**Figure**

2.10D). Overall, 9 of the surveyed transcripts without observable membrane localization at the 4-cell stage (*F07C6.4*, *frm-2*, *nfm-1*, *ptp-1*, *unc-112*, *efa-6*, *mtm-1*, *let-502*, *ani-2*, and *dyn-1*)

Table 2.1: FERM and PH domain-containing, maternally inherited transcripts screened for subcellular localization patterns. Seventeen transcripts containing either FERM domain or PH-like domains were selected from known maternally inherited mRNAs (Osborne Nishimura et al., 2015, Tintori et al., 2016). Cell enrichment at the 4-cell stage from scRNA-seq data is shown. Transcript localization is briefly described.

Protein Domain	Enrichment at 4-cell	Transcript	Localization at 4-cell	Notes	
FERM	anterior	<i>F07C6.4</i>	uniform	apparent membrane localization at the 100 cell stage	
		<i>frm-2</i>	N/A (low RNA count)	pharyngeal localization 2.5-fold stage	
		<i>frm-7</i>	cell membrane		
		<i>nfm-1</i>	N/A (low RNA count)	apparent membrane localization at the 100 cell stage	
	uniform	<i>frm-4</i>	cell membrane		
		<i>ptp-1</i>	N/A (low RNA count)	apparent membrane localization at the bean stage	
		<i>Y41E3.7</i>	clustered		
	posterior	<i>unc-112</i>	clustered	Body wall enrichment around 3-fold stage	
	PH-like	anterior	<i>ani-1</i>	cell membrane	
			<i>efa-6</i>	pericentriolar	midline enrichment at the 3-fold stage
<i>mtm-1</i>			uniform	apparent membrane localization in PGCs at 3-fold stage	
uniform		<i>let-502</i>	uniform	membrane localization at junction points at 2-fold stage	
		<i>mrck-1</i>	clustered		
		<i>wsp-1</i>	clustered		
posterior		<i>ani-2</i>	clustered	remains P granule enriched through the 32-cell stage. At bean stage is excluded from P granules and remains at the Z2/Z3 interface	
		<i>dyn-1</i>	clustered	apparent membrane localization in PGCs at 3-fold stage	
		<i>exoc-8</i>	clustered		

displayed membrane localization at later stages of development, frequently coinciding with where their encoded proteins function [163,164,166–170]. These findings suggest subcellular patterning is developmentally dynamic.

By conducting a visual screen on a subset of FERM and PH-like domain containing transcripts, we identified additional transcripts that enrich at membranes, adding to the small but growing list of transcripts with this behavior in *C. elegans* [48,117]. 12 out of the 17 (70%) FERM and PH-like domain containing transcripts we surveyed exhibited membrane localization at some stage during development. These findings illustrate that translated mRNAs encoding PIP₂-binding domains often localize to plasma membranes and suggests that they may locally translated at the sites where their proteins are required. Furthermore, results from this screen reinforce the trend that transcripts concentrated within the P lineage in the early embryo are lowly translated and display clustered patterning, likely within P granules.

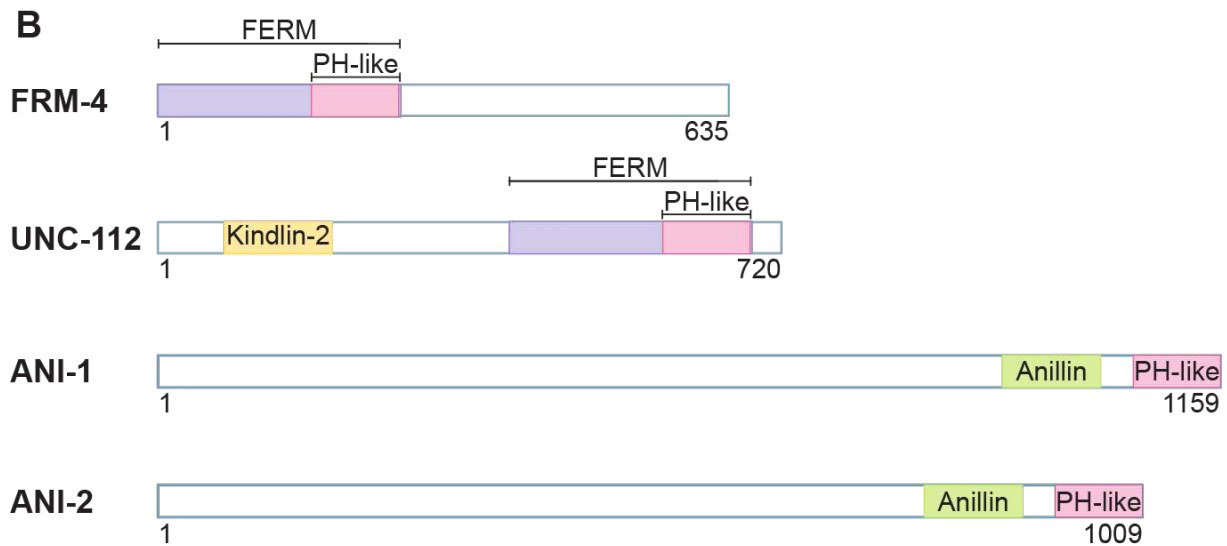
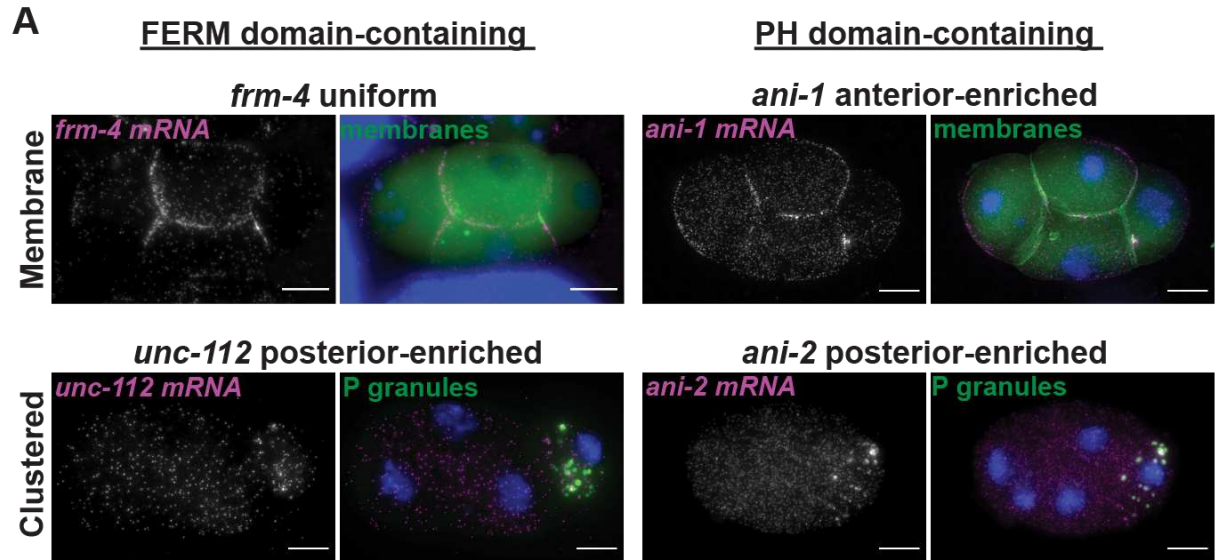


Figure 2.8: FERM and PH domain-containing, maternally-inherited transcripts display mRNA patterning. (A) smFISH micrographs of 4-cell embryos imaging two FERM domain containing transcripts, *frm-4*, *unc-112*, (magenta, left) and two PH-domain containing transcripts *ani-1*, *ani-2* (magenta, right). *frm-4* mRNA and *ani-1* mRNA (top) were imaged in a PH::GFP membrane marker transgenic background (membranes, green). *unc-112* mRNA and *ani-2* mRNA (bottom) were imaged in the GLH-1::GFP P granule marker strain (P granules, green). DNA (DAPI, blue). Scale bars 10 μ m.

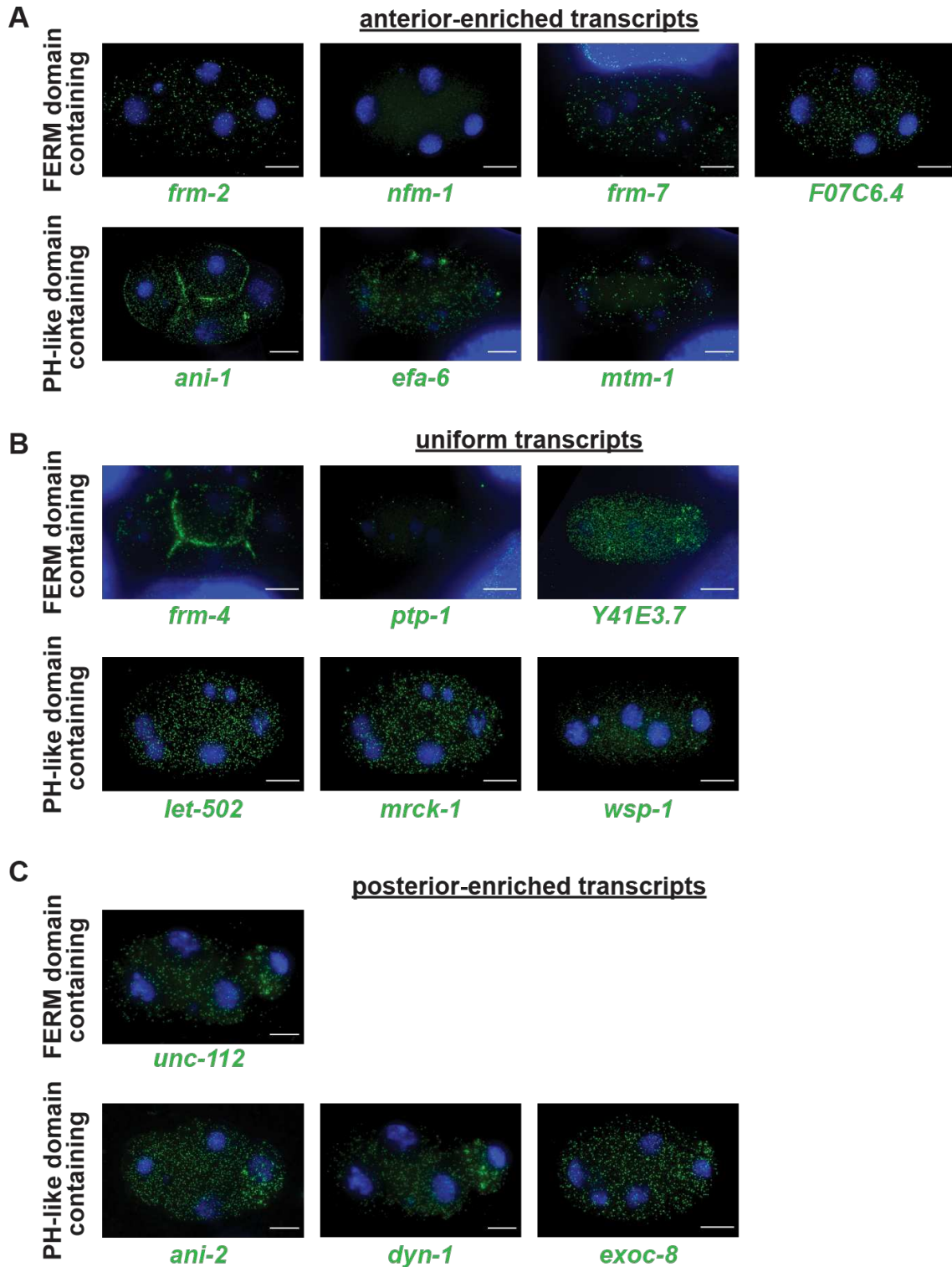


Figure 2.9: Subcellular localization patterns of surveyed FERM and PH domain-containing transcripts. (A) Seven anterior-enriched transcripts *F07C6.4*, *frm-2*, *frm-7*, *nfm-1*, *ani-1*, *efa-6*, and *mtm-1*, (B) six uniformly distributed transcripts *frm-1*, *ptp-2*, *Y41E3.7*, *let-502*, *mrck-1*, and *wsp-1*, and (C) four poster-enriched transcripts *unc-112*, *ani-2*, *dyn-1*, and *exoc-8* are shown.

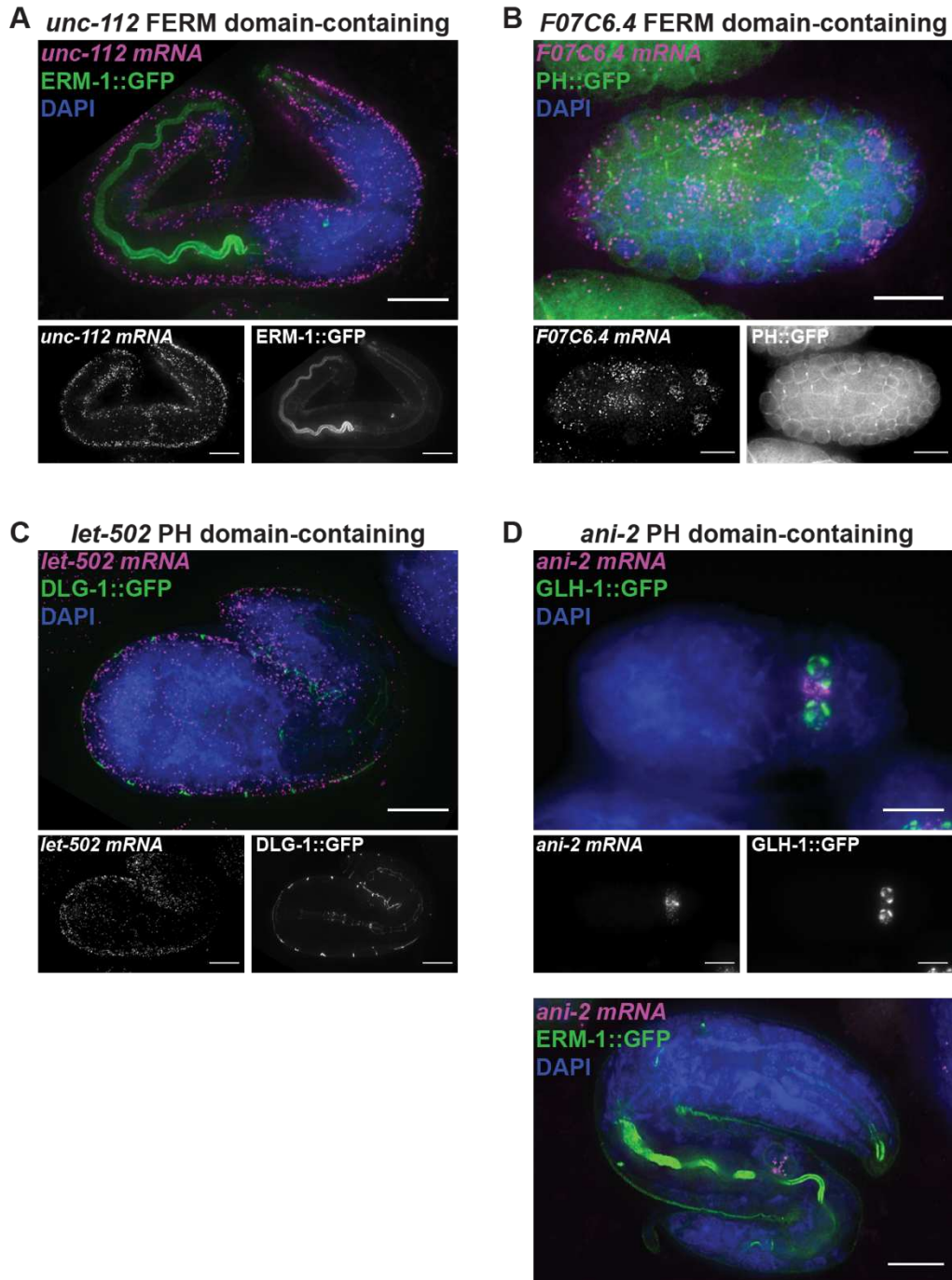


Figure 2.10: Subcellular localization patterns of surveyed FERM and PH domain-containing transcripts at mixed later stages. (A) smFISH micrograph of 3-fold *C. elegans* embryo imaging the posterior-enriched, FERM domain encoding transcript *unc-112* (magenta) in ERM-1::GFP background (green) with DNA (DAPI, blue). (B) smFISH micrograph of 100-cell *C. elegans* embryo imaging the anterior-enriched, FERM domain encoding transcript *F07C6.4* (magenta) in PH::GFP membrane marker background (green) with DNA (DAPI, blue). (C) smFISH micrograph of 1.5-fold *C. elegans* embryo imaging the uniformly-distributed, PH-like domain encoding transcript *let-502* (magenta) in DLG-1::GFP background (green) with DNA (DAPI, blue). (D) smFISH micrograph of a bean (top) and 3-fold (bottom) *C. elegans* embryo imaging the posterior-enriched, PH-like domain encoding transcript *ani-2* (magenta) in GLH-1::GFP P granule marker background (green, top) and ERM-1::GFP background (green, bottom) with DNA (DAPI, blue).

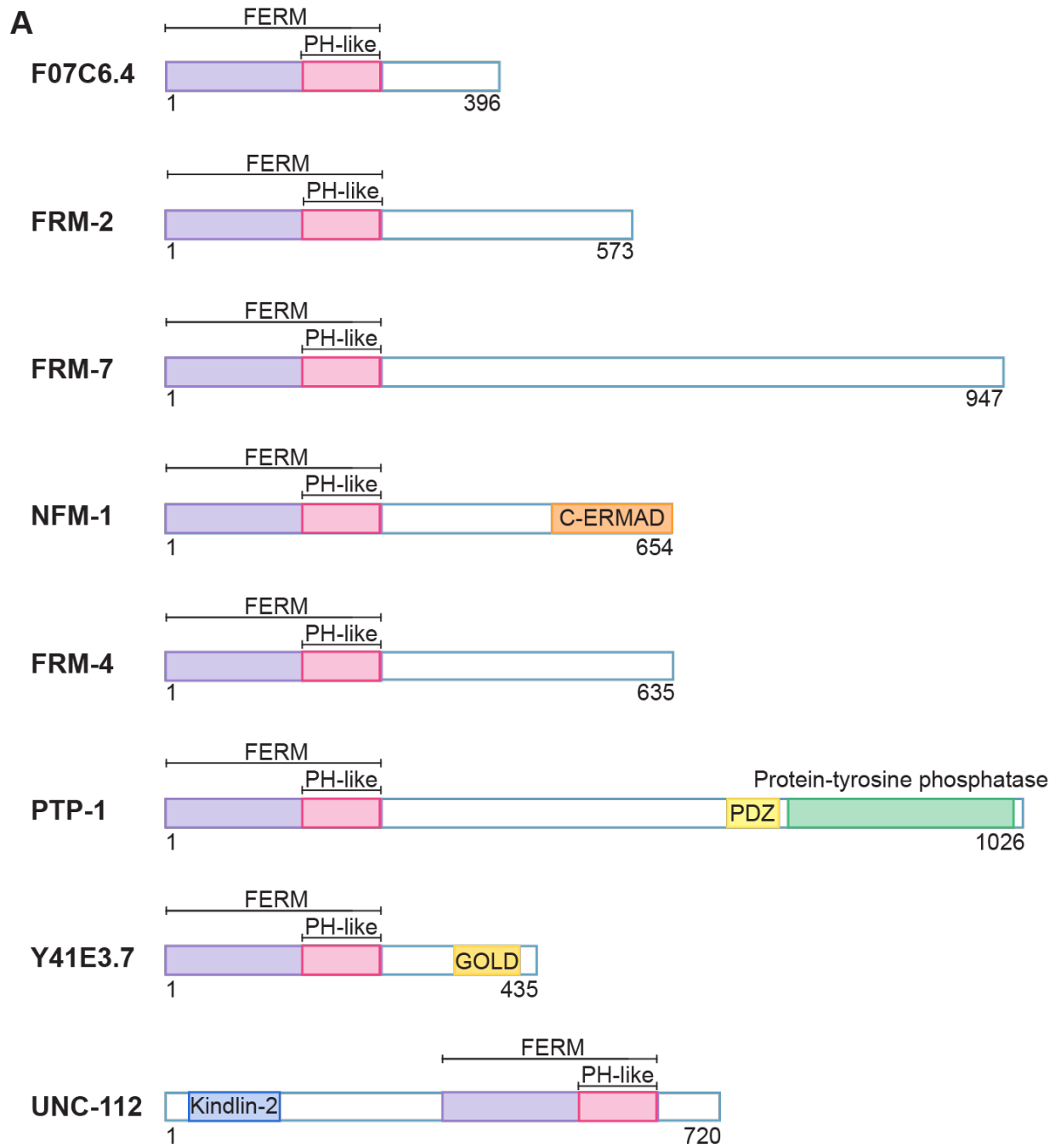


Figure 2.11: Depictions of the encoded protein domains for the surveyed FERM domain-containing transcripts.

A

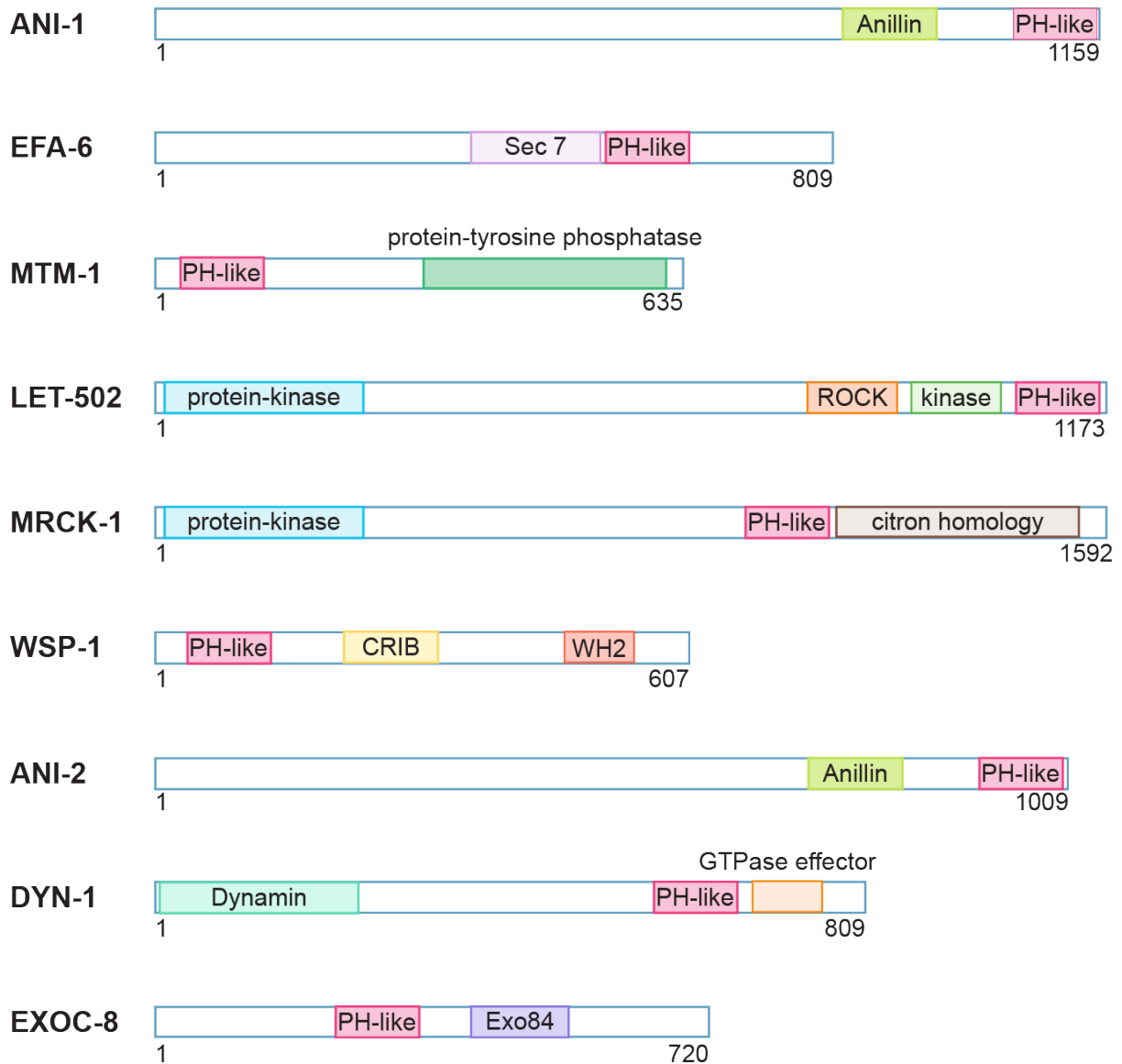


Figure 2.12: Depictions of the encoded protein domains for the surveyed PH/PH-like domain-containing transcripts.

2.3 Discussion

Here, we report that *C. elegans erm-1* mRNA is localized to the plasma membrane in a translation-dependent manner during early embryonic development (**Figure 2.13**). We showed that in the absence of active translation, an intact ribosome-nascent chain complex (RNC) was

required to maintain *erm-1* mRNA localization. We also demonstrated that 36% of the *erm-1* mRNA sequence could be altered but the transcript would still localize properly provided the ERM-1 protein sequence was preserved. This finding further suggests that the localization determinant is specified in the nascent chain of the ERM-1 protein, not as a *cis*-acting element in the mRNA sequence or structure. Furthermore, we narrowed down a domain required for localization and determined it resided within the FERM domain and depended on that domain's ability to bind PIP₂. We identified 3 additional FERM or PH-like domain encoding genes (*frm-7*, *frm-4*, and *ani-1*) with mRNA localization at the plasma membrane in the early embryo by a smiFISH visual screen and an additional 9 genes with mRNA localization later in development. Our data indicate subcellular localization is a generalizable feature of transcripts encoding FERM or PH-like domains.

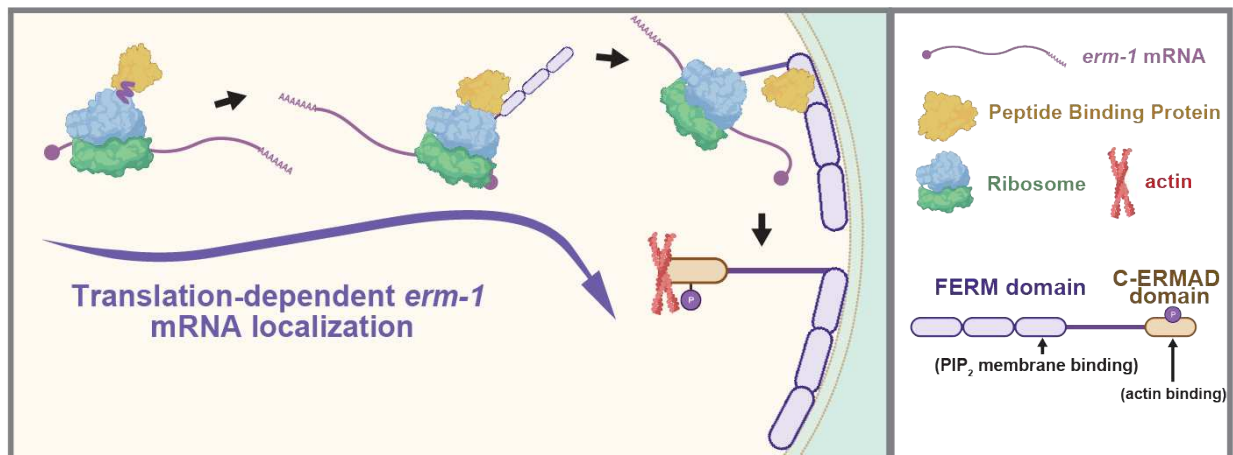


Figure 2.13: Model of translation-dependent *erm-1* mRNA localization in the early *C. elegans* embryo. *erm-1* mRNA is localized in a translation-dependent manner requiring the intact RNC and PIP₂-binding region of the FERM domain.

Complementarily to our findings in the early embryos, recent studies of later developmental stages identified 8 transcripts (*dlg-1*, *ajm-1*, *sma-1*, *vab-10a*, *erm-1*, *pgp-1*, *magu-2*, and *let-413*), including *erm-1*, that enrich to regions of the plasma membrane adjacent to apical junctions [117,171]. In particular, *dlg-1* mRNA localizes through a translation-dependent

pathway [117]. *dlg-1* localization requires the translation of N-terminal L27-PDZ domains, C-terminal SH3, Hook, and Guk domains to fully recapitulate the localization patterns of the *dlg-1* mRNA. These data, in combination with our findings, suggest translation-dependent localization could be a prevalent feature of mRNA that generally encode apical junction components or membrane associated proteins.

An outstanding question is whether *erm-1* mRNA localization is critical for ERM-1 function. The ERM-1[4KN] mutation yields *erm-1* mRNA and ERM-1 protein that are mis-localized and results in lethality. However, the localization of the mRNA and protein are confounded, and it is difficult to test whether the proper localization of *erm-1* mRNA is required. Do ERM-1 proteins need to be locally translated at the plasma membrane for proper function? Because ERM proteins link the plasma membrane and actin cytoskeleton, ERM proteins often function in cell movement, membrane trafficking, cell signaling, and cell adhesion. They contribute to cancer-associated processes such as cell metastasis and chemotherapy resistance [134,135,172,173]. Local translation of ERM-1 could be important for producing ERM-1 linker proteins at the exact sites and at the exact concentrations in which they are needed. This process could be responsive to signaling, polarity, or stability cues. Indeed, during embryonic development, the landscape of the plasma membrane is constantly changing and coordination between cell membrane and actin cytoskeletal structures are of paramount importance to cell morphology and cell migration processes. Therefore, local translation of ERM-1 could be sensitive to incoming signals or developmental needs.

As an example of this concept, the protein PCNT (Pericentrin) in human cells and zebrafish embryos is shown to cotranslationally localize to dividing centrosomes during early mitosis [65]. This is hypothesized to supply sufficient PCNT protein where it is expeditiously

needed for cell division and to mitigate the kinetic challenge of trafficking a large protein. Alternatively, some proteins are locally translated to promote proper folding, facilitate interactions with effector proteins, or to promote their ultimate integration into membranes or vesicles [174]. We postulate another idea, that local translation may temporarily stabilize ERM associations at membranes until phosphorylation in the C-terminal domain can facilitate actin binding. By this logic, ERM proteins could be translated in an “ON” state, ready to perform their function.

What pathways localize translationally competent *erm-1* transcripts to the plasma membrane in the early embryo? The pathway that directs (transmembrane protein and secretory protein encoding) mRNAs to the ER is the most well-characterized translation-dependent mRNA trafficking pathway and requires the presence of a signal peptide. As ERM-1 lacks a discernable ER-directing signal peptide and fails to pull down ER associated-components in IP assays, we surmise the pathway that directs translating *erm-1* to the plasma membrane is likely distinct from the ER secretory pathway [103,175,176]. Alternatively, if *erm-1* is localized in an ER-dependent pathway it would likely be noncanonical.

Future studies will determine the machinery required to traffic *erm-1*, and transcripts like it. A recent study live-imaging *erm-1* mRNA movements reported reduced *erm-1* enrichment at the membrane upon knocking down a dynein motor (DHC-1), suggesting *erm-1* localization could require this component of cytoskeletal trafficking [171]. It will also be interesting to determine whether *erm-1* translation is paused or active during the trafficking process and whether multiple rounds of translation occur at the membrane.

Our screen of FERM and PH-like domain containing genes yielded multiple transcripts with mRNA localization at the plasma membrane suggesting this property is conserved across

species. The *ani-1* and *ani-2* ortholog in *Drosophila*, *anillin*, concentrates at the pseudo-cleavage furrow of *Drosophila* embryos dependent on translation of both its PH and actin binding domains [116]. Indeed, the expanded use of mRNA imaging and sub-cellularly enriched RNA-seq technologies has led to a greater appreciation that localization of mRNA is a widespread feature of cell biology, not only to the plasma membrane but to a wide diversity of membranes and other subcellular structures [20,120]. These findings suggest that many proteins may benefit from local translation at their destination site.

2.4 Materials and Methods

2.4.1 Worm husbandry

C. elegans strains were cultured according to standard methods [177]. Worm strains were maintained and grown at 20°C on nematode growth medium (NGM: 3 g/L NaCl; 17 g/L agar; 2.5 g/L peptone; 5 mg/L cholesterol; 1mM MgSO₄; 2.7 g/L KH₂PO₄; 0.89 g/L K₂HPO₄). Strains used in this study are listed in (Table 2.2).

2.4.2 Heat Shock Experiments

Heat shock experiments were performed by transferring harvested embryos to pre-warmed M9 liquid media and incubating at 30°C for 25 minutes. After heat shock, worms were immediately fixed for smFISH.

Table 2.2: Worm strains used in study

Strain	Description	Genotype	Source/Reference
N2	N2	<i>C. elegans</i> wildtype	CGC
LP306	GFP::PH	cpIs53 [mex-5p::GFP-C1::PLC(delta)-PH::tbb-2 3'UTR + unc-119 (+)] II	Heppert JK, et al. Mol Biol Cell. 2016
Box213	erm-1::GFP	erm-1 [Perm-1::erm-1::GFP::erm-1 3'UTR] I	Ramalho et al., Development. 2020
WRM24	MODC PEST::GFP::H2B	sprSi17 [mex-5p::MODC PEST::GFP::H2B::mex-3 3'UTR + Cbr-unc-119(+)] II	CGC/Kaymak et al., Dev Dyn. 2016
wLPW007	erm-1::GFP	COP2295 - knuSi874 [pNU2555(erm-1p::erm-1::GFP::erm-1u in cxTi10882, unc-119(+))] IV ; unc-119(ed3) III	This study, made in collaboration with InVivo Biosystems
wLPW008	erm-1 synonymous::GFP	COP2296 - knuSi874 [pNU2556(LWIN04 - erm-1p::erm-1scmbl::GFP::erm-1u in cxTi10882, unc-119(+))] IV ; unc-119(ed3) III	This study, made in collaboration with InVivo Biosystems
Box233	erm-1[4KN]::GFP	erm-1(mib21[erm-1[4KN]::GFP]) I / dpy-5(e61); unc-29(e403) I	Ramalho et al., Development. 2020
Box218	erm-1[T544A]::GFP	erm-1(mib16[erm-1[T544D]::GFP]) I	Ramalho et al., Development. 2020
DUP64	GLH-1::GFP	glh-1(sam24[glh-1::gfp::3xFlag]) I	Andraloje et al., 2017

2.4.3 RNAi Feeding for smFISH Microscopy

RNAi feeding constructs were obtained from the Ahringer library [178]. Bacteria containing inducible dsRNA vectors were grown at 37°C in LB + ampicillin (100 µg/mL) media for 16 hr, spun down and resuspended at 10X original concentration with M9, plated on NGM + Carbenicillin (100 µg/mL) + IPTG (1 mM) plates, and grown at room temperature overnight, or until plates were dry. Embryos were harvested for synchronization from mixed staged worms. Harvested embryos were incubated in M9 for 24 hrs at RT while nutating until all arrived at L1 developmental stage. L1 worms were deposited on RNAi feeding plates and grown at 20°C for 48 hrs. Embryos were harvested from gravid adults and smFISH was conducted. For each gene targeted by RNAi, we performed at least three independent replicates. L4440 RNAi empty vector was used as a negative control and *pop-1* RNAi used as an embryonic lethal positive control. For experiments performing *ifg-1* RNAi, synchronized L1 worms were grown to L2 on

OP50 plates before being washed in M9 and transferred to RNAi plates for 48 hrs. *E. coli* strains used in this study can be found in (Table 2.3).

Table 2.3: *E. coli* strains used in study.

Strain description	Plasmid description	Detailed description	Reference
OP50	OP50	OP50	
L4440	pPD129.36	empty worm RNAi plasmid	Fire Lab C. Elegans Vector Kit 1999
<i>ifg-1</i> RNAi	M110.4 from the Ahringer library	worm RNAi plasmid + <i>ifg-1</i> gene fragment	Fraser et al, 2000, Nature

2.4.4 Permeabilization and drug delivery

For small molecule inhibitor experiments, *perm-1* RNAi was performed to permeabilize the eggshell as described in [152]. Briefly, synchronized L1 worms were fed on RNAi for 48 hrs and embryos were hand-dissected from the treated mothers. Permeabilization by *perm-1* RNAi was tested by submerging embryos in water to induce bursting from to increased internal osmotic pressure. Additionally, RNAi efficacy was confirmed by *pop-1* RNAi positive control. To harvest embryos, young adult worms were washed off plates in 5ml S-buffer (129 mL 0.05 M K₂HPO₄; 871 mL 0.05 M KH₂PO₄; 5.85 g NaCl' 300 +/- 5 mOsm) and allowed to settle to the bottom of a 15 ml conical (no longer than 5min). S buffer was removed, and worms were resuspended in 100 µl S-buffer alone (negative control) or drug diluted in 100 µl S-buffer (500 µg/mL Cycloheximide and 100µg/mL Puromycin final concentrations). The 100 µl drug solution and young adult worms were transferred to a concavity slide, hand dissected in a concavity slide, transferred to a 1.5 mL Eppendorf tube and incubated for 20 min. After incubation with drug solution, 1 mL of -20°C methanol was added to fix the embryos. Embryos were freeze-cracked in liquid nitrogen for 1 min then incubated overnight in methanol at -20°C to continue the

fixation. smFISH was performed as described. Due to the fragility of *perm-1* depleted embryos, all spins required in their smFISH preparation were performed at 250 rcf instead of 2000 rcf.

2.4.5 smFISH

single molecule Fluorescence *In Situ* Hybridization (smFISH) was performed based on the TurboFish protocol (Femino et al., 1998; Nishimura et al., 2015; Parker et al., 2021; Raj and Tyagi, 2010; Raj et al., 2008; Shaffer et al., 2013). Updates specific to *C. elegans* were made using new Biosearch reagents and outlined in [179]. Using the Stellaris RNA FISH Probe Designer, custom FISH probes were designed for transcripts of interest (Parker et al., 2020; Parker et al., 2021). Biosearch Technologies, Inc., Petaluma, CA) available online at www.biosearchtech.com/stellarisdesigner (version 4.2). Embryos were hybridized with Stellaris RNA FISH Probe sets labeled with CalFluor 610 or Quasar 670 (Biosearch Technologies, Inc.), following the manufacturer's instructions available online at www.biosearchtech.com/stellarisprotocols. Briefly, adult worms were bleached for embryos, suspended in 1 ml -20°C methanol, freeze cracked in liquid nitrogen for 1 min, and fixed overnight in methanol at -20°C for 1-24 hours. Alternatively, fixation was done at 4 min incubation following the 1 min freeze crack, switching to -20°C acetone incubation for an additional 5 min. ERM-1::GFP worms were freeze-cracked in 1 mL acetone followed by a 35 min incubation at -20°C. After fixation, embryos incubated in Stellaris Wash Buffer A for 5min at RT (Biosearch, SMF-WA1-60) before hybridization in 100 µl Stellaris Hybridization buffer [(Biosearch, SMF-HB1-10) containing 50 pmols of each primer set (up to two channels per experiment) and 10% formamide] 16-48 hrs at 37°C mixing at 400 rpm in a thermomixer (Eppendorf ThermoMixer F1.5). Embryos were washed for 30 min in Stellaris Wash Buffer A, followed by a second wash of Stellaris Wash Buffer A containing 5 µg/ml of DAPI, then 5 min

in Wash Buffer B followed by a second 5 min wash (Biosearch, SMF-WB1-20) before incubation in N-propyl gallate antifade (10 mL 100% glycerol, 100 mg N-propyl gallate, 400 μ L 1M Tris pH 8.0, 9.6 mL DEPC treated H₂O) prior to slide preparation. All embryos were centrifuged in spin steps at 2,000 rcf unless otherwise noted. Embryos were mounted using equal volumes hybridized embryos resuspended in N-propyl gallate antifade and Vectashield antifade (Vector Laboratories, H-1000). smFISH image stacks were acquired as described in Parker et al., 2020. on a Photometrics Cool Snap HQ2 camera using a DeltaVision Elite inverted microscope (GE Healthcare), with an Olympus PLAN APO 60X (1.42 NA, PLAPON60XOSC2) objective, an Insight SSI 7-Color Solid State Light Engine, and SoftWorx software (Applied Precision) using 0.2 μ m z-stacks. Deltavision (SoftWorx) deconvolution software was applied for representative images. Images were further processed using FIJI [180]. For each condition described a minimum of 5 embryos per 4-cell stage, but often many more across multiple cell stages, were imaged. All smFISH and smiFISH probes can be found in (**Table A.1**). All raw microscopy images are deposited on Mountain Scholar, a digital, open access data repository associated with Colorado State University Libraries:

2.4.6 smiFISH

single molecule inexpensive Fluorescence *In Situ* Hybridization (smFISH) was performed as described in [48]. Briefly, custom primary DNA oligos were designed as described [181] complementary to the 17 FERM and PH-like domain containing transcripts screened and ordered from IDT (<https://www.idtdna.com/pages/products/custom-dna-rna/dna-oligos>) (**Table A.1**). Secondary FLAPX probes were ordered with dual 5' and 3' fluorophore labeling, Cal Fluor 610 or Quasar 670, from Stellaris LGC (Biosearch Technologies, BNS-5082 and FC-1065,

respectively). Secondary, fluorophore labeled probes were annealed to primary probes fresh for every experiment in a thermocycler at 85°C for 3 min, 65°C for 3 min, and 25°C for 5 min.

2.4.7 Quantification of plasma membrane RNA localization

Quantification of transcript localization with reference to the cell membrane was performed as previously described [48] using the web application ImJoy [182]. Briefly, RNAs were first detected from raw images using the Matlab code FISH-quant [183]. Individual cell outlines were then manually annotated in FIJI for each Z-stack in the micrograph, excluding the uppermost and lowermost stacks where cells are flattened against the slide or coverslip or there is out-of-focus light. The distance of each RNA was then measured from the nearest annotated membrane and binned in 10% distance increments away from nearest membrane to account for change in size between embryos. Total number of RNAs per bin were then normalized by the volume of the concentric areas they occupied. After this normalization, values larger than 1 indicate that for this distance more RNAs are found compared to a randomly distributed sample.

2.4.8 Quantification of total mRNA

Detection of RNA molecules was performed in the 3D image stacks with FISH-quant [183]. Post-processing to calculate the different location metrics was performed as described above with custom written Matlab and Python code. The Python code is implemented in user-friendly plugins for the image processing platform ImJoy [182]. Source code and all scripts used for analysis and figure generation are available here <https://github.com/muellerflorian/parker-rna-loc-elegans>

To quantify the number of individual mRNAs in the ERM-1[4KN] strain a custom MATLAB script was implemented. FISH-quant detection settings were used to identify

candidate mRNA clusters from smFISH micrographs using a Gaussian Mixture Model (GMM). The GMM differentiates independent, single mRNAs from groups of clustered mRNAs by probabilistically fitting a predicted RNA of average intensity and size over each FISH-quant detected RNA.

2.4.9 Domain search

A smiFISH-based screen was utilized to identify if transcripts with protein domains similar to *erm-1* also displayed membrane localization. WormBase ParaSite was utilized to generate a list of proteins with domain IDs matching those annotated for ERM-1. Proteins with domain IDs matching ERM-1 were subset for genes present in 2-cell stage embryos [126]. This resulted in a list of 149 maternally inherited genes encoding either a FERM or PH-like domain. (**Table B.1**).

Candidate genes were further subset using the “Interactive visualizer of differential gene expression in the early *C. elegans* embryo” (<http://tintori.bio.unc.edu/>, [130]). Candidate genes were manually curated based on the following criteria: 1) persistence of enrichment in the 4-cell stage embryo, 2) high transcript abundance in the 4-cell stage embryo, 3) homology to genes encoding transcripts with known localization in other biological systems, and 4) existing protein expression data available on Wormbase (<https://wormbase.org/>) (**Table B.1**). Manual curation resulted in 17 candidate genes that are simultaneously maternally inherited and contain FERM or PH-like domains to screen for membrane localization (**Table 2.1**).

2.5 Acknowledgements

We are grateful to Michael Boxem, Susan Mango, Cristina Tocchini, Brooke Montgomery, Tai Montgomery, Jessical Hill, and WormBase for reagents, protocols, equipment, advice,

productive discussion, and critical feedback on the manuscript. This work utilized resources from the University of Colorado Boulder Research Computing Group, which is supported by the National Science Foundation (awards ACI-1532235 and ACI-1532236), the University of Colorado Boulder, and Colorado State University. This work utilized microscopy resources from NIH grant 1S10 OD025127 and support from the CSU Microscope Imaging Network. Some strains were provided by the Caenorhabditis Genetics Center, which is funded by National Institutes of Health Office of Research Infrastructure Programs (P40 OD010440). Some figure elements were created in BioRender.

2.6 Competing Interests

The authors have no competing interests

2.7 Funding

Funder	Grant reference number	Author
National Institutes of Health	R35GM124877	Erin Osborne Nishimura
NSF MCB CAREER	2143849	Erin Osborne Nishimura
NSF GAUSSI training grant	DGE-1450032	Lindsay Winkenbach
NSF GAUSSI training grant	DGE-1450032	Dylan Parker
Bridge to Doctorate at Colorado State University	1612513	Robert Williams

Chapter 3

Translation-dependent localization of *imb-2* mRNA to the nuclear periphery²

3.1 Introduction

In eukaryotic cells, transporting macromolecules between the nucleus and cytoplasm is critical for replication, transcription, cell cycle regulation, and gene expression regulation broadly [184]. Transport between the nucleus and cytoplasm, nucleocytoplasmic transport, is orchestrated by carrier protein complexes which recognize specific localization signals on cargo and facilitate interactions with nuclear pore complexes (NPCs) [185]. Active nucleocytoplasmic transport is primarily carried out by β -karyopherins, which are functionally divided into Importins and Exportins. Importins and their associated cargo enter the nucleus through an NPC, where the binding of Ran-GTP with Importin releases cargo into the nucleus. Upon export back into the cytoplasm, Ran-GTP is hydrolyzed to Ran-GDP, releasing Ran-GDP from the Importin [184]. In mammals, the best-characterized Importins are Importin- α , Importin- β , and Transportin 1. Transportin 2 is less well characterized but shown to have redundant cargo with Transportin 1 and other importins [186]. The Transportin subfamily appears to derive from a single ancestral gene. A single gene still comprises the Transportin subfamily in yeast (*kap104*) and *C. elegans*

² The work described in chapter 3 is ongoing and unpublished

(*imb-2*) making *C. elegans* an excellent model for further exploring fundamental characteristics of the Transportin subfamily [187].

In *C. elegans*, *imb-2* is predicted to be a homolog of human TNPO2 (Transportin 2) and function in protein import into the nucleus through direct binding of nuclear localization sequences on associated cargo [138]. IMB-2 is also a highly conserved homolog of human TNPO1 (Transportin 1) [188]. Deletion or depletion of the *imb-2* gene is embryonic and larval lethal [189–192]. As part of its role in nuclear import, IMB-2 is functions in the conserved insulin signaling and reactive oxygen species (ROS) signaling pathways [188]. In the insulin signaling pathway, IMB-2 imports the *C. elegans* DAF-16 (homolog of human Forkhead Box O FOXO) into the nucleus in response to environmentally induced oxidative stress [188]. Additionally, *imb-2* functions in olfactory neuron development by importing the transcription factor NSY-7 to activate *sox-2* expression [192]. This study also detected IMB-2 protein in the nucleus and around the nuclear envelope of cells in the head and body during embryogenesis, larval development, and adulthood [192] (Alqadah et al., 2019). More recently, the maternally-inherited *imb-2* mRNA was detected with perinuclear localization in early embryos where the IMB-2 protein is predicted to localize **Figure 3.1**) [48] .

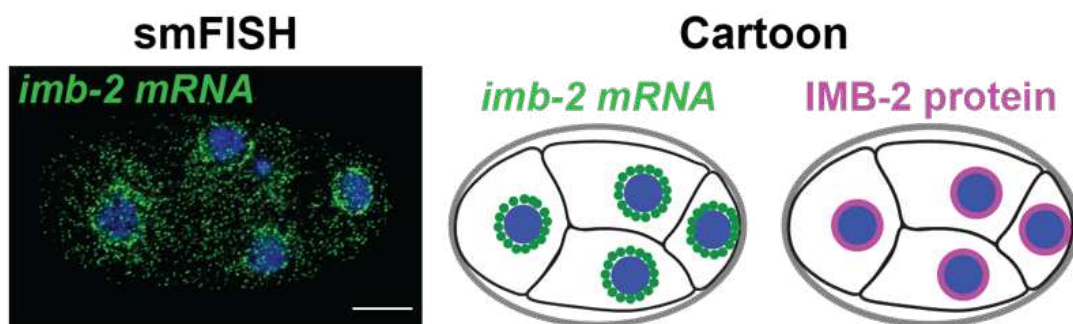


Figure 3.1: *imb-2* localizes to the nuclear periphery where the encoded IMB-2 protein is reported to function. *imb-2* mRNA was visualized using smFISH (green) in a 4-cell embryo (left). Schematic illustration of perinuclear localization of *imb-2* mRNA (green) and IMB-2 protein (magenta) (right). Scale bars 10 μ m.

Many studies have demonstrated that mRNA localization functions in cellular processes such as development, differentiation, and cell migration. The two primary mechanisms by which mRNAs localize subcellularly are translation-independent or translation-dependent pathways. The translation-independent pathway typically relies upon an RNA localization sequence element (zip code), often located in the 3'UTR, that is recognized and bound by an RNA binding protein (RBP). The translation-dependent pathway relies upon the translation of a localization signal peptide for delivery to its specific compartment. Translation-dependent localization of mRNAs encoding for secreted and membrane proteins on the endoplasmic reticulum (ER) are well described [102]. In this canonical model (**reviewed in Chapter 1.3.3.1**), a translated nuclear localization signal (NLS) is recognized and bound by the signal recognition peptide (SRP) and directed to the ER. Recent studies demonstrate that transcripts can associate with the ER through translation-dependent and translation-independent mechanisms [107,193,194].

Previous work in *C. elegans* demonstrated that the *imb-2* 3'UTR was insufficient to direct a neogreen-encoding reporter transcript to the nuclear periphery indicating that the *imb-2* localization element resides elsewhere in the RNA sequence or the encoded protein [48]. In that same sufficiency assay, fusion of the *imb-2* 3'UTR to neogreen reduced the abundance of the *imb-2* 3'UTR sufficiency transcript compared to control. This reduction suggests that the *imb-2* 3'UTR may promote transcript instability in the cytoplasm out of context with the whole *imb-2* gene [48]. Additionally, *imb-2* does not encode a nuclear localization signal, which suggests a translation-dependent localization mechanism would occur by a non-canonical pathway [48].

This chapter provides preliminary evidence that *imb-2* mRNA localization to the nuclear periphery is translation-dependent and is sensitive to stress. Additionally, treatment with small molecule inhibitors preliminarily indicates *imb-2* localization requires remaining intact with

translating ribosomes and the nascent polypeptide. Further, while translation inhibition experiments demonstrated dependence on translation for localization, preliminary experiments altering the mRNA sequence context resulted in silencing of the synonymous transcript. This could indicate that *imb-2* localization relies on both translation-dependent and translation-independent elements for the stability of the transcript and successful perinuclear enrichment.

3.2 Results

3.2.1 *imb-2* mRNA localization to the nuclear periphery requires translation initiation

Previous evidence from Parker et al. demonstrated that the *imb-2* 3'UTR was insufficient to direct localization to the nuclear periphery [48]. We therefore began testing the translation-dependent localization model. To test the translation-dependent model for *imb-2* perinuclear localization, we disrupted translation initiation globally by depleting the translation initiation factor *ifg-1* (*Initiation Factor 4G (eIF4G) family*) by RNA interference (RNAi). IFG-1 is the sole *C. elegans* ortholog of the human initiation factor eIF4G and functions in both cap-dependent and -independent translation initiation [137–140]. Depleting *ifg-1* by RNAi prevents translation initiation by blocking the recruitment of the 40S ribosomal subunit to the transcript (**Figure 3.2A**) [137]. Translation inhibition was confirmed using a destabilized GFP as a translation reporter (MODCPEST GFP::*H2B*) with a reduced fluorescence half-life of roughly 2 hrs from the typical half-life of roughly 26 hrs [143]. We confirmed translation inhibition in embryos by a reduction in the degradable GFP fused to *H2B* reporter signal (**Figure 3.2B**). Embryos with reduced *H2B* fluorescence also displayed a loss of perinuclear *imb-2* mRNA localization

compared to the control (**Figure 3.2C**). These results support the model in which *imb-2* mRNA localization to the nuclear periphery is translation-dependent. However, this assay does not indicate whether localization requires an intact ribosome nascent chain complex (RNC) or ongoing translation.

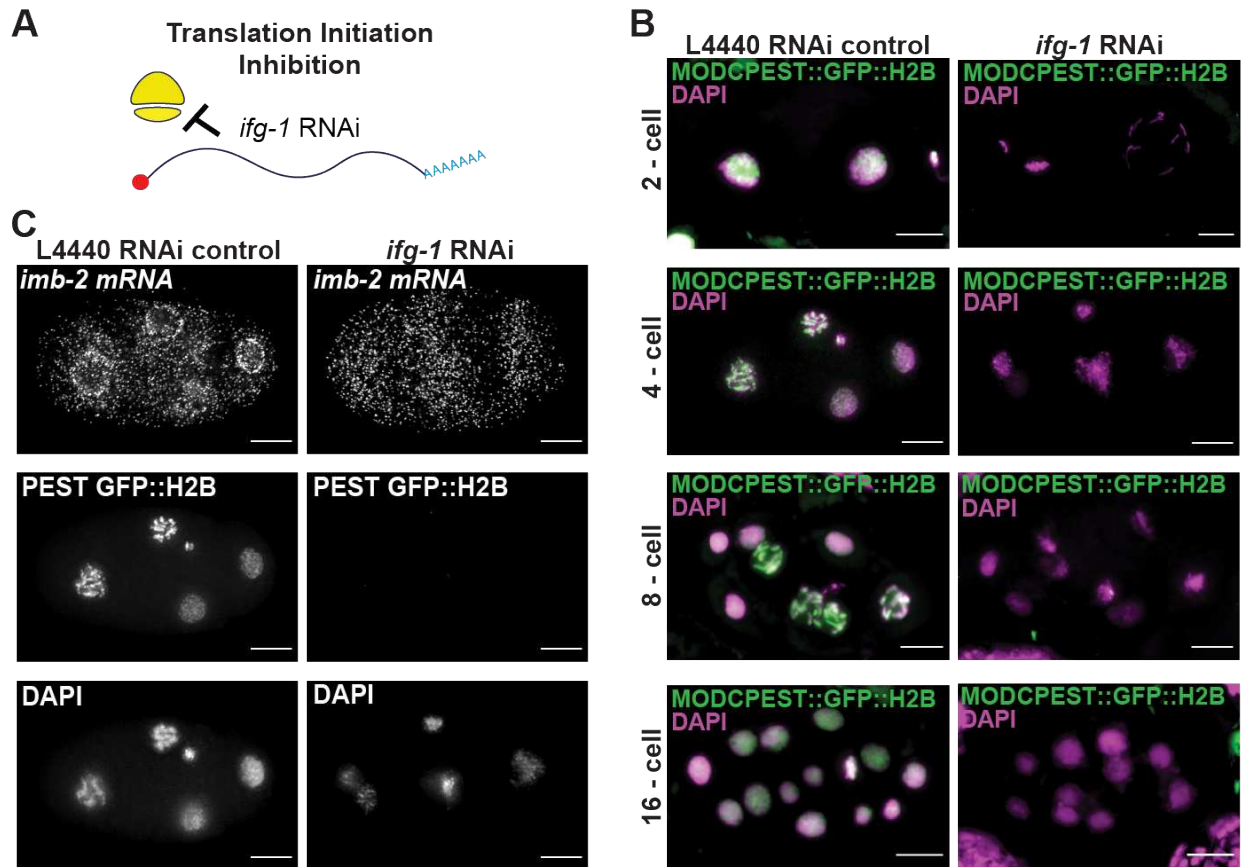


Figure 3.2: *imb-2* loses perinuclear localization when translation initiation is inhibited by *ifg-1* RNAi. (A) Schematic of translation initiation inhibition by *ifg-1* RNAi preventing ribosome binding to the transcript. (B) Translation inhibition by *ifg-1* RNAi confirmed in the translation reporter strain MODCPEST GFP::H2B (green) between 2-cell and 16-cell stage marked by DAPI stained nuclei (magenta). (C) Fluorescent micrographs of 4-cell embryos in control RNAi conditions (L4440, left) and treated with *ifg-1* RNA (right) probing *imb-2* mRNA with smFISH in the translation reporter strain MODCPEST GFP::H2B with nuclei stained with DAPI. Scale bars 10 μ m.

3.2.2 IMB-2 localization requires the intact ribosome-nascent chain complex

To test whether *imb-2* mRNA localization requires intact ribosome-nascent chain complexes (RNCs), we inhibited translation elongation using two different small molecule inhibitors. Cycloheximide stalls elongation and preserves RNCs, while puromycin induces dissociation of the ribosome and nascent chain from the transcript [148,149].

To overcome the challenge of introducing small molecules through the eggshell and permeability barrier in the *C. elegans* embryo, we disrupted the sugar modifying enzyme and permeability barrier protein PERM-1 by RNAi [150,152,195]. *perm-1* RNAi permits small molecule entry while not altering early developmental progression, though *perm-1* RNAi eventually leads to lethality in late embryos [152]. Additionally, through alterations to standard smFISH protocols, *perm-1* RNAi is compatible with drug treatment followed by smFISH imaging of *imb-2* mRNA.

We observed that treatment with cycloheximide, which preserves the RNC while stalling during translation elongation, did not disrupt observable *imb-2* mRNA localization (**Figure 3.3A**). In contrast, treatment with puromycin, which dissociates the ribosome and nascent chain, resulted in the loss of *imb-2* mRNA localization to the nuclear periphery (**Fig. 3.3A**). Treatment with puromycin suggests that the *imb-2* mRNA must maintain association with the ribosome and nascent chain for *imb-2* transcripts to concentrate at the nuclear periphery. Puromycin-treated embryos did not display an apparent reduction in the number of mRNA molecules compared to control. This could indicate that the stability of the transcript does not require bound ribosomes or localization to the nuclear periphery. However, the 15-minute treatment could also be too short of a timeframe in which to observe degradation. Embryos treated with cycloheximide retained localization, indicating *imb-2* mRNA enrichment to the nuclear periphery does not require ongoing translation elongation provided the mRNA remains intact with the ribosome and

nascent IMB-2 polypeptide. These findings further support the translation-dependent model for perinuclear *imb-2* mRNA localization and indicate that an intact RNC is necessary.

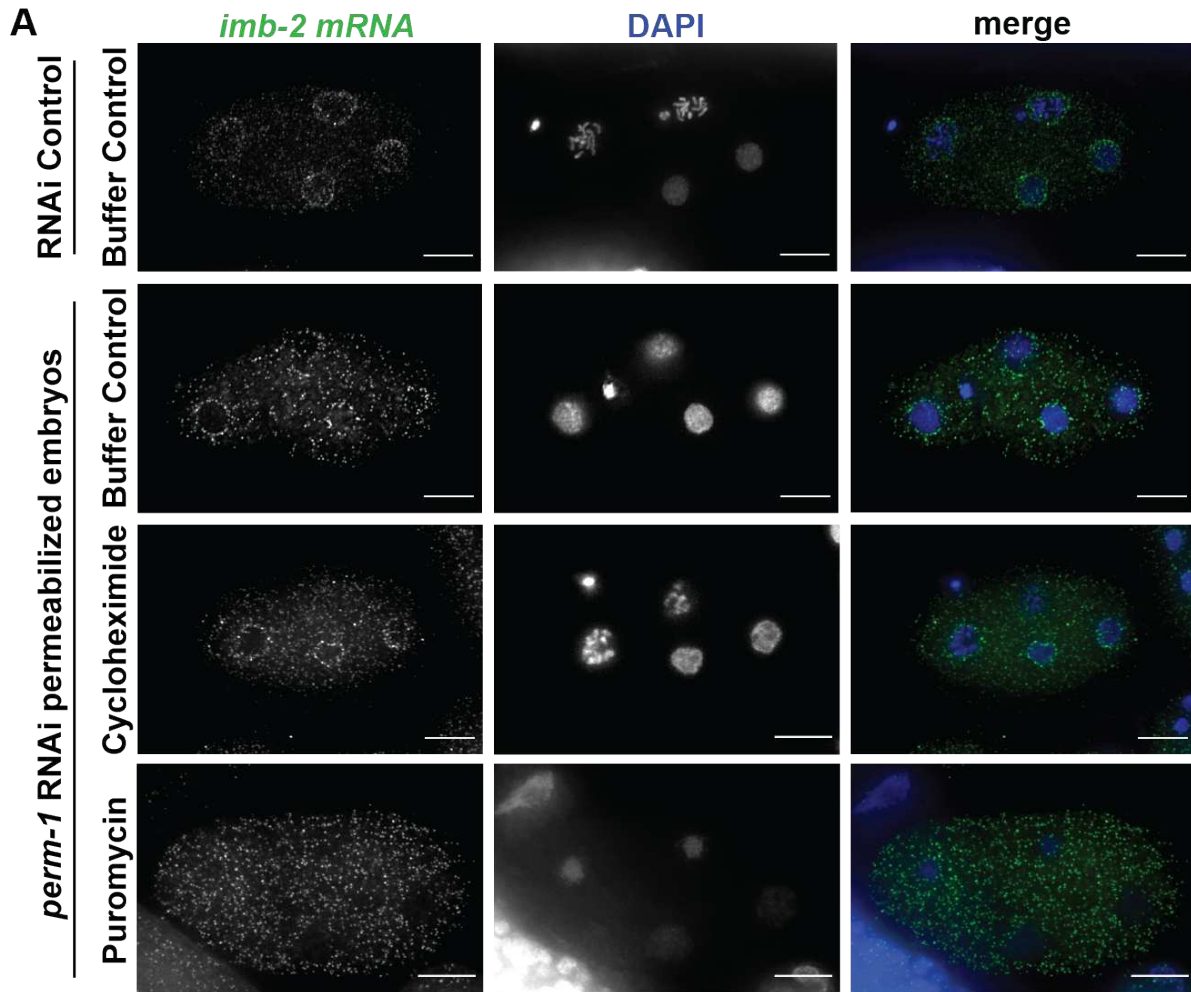


Figure 3.3: Translation elongation inhibition through treatment with puromycin and cycloheximide. (A) 4-cell embryos under RNAi control conditions or permeabilized by *perm-1* RNAi and subsequently treated with small molecule inhibitors cycloheximide, puromycin, or buffer control. *imb-2* mRNA (green) was imaged by smFISH with nuclei stained with DAPI (blue). Scale bars 10 μ m.

3.2.3 *imb-2* mRNA localization is susceptible to heat stress

Previous work identifying IMB-2 as a homolog of human Transportin-1 (TNPO1) demonstrated that in worms, IMB-2 also functions in the nucleocytoplasmic transport of DAF-16 in response to environmental stress [188,196]. The environmental stress tested, heat stress, occurs in animals

or cells by exposure to temperatures higher than normal body temperature and prevents protein synthesis primarily through changes in phosphorylation states of translation initiation factors followed by their subsequent inactivation [144,147,197,198]. In *C. elegans*, a well characterized pathway to combat heat stress is the IGF/insulin-like signaling (ILS) pathway [197]. The ILS pathway depends on the downstream nuclear import of the transcription factor DAF-16, a homolog of human FOXO [199]. In *C. elegans*, the DAF-16 transcription factor is imported into the nucleus in an IMB-2-dependent manner when acute heat stress is applied [188]. However, in human and yeast models, Transportin-1 (TNPO1/Kap104) is detected in cytoplasmic stress granules (SGs) in response to stress (**reviewed in Chapter 1.2.1**) [200,201]. In these instances, Transportin-1 is observed moving in and out of SGs rapidly, and a significant fraction of Transportin-1 remains outside SGs [201]. Given the translation-dependent nature of *imb-2* mRNA localization, we wanted to test whether *imb-2* localization would also be susceptible to heat stress. Additionally, we wanted to observe if *imb-2* mRNA would retain colocalization with IMB-2 protein. Further, we wanted to determine whether *imb-2* mRNA or IMB-2 protein would retain perinuclear localization or relocalize to stress granules, the two subcellular locales where IMB-2 or its homologs are detected after exposure to stress [188,192,196,200,201].

We used a stress granule marker worm strain (TIAR-1::GFP) to observe whether *imb-2* mRNA accumulates in SGs after exposure to heat. TIAR-1 is an ortholog to human stress granule-associated RNA binding protein TIA-1 [202]. Under control conditions, *imb-2* mRNA accumulated at the nuclear periphery, and TIAR-1 protein aggregated in the posterior lineage, where TIAR-1 resides in P granules (**Figure 3.4A, left panel**) [203]. When no heat stress was applied, *imb-2* mRNA did not colocalize with TIAR-1 (**Figure 3.4A, left panel**). In acute heat-treated 4-cell embryos (37 °C for 15 min), we observed distinct stress granule formation by our

TIAR-1::GFP reporter with *imb-2* mRNA colocalizing with TIAR-1 cytoplasmic clusters (Figure 3.4A, right panel).

While *imb-2* mRNA could be observed in cytosolic clusters overlapping with the stress granule marker TIAR-1::GFP, we wanted to test whether IMB-2 protein would display similar changes in localization patterning. Given the translation-dependent localization model for *imb-2* localization, we expect to observe IMB-2 protein in cytosolic clusters colocalizing with *imb-2* mRNA. However, according to the study demonstrating the necessity of IMB-2 protein for the nuclear import of DAF-16 in response to heat stress, we could also expect to observe some retention of IMB-2 protein localization to the nuclear periphery [188]. To test this hypothesis, we worked with InVivo Biosystems to generate a single copy insertion worm strain expressing *imb-2::gfp* at a transgenic locus on Ch IV. In this worm strain, both *imb-2* mRNA and IMB-2 protein are enriched at the nuclear periphery (Figure 3.4B, left panel; Figure 3.5A).

After exposing embryos acute heat stress, IMB-2 protein formed cytosolic clusters colocalizing with *imb-2* mRNA, similar to *imb-2* mRNA colocalizing with the stress granule marker TIAR-1::GFP (Figure 3.4A, left panel; Figure 3.4B, right panel). In those same heat-treated embryos IMB-2 protein retained localization at the nuclear periphery colocalizing with *imb-2* mRNA (Figure 3.4B, right panel). This suggests that in *C. elegans*, IMB-2 protein accumulates in stress granules as reported with human and yeast Transportins (TNPO1 and TNPO2/KAP104) as well as at the nuclear periphery as previously reported [22,54,188,200,201].

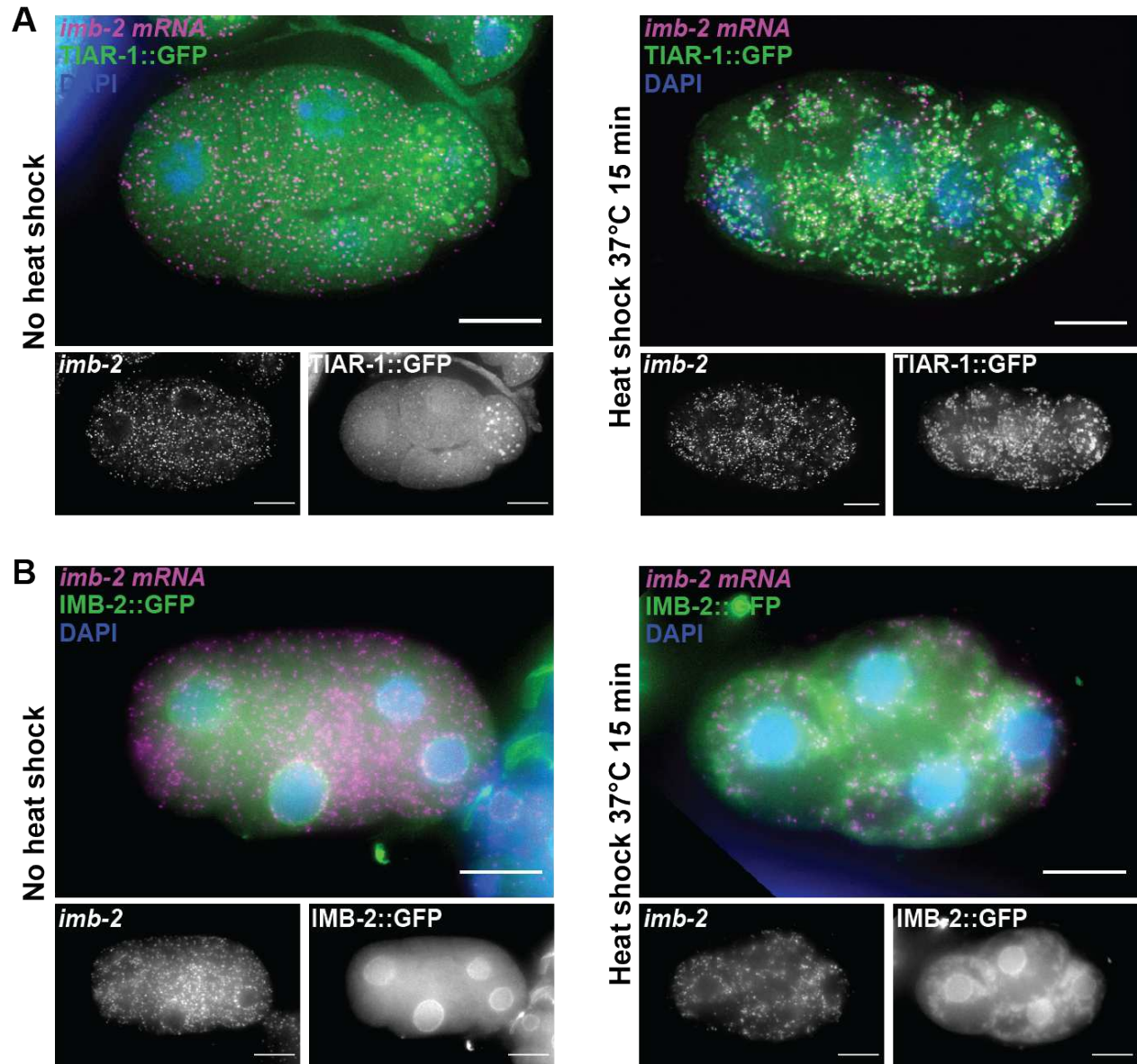


Figure 3.4: Effect of heat stress on *imb-2* mRNA and IMB-2 protein localization. (A) 4-cell embryos with the stress granule protein marker TIAR-1::GFP (green) probing for *imb-2* mRNA (magenta) by smFISH under not heat shock (control 20C) and acute heat stress (37 °C for 15 min). Nuclei stained with DAPI (blue). (B) 4-cell embryos with the IMB-2 protein marker IMB-2::GFP (green) probing for *imb-2* mRNA (magenta) by smFISH under not heat shock (control 20C) and acute heat stress (37 °C for 15 min). Nuclei stained with DAPI (blue). Scale bars 10 μm.

3.2.4 *imb-2* mRNA stability depends on nucleic acid sequence

context

Based on translation inhibition experiments, *imb-2* localization to the nuclear periphery is translation-dependent. However, it remains unclear whether the mRNA sequence could also be

critical for localization and stability. The study that demonstrated the *imb-2* 3'UTR was insufficient to direct a reporter construct to the nuclear periphery also showed that appending the *imb-2* 3'UTR to a neogreen reporter yielded fewer mRNA molecules than endogenous *imb-2* [48]. This indicates that a property of the holistic *imb-2* gene could be necessary for localization and protection from degradation.

In Chapter 2, we demonstrated that altering the *erm-1* mRNA sequence context by using alternative codons and synthetic introns did not affect the *erm-1* mRNA localization. The same study that demonstrated the *imb-2* 3'UTR being insufficient to direct localization also demonstrated the *erm-1* 3'UTR was insufficient to direct localization, but the *erm-1* transcript number did not appear reduced. As IMB-2 lacks a discernable NLS, an mRNA sequence element could be required for licensing *imb-2* for translation and protection from degradation. In yeast, there are examples of ER-bound transcripts requiring both translation-dependent and -independent elements for successful localization. Ribosome profiling combined with biochemical fractionation identified that a subset of ER-targeted transcripts had SRP pre-recruited to non-coding mRNA elements prior to the onset of translation [107].

To test whether other *imb-2* mRNA nucleotide sequences are necessary for localization, we synthetically recoded the *imb-2* mRNA nucleotide coding sequence while preserving the amino acid sequence. For this experiment, we generated three new worm strains (**Figure 3.5A**). We made a GFP knock-in at the C-terminal of the endogenous *imb-2* locus on chromosome II. We generated a strain with a single copy insertion on Chr IV of recoded *imb-2* nucleotide sequence yet synonymous IMB-2 amino acid sequence. Additionally, we created a single copy insertion of wt sequence *imb-2::gfp* at the same locus on chromosome IV. All three strains were generated and genotyped by InVivo Biosystems.

When imaging the endogenously GFP knock-in strain, *imb-2* mRNA was detected at the 4-cell stage, but *gfp* mRNA was not (**Figure 3.5B**). GFP signal was also not detected (**Figure 3.5B**). Additionally, the *imb-2* mRNA at the 4-cell stage was very poorly localized to the nuclear periphery. However, around the 200-cell stage, *gfp* mRNA was detected but GFP signal still was not. These embryos developed normally and produce viable offspring under typical growing conditions. This was a surprising result because the Chuang lab successfully generated an *imb-2::NeonGreen* worm strain with detectable NeonGreen protein signal at the nuclear periphery and in the nuclei during embryogenesis, larval stages, and adulthood [192]. The *imb-2* gene has three isoforms. It is possible that some isoforms are failing to be expressed properly upon addition of the C-terminal GFP sequence. Additionally, it could be that the isoform that successfully expressed *gfp* mRNA at the 200-cell stage, if not GFP protein, is not maternally loaded and therefore is not observed at the 4-cell stage.

The single copy insertion at the MosSci locus of *imb-2::gfp* encodes the long isoform *imb-2* sequence under the endogenous *imb-2* promoter. 4-cell embryos from this worm strain displayed *imb-2* mRNA and IMB-2::GFP localized to the nuclear periphery (**Figure 3.5C**). The synonymous *imb-2* strain expresses the recoded long isoform with the addition of synthetic introns. At the 4-cell stage, *imb-2 synonymous* mRNA and protein are not detected, indicating amino acid sequence alone is not sufficient to recapitulate mRNA and protein localization patterning (**Figure 3.5D**).

The *imb-2* synonymous strain displayed greatly reduced levels of synonymous transcript and no apparent IMB-2 SYNON protein. This indicates that the coding region sequence is important for the localization and expression of both the mRNA and the protein. Additionally, this indicates that scrambling the CDS and/or introducing synthetic introns likely targeted the

transcript for a decay or other silencing pathway. The *imb-2* native sequence tagged with GFP inserted at the same transgenic locus demonstrated that the altered *imb-2* nucleic acid sequence, not the expression from the MosSci locus, changes the transcript behavior.

A

<i>imb-2</i> worm strains		
<i>imb-2::gfp</i> (endogenous)	<i>imb-2p::imb-2::gfp::imb-2 3'UTR II</i>	<i>gfp</i> knock-in at endogenous <i>imb-2</i> locus on Chr II (this study)
<i>imb-2::gfp</i> (transgene)	<i>imb-2p::imb-2::gfp::imb-2 3'UTR IV</i>	single copy insertion at Chr IV MosSCI locus (this study)
<i>imb-2 synon::gfp</i> (transgene)	<i>imb-2p::imb-2 synon::gfp::imb-2 3'UTR IV</i>	single copy insertion at Chr IV MosSCI locus (this study)

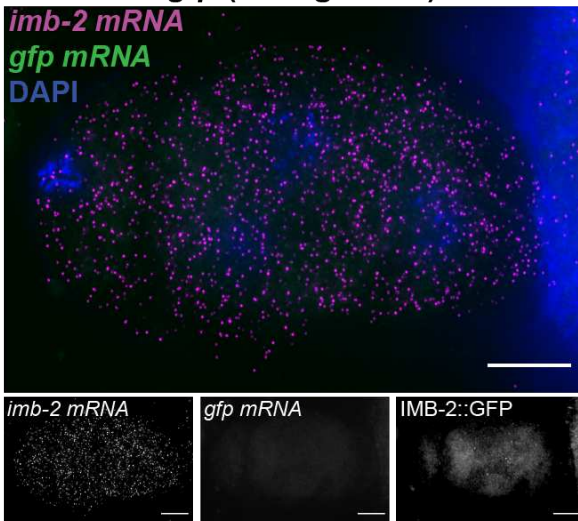
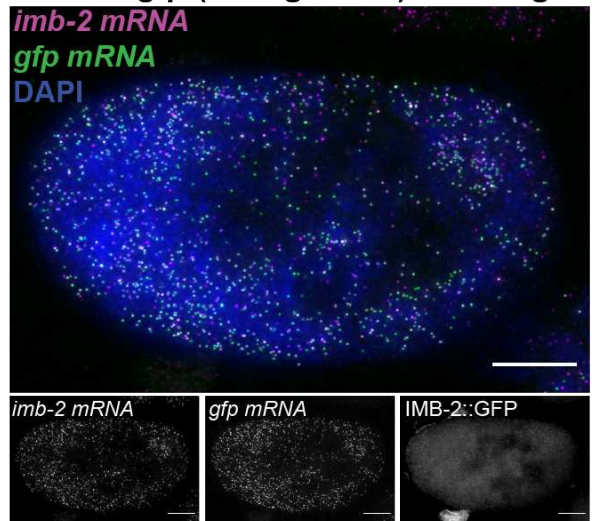
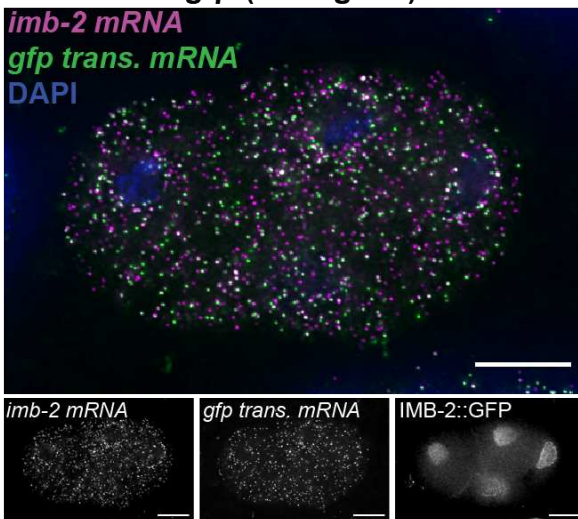
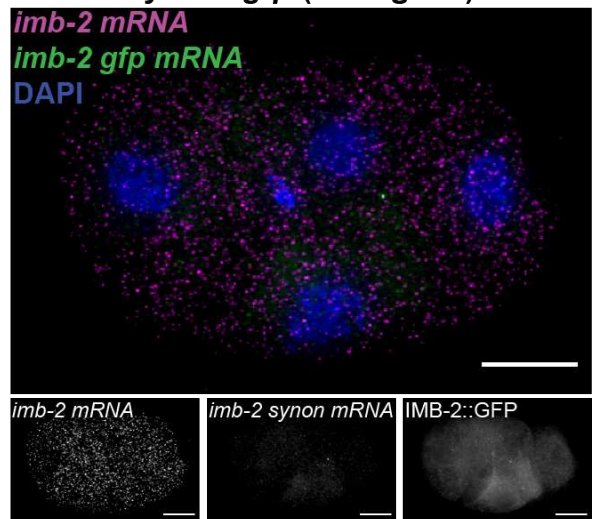
B *imb-2::gfp* (endogenous) 4-cell*imb-2::gfp* (endogenous) mid-stage**C** *imb-2::gfp* (transgene) 4-cell**D** *imb-2 synon::gfp* (transgene) 4-cell

Figure 3.5: *imb-2* mRNA localization to the nuclear periphery is mRNA sequence context dependent. (A) Table describing the three worm strains generated to test the mRNA context dependence for *imb-2* mRNA localization. (B) 4-cell and 200-cell embryos imaging the GFP knock in at the endogenous *imb-2* locus. (C) 4-cell embryo of *imb-2::gfp* inserted as a single copy at the MosSci locus on Chr IV. (D) 4-cell stage of the *synonymous imb-2* mRNA (*gfp synon.*, green) and wt *imb-2* (magenta). Nuclei stained with DAPI (blue). Scale bars 10 μ m.

3.3 Discussion

This chapter provided preliminary evidence supporting a translation-dependent model of *imb-2* mRNA localization to the nuclear periphery during early embryonic development. Through genetically depleting the translation initiation factor IFG-1, we demonstrated that translation initiation is required for localization. Additionally, by treating embryos with translation elongation inhibitors with differing mechanisms of action, we demonstrated that an intact ribosome-nascent chain complex (RNC), but not ongoing translation, is required for perinuclear localization. Exposing embryos to acute heat stress demonstrated that *imb-2* mRNA and IMB-2 protein could obtain a dual localization pattern in stress granules and at the nuclear periphery. Preliminary evidence altering the mRNA coding sequence of *imb-2* resulted in apparent silencing of the synonymous transcript with no translation. The data in this chapter indicate that non NLS-encoding transcripts can localize to the nuclear periphery, which is distinct from the canonical NLS-dependent localization pathway.

The *C. elegans* IMB-2 protein contains an Importin N-terminal domain followed by a short, disordered region. According to Gene Ontology (GO) annotation and structure data from other Importin N-terminal domain-containing proteins, this domain binds Ran GTPase protein and facilitates import into the nucleus [204,205]. The intrinsically disordered region contains a patch of basic and acidic residues with NLS binding capability to facilitate cargo binding [204]. Additionally, knocking down IMB-2 is embryonic lethal [190,191]. The orthologs of IMB-2 in humans, Transportin-1 and Transportin-2, contain the conserved Importin N-terminal domain with some variation in the disordered region, though cargo binding by NLS is preserved [186]. The specificity of Transportin proteins for NLSs has primarily been studied in mammals and

yeast, with an overlap in cargo binding between members of the Transportin subfamily and other Importins [186].

In *C. elegans*, the most studied nuclear import substrate bound by IMB-2 is the longevity factor DAF-16 (Forkhead box O FOXO in humans) [188,206,207]. Other longevity factors speculated to be imported by IMB-2 into the nucleus include the lipid binding protein LBP-8 and OCR-2, but the complete set of substrates bound by IMB-2 remains unknown [208–210]. Mammalian Transportin-1 and Transportin-2 bind cargoes including proteins involved in mRNA processing (hnRNP family members and FUS), core histones, ribosomal proteins, and the transcription factor FOXO4 [211]. Yeast Transportin-1 also binds RNA binding proteins involved in mRNA processing, transcription factors, and ribosomal proteins [186]. These findings point to conservation between the nucleocytoplasmic transport facilitated by the Transportin subfamily between yeast, worms, and humans.

A conserved part of cellular response to acute stress includes the formation of stress granules in the cytoplasm (**reviewed in chapter 1.2.1**). In mammalian cells, Transportin-1 and Transportin-2 are found in SGs, along with known cargoes [54,201]. Yeast Transportin and associated cargo are also identified in SGs [22,54]. Coimmunoprecipitation in human cells shows Transportin-1 bound to the transcription factor FOXO in response to acute stress, which was further corroborated in *C. elegans* with IMB-2-dependent import of FOXO homolog DAF-16. This suggests that, depending on cargo bound, Transportin proteins can assume dual locations in response to stress exposure (**Figure 3.6**). This may vary depending on the type of stress the cells or organism is exposed to.

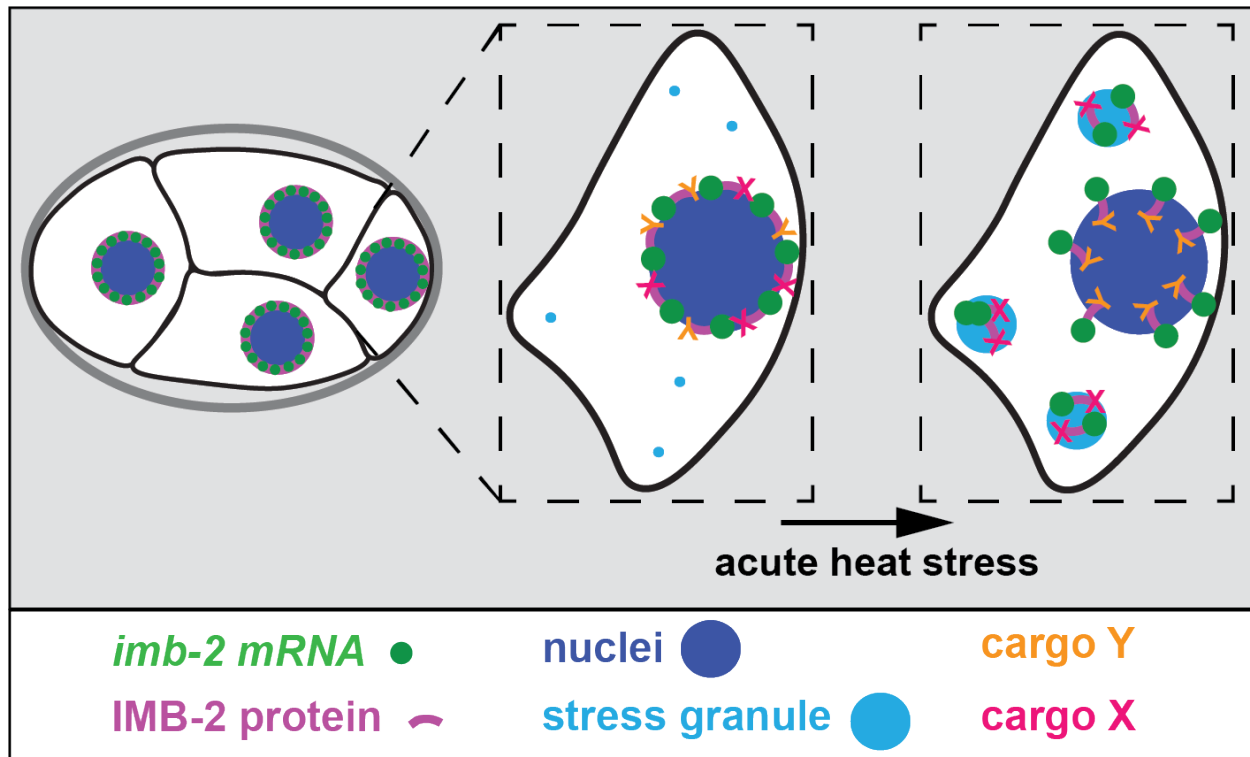


Figure 3.6: *imb-2* mRNA and IMB-2 protein localization after stress depends on the cargo to which IMB-2 is bound.

What could be the function of *imb-2* mRNA localization to the nuclear periphery and stress granules post-stress exposure? Under standard conditions, perinuclear *imb-2* localization could function in co-translationally binding cargo upon translation of the NLS-binding region. *imb-2* could also be translated at the nuclear periphery to achieve successive rounds of translation, given the rapid cell divisions during development and high demand for nucleocytoplasmic transport. Specific to maternally deposited transcripts, *imb-2* localization could locally translate so that nucleocytoplasmic transport machinery is poised to respond to gene expression regulation demands at the onset of zygotic transcription.

Alternatively, *imb-2* localization could be a passive function of IMB-2 localizing to the nuclear periphery upon binding Ran and cargo. *imb-2* could localize passively to stress granules upon stress exposure while it remains in complex with the nascent IMB-2 protein and its bound substrate. According to the stress granule transcriptomes in humans and yeast, the Transportin

encoding transcripts are neither enriched nor depleted in SGs [21,212]. This could indicate the dual localization between the nuclear periphery and stress granules following IMB-2 distributions.

In the context of the maternal-to-zygotic transition, what would be the function of IMB-2 maintaining perinuclear localization to import a transcription factor, such as DAF-16, when zygotic transcription is paused? Would DAF-16 import poise the nucleus for a transcriptional response to stress in early development? What other cargo could IMB-2 be importing prior zygotic transcription initiation?

Follow-up experiments are required to support and further instruct the model formed from the preliminary data in this chapter (**Figure 3.6**). First, translation-dependence of *imb-2* localization could be confirmed by introducing a TG deletion in the start codon of *imb-2* in a background with a silenced nonsense-mediated decay (NMD) pathway to prevent degradation of the transcript. This would test the effect *imb-2* specific translation inhibition on localization. Additionally, it would be informative to inject the *imb-2* 3'UTR sufficiency construct into an NMD silenced background to observe the stability and localization of the *imb-2* 3'UTR. To test whether *imb-2* mRNA and IMB-2 protein are in complex with DAF-16 during early development, immunofluorescence and smFISH could be performed in the transgenic IMB-2::GFP strain to simultaneously observe all three inquiries in the same embryo. To test whether localization changes in response to different types of stress, embryos could be exposed to different types of stress, such as starvation.

IMB-2 is the only member representing the Transportin subfamily in *C. elegans*, providing an opportunity to understand better the potential functions of translation-dependent maternal *imb-2* mRNA localization for IMB-2 protein function. Compared to other Importin

proteins, the Transportin family is less studied. Beyond the context of embryonic development, the mislocalization of known mammalian Transportin-1 cargoes, such as FUS, is linked to the development of neurological disease, illustrating the importance of Transportin-dependent nuclear import [213].

3.4 Materials and Methods

3.4.1 Worm husbandry

For details on worm husbandry reference chapter 2.4.1. (**Table 3.1**)

Table 3.1: Worm strains used in Chapter 3

Strain	Description	Genotype	Source/Reference
N2	N2	<i>C. elegans</i> wildtype	CGC
wLPW001	MODC PEST::GFP::H2B	sprSi17 [mex-5p::MODC PEST::GFP::H2B::mex-3 3'UTR + Cbr-unc-119(+)] II	CGC/Kaymak et al., Dev Dyn. 2016
wLPW004	imb-2p::imb- 2_scrambled::eGFP::imb- -2 3'UTR	imb-2p::imb- 2scrmbl::GFP::imb-2u in 10882, unc-119(+)] IV ; unc-119(ed3) III	This study
wLPW005	endogenous KI of eGFP at imb-2 locus	imb-2 (knu972[imb- 2::GFP::loxP::hygR::locP])	This study
wLPW006	imb-2p::imb- 2::eGFP::imb-2 3'UTR	imb-2p::imb- 2::GFP::imb-2u in 10882, unc-119(+)] IV ; unc- 119(ed3) III	This study
wLPW019	TIAR-1::GFP	tiar-1(tn1545[tiar- 1::s::tev::GFP]) II	CGC/ Huelgas-Morales G., et al. G3 (Bethesda). 2016 Apr; 6(4): 1031- 1047

3.4.2 Heat Shock Experiments

Heat shock experiments were performed by transferring harvested embryos to pre-warmed M9 liquid media and incubating at 37°C for 15 minutes. After heat shock, worms were immediately fixed for smFISH.

3.4.3 RNAi Feeding for smFISH Microscopy

For details on RNAi feeding for smFISH microscopy reference chapter 2.4.3. (**Table 3.2**).

Table 3.2: E. coli strains used in Chapter 3

Strain description	Plasmid description	Detailed description	Reference
OP50	OP50	OP50	
L4440	pPD129.36	empty worm RNAi plasmid	Fire Lab C. Elegans Vector Kit 1999
<i>ifg-1</i> RNAi	M110.4 from the Ahringer library	worm RNAi plasmid + <i>ifg-1</i> gene fragment	

3.4.4 Permeabilization and drug delivery

For details on RNAi feeding for smFISH microscopy reference chapter 2.4.4.

3.4.5 smFISH

For details smFISH reference chapter 2.4.5. (**Table A.1**).

3.4.6 smiFISH

For details smiFISH reference chapter 2.4.6. (**Table A.1**).

Chapter 4

Discussion and future perspectives

4.1 *C. elegans* as a model for studying mRNA localization in the context of development

As reviewed in Chapter 1 and Chapter 2.1, mRNA localization is a widespread form of post-transcriptional regulation in organisms ranging in complexity from single-cell bacteria to complex mammals. At the latest RNALocate database count, more than 210,000 RNA-associated subcellular localization events have been documented in 104 species [23]. The first example of mRNA localization was β -actin mRNA to lamellae in chicken embryonic fibroblasts [2]. Soon after, the first localized maternal mRNAs were discovered in *Xenopus* and *Drosophila* [10,79,214]. Further studies in *Drosophila* identified that the localization of morphogenic transcripts functioned to establish embryonic polarity and determine body axis orientation [32]. More recently, *C. elegans* has emerged as an important developmental model for understanding and studying mRNA localization patterns, mechanisms, and functions.

Previous work in our group began establishing *C. elegans* as a tractable model for exploring mRNA localization patterns of maternally inherited transcripts [48,126]. Prior to this work, examples of subcellular localization in *C. elegans* were limited to a select few transcripts identified in the membraneless organelles P granules, effectively worm germ granules [35,46]. Single-cell RNA-sequencing in 2-cell embryos identified the maternally-inherited transcriptome and a subset of asymmetrically-enriched transcripts [126]. Further single-cell sequencing from

the 1- to 16-cell stages identified subsets of maternal transcripts that were degraded, zygotically transcribed, and provided further evidence for asymmetric inheritance [130]. These data sets provided candidates to screen for subcellular localization patterns using single molecule Fluorescence *in situ* Hybridization (smFISH). smFISH on maternally-inherited and zygotically transcribed candidates revealed that maternally-loaded transcripts are enriched for subcellular localization patterning compared to zygotic transcripts [48].

These findings were remarkable for a few reasons. First, these observations demonstrated a pattern of transcripts enriched in the posterior cell clustered in P granules downstream of translation repression mediated through sequences in their 3'UTRs. Second, this screen increased the number of known transcripts to possess subcellular localization patterning while identifying additional localization patterns beyond clustered in P granules, namely *imb-2* enriched to the nuclear periphery and *erm-1* localization to the plasma membrane. Also, these findings demonstrated that diverse subcellular localization patterning of maternally-inherited transcripts is a more widespread feature of embryos. This last finding was critical because the majority of studies exploring the diversity and prevalence of mRNA localization patterning were performed in *Drosophila* embryos [16,17,32]. While this is undoubtedly a fascinating observation, it was thought that the magnitude of localization patterning was due to the syncytial environment of early embryogenesis in *Drosophila*. The first 13 divisions in *Drosophila* are nuclear, meaning there is no cellular compartmentalization and therefore a shared cytoplasm during this time. Thus, mRNA localization would be a powerful form of post-transcriptional regulation to establish polarity and cell fate in the absence of physical barriers offered by the cell membrane. Identifying a diversity of localization patterns in *C. elegans* on par with those observed in *Drosophila* demonstrated that subcellular localization is prevalent in early embryogenesis even

in a cellularized environment. This makes *C. elegans* an excellent model for exploring other localization patterns, mechanisms of localization, and functions in development. More generally, *C. elegans* has the advantages of being inexpensive, genetically tractable, short generation times, a fully mapped cell lineage from 1-cell to adulthood, transparent structures ideal for microscopy, and can survive as a frozen stock.

In Chapter 2, we expanded the known list of membrane-localized maternal transcripts from 4 to 7 while identifying an additional nine genes with apparent mRNA localization patterns later in development. We identified that the presence of a PH or PH-like domain could be predictive of plasma membrane localization while also observing that a single gene can change localization patterns over developmental time. Our translation-inhibition studies identified *erm-1* as the first maternally-deposited transcript with translation-dependent localization in *C. elegans*. A similar study by the Mango lab simultaneously identified a zygotically transcribed mRNA with translation-dependent localization to the apical membranes of developing epithelia [117]. In combination with our findings, these data further developed *C. elegans* as a model for studying translation-dependent mRNA localization while establishing methods to probe translation dependence. Developing a technique to combine treatment with small molecules and smFISH will allow other researchers to test questions of localization mechanisms in early *C. elegans* embryos. Further, through collaboration, the *erm-1* gene provides us with an opportunity to link mRNA localization to function.

In addition to establishing *erm-1* as a model for studying translation-dependent mRNA localization of maternal transcripts to the plasma membrane, Chapter 3 identified *imb-2* as a potential model for non-canonical, translation-dependent localization to the nuclear periphery. Beyond establishing *imb-2* mRNA localization is translation-dependent, studies in stress

conditions showed that both *imb-2* mRNA and IMB-2 protein could localize either to stress granules or retain perinuclear localization. These preliminary findings indicate that IMB-2 displays behavior consistent with other organisms and participates in conserved stress response pathways. *imb-2* is the single gene in *C. elegans* representing the Transportin subfamily, making *C. elegans* an excellent model for further exploring the function of Transportins in nucleocytoplasmic transport during development.

4.2 Contributions of mRNA localization to the maternal-to-zygotic transition

More broadly, the work presented in this thesis presents an opportunity to study the potential contributions of mRNA localization, specifically translation-dependent localization, to regulating the maternal-to-zygotic transition (MZT). During animal development, early embryonic development is directed by maternally inherited components. Then, after a pause in transcription that varies in cell division length depending on the organism, the zygotic transcription initiates to complete the MZT hand-off to the zygotic genome. During the initial phase of the MZT, gene regulation is exclusively on post-transcriptional and post-translational. This initial phase is followed by a gradual switching on of the zygotic genome and activation of zygotic transcriptional regulation. mRNA localization is a form of post-transcriptional gene regulation during the initial phase of the MZT. The majority of maternal mRNAs observed in model organisms display subcellular localization patterning compared to zygotically transcribed transcripts [17,48]. Why would the maternal population of transcripts be enriched for subcellular patterning compared to their zygotically transcribed counterparts?

While *Drosophila*, *Xenopus*, and *C. elegans* have been the formative models of exploring the contribution of maternal mRNA to the MZT, further studies in varying organisms are revealing conserved patterns between them. So far, *Drosophila* is the best-studied model for the regulation of maternal mRNA translation. During egg activation and oocyte maturation, translation efficiency increases for up to 50% of the maternal transcriptome [215]. Of this subset, a correlation between poly(A) tail length and translation efficiency has been observed [216,217]. This correlation diminishes upon zygotic genome activation (ZGA) [217]. Further studies in *Drosophila* and other developmental models suggest that polyadenylation and deadenylation regulation can affect the stability and translation of maternal mRNAs during the MZT.

Global analyses indicate that maternal transcripts represent a large range of the protein-coding transcriptome, or translome, though a significant portion of maternal transcripts undergo degradation and clearing prior to zygotic genome activation [218–225]. In *Drosophila*, roughly 65% of maternally-inherited transcripts is cleared during the maternal-to-zygotic transition. Only 2% of the maternal proteome is cleared [226]. In *C. elegans*, roughly 30% of the maternal mRNAs are cleared during the single cell stage, followed by an additional 30% by the 4-cell stage [126,130,219,220]. By the onset of the MZT, roughly 60% of the maternal transcriptome is cleared. What about the remaining 35-40% of transcripts that aren't cleared? Maternal mRNAs are posited to be cleared due to dNTP depletion and turnover during the MZT. Due to the pause in transcription and depleted reservoir of dNTPs, translation-dependent/co-translational localization could be an efficient strategy of the early embryo for locally regulated proteomes. Additionally, the presence of translation machinery bound to maternal mRNA might preserve its stability and prevent degradation. Addressing these questions requires advancing

techniques that yield information on mRNA localization with translation dynamics, both in fixed and live samples.

4.3 Advancing techniques pair mRNA localization with translation dynamics, lending insight into function

As reviewed in Chapter 1, genomics and imaging technologies to detect mRNAs and their localization patterns, mRNA localization is appreciated as a conserved part of post-transcriptional gene expression regulation. Additionally, as techniques to detect translation status improve mRNA localization can be linked to translation and therefore lead insight into contributions towards precise temporal and spatial control of gene expression. Subcellular mRNA localization has emerged as a highly conserved post-transcriptional mechanism for the spatial and temporal control of protein synthesis. As new imaging and sequencing methods of detecting mRNA localization and translation are developed, it is now possible to study mRNA localization across species of varying complexity and size. This provides the opportunity to uncover conserved mechanisms and prospective functions. Single-gene and single-molecule studies are uncovering mechanisms of local translation through translation-dependent and -independent localization at various subcellular locales. Excitingly, the impact of mRNA localization on the physiology of the development of specific, multicellular tissues and complete organisms is unveiling the impact of local translation in cell-to-cell interactions, tissue organization, and cell fate determination.

Single molecule fluorescence *in situ* Hybridization (smFISH) has been a gold standard for visualizing and quantifying individual transcripts in fixed samples. Combining smFISH with immunofluorescence permits visualization of protein and mRNA but does not yield information

on translation dynamics. Techniques have been developed to visualize specific mRNAs interacting with ribosomes, such as FLAIRM (fluorescence assay to detect ribosome interactions with mRNA) [227]. Alternatively, probes can be designed complementary to both an mRNA of interest and ribosomal RNA (rRNA) to reveal whether a transcript is associated with ribosomes [228]. However, these techniques only provide insight into a few individual transcripts and do not provide scope for whole cell or organism RNA localization.

In response, groups are scaling up FISH-based and other techniques for transcriptome and subcellular transcriptome level data generation. These techniques include RNA SPOTS (RNA Sequential Probing of Targets) and MERFISH (Multiplex Error Robust Fluorescence *in situ* Hybridization), amongst others [229–231]. Other RNA-seq based techniques can yield subcellular information by micro-dissecting tissue samples (Laser capture micro-dissected RNA-seq (LCM-RNAseq)) or by using proximity labeling techniques (APEX-seq) [22,232]. The proximity labeling technique APEX-seq comes with the additional advantage of collecting both spatial transcriptome data as well as spatial proteome data through complementation with mass spectrometry. APEX-seq expanded the knowledge of the subcellular mRNA and protein content of stress granules in mammalian cells [21,22]. Another proximity tagging technique, HALO-seq, has yielded major insights into neurobiology [128,233]. The Shechner lab is developing a new technique, O-MAP (oligonucleotide-directed *in situ* proximity), to take advantage of the specificity of smFISH to reduce off-target tagging and reduce experimental difficulty (RNA 2022). These techniques can be combined with ribosome profiling techniques such as Ribo-Seq (ribosome sequencing), ART-Seq (active mRNA translation sequencing), or TRAP-Seq (translating ribosome affinity purification RNA sequencing) to isolate the population of mRNAs associated with ribosomes and give insight into translation-dynamics [234].

While techniques in fixed samples have revealed insights into subcellular transcriptomic and proteomic organization and abundance, fluorescence-based imaging techniques are making it possible to visualize translation dynamics in live cells. Real-time visualization of translation paired with mRNA localization has been made possible with translating RNA imaging by coat protein knock-off (TRICK), single-molecule imaging of nascent peptides (SINAPS), and nascent chain tracking (NCT) [235–237]. These live-cell approaches have been instrumental in measuring translation kinetics related to the first round of translation or ongoing translation.

4.4 Perspectives and future directions

The work described in this thesis expands *C. elegans* as a model for studying translation-dependent mRNA localization in the early embryo, identifying the first translation-dependent localized maternal mRNA, *erm-1*. We characterized two transcripts as potential models for their subcellular locales to the plasma membrane or nuclear periphery. Additionally, we expanded techniques to perturb translation while able to visualize mRNA in early embryos. These insights add to the growing RNA biology field, translation-dependent localization, and RNA localization as a powerful form of post-transcriptional gene regulation during early development and beyond. The techniques described in this work have expanded the known membrane localized transcripts list and demonstrated how localization patterns can change over time and in response to environmental cues.

There are a few key challenges that are an obstacle towards linking mRNA localization to potential function and contribution towards gene regulation. First, there are few methods currently developed that can alter mRNA localization for context in vivo. I.e., tethering *erm-1* mRNA to a different subcellular locale like the nuclear periphery to observe whether or not there

were functional consequences for the ERM-1 protein and ultimate embryonic development. Tethering can affect mRNA stability or alter translation efficiency making interpreting results difficult, among other considerations. Additionally, techniques to tag transcripts *in vivo*, such as the MS2/MCP or PP7/PCP, can alter endogenous behavior by preventing nuclear export, forming cytoplasmic aggregates, altering localization patterns, etc. Further, the development of *in situ* high throughput transcriptomics technologies has generated a vast amount of mRNA localization patterns that require further interpretation and analysis. The development of machine learning tools will facilitate the interpretation and analyses of these data sets to identify conserved patterns and give insight into potential function when paired with additional *in vivo* analyses.

Next, it will be interesting to apply some of the growing compendium of subcellular transcriptomics assays to characterize the full collection of maternal and zygotic transcripts at the plasma membrane, nuclear periphery, and other locales. It will be very insightful to pair this with ribosome profiling and other translation techniques for future studies understanding the landscape during the MZT. It will be fascinating to uncover the set of genes that are actively translated vs. bound by ribosomes poised for translation upon ZGA vs. degraded and identify conserved features that specify the fate of the transcript. Finally, it will be thrilling when we can consistently link mRNA localization to function, or lack thereof, and understand the true impact and contribution of mRNA localization to gene expression regulation and biology.

Bibliography

1. Jeffery WR, Tomlinson CR, Brodeur RD. Localization of actin messenger RNA during early ascidian development. *Dev Biol.* 1983;99:408–17.
2. Lawrence JB, Singer RH. Intracellular localization of messenger RNAs for cytoskeletal proteins. *Cell.* 1986;45:407–15.
3. Kislauskis EH, Zhu X, Singer RH. Sequences responsible for intracellular localization of beta-actin messenger RNA also affect cell phenotype. *J Cell Biology.* 1994;127:441–51.
4. Ross AF, Oleynikov Y, Kislauskis EH, Taneja KL, Singer RH. Characterization of a beta-actin mRNA zipcode-binding protein. *Mol Cell Biol.* 1997;17:2158–65.
5. Hüttelmaier S, Zenklusen D, Lederer M, Dichtenberg J, Lorenz M, Meng X, et al. Spatial regulation of β -actin translation by Src-dependent phosphorylation of ZBP1. *Nature.* 2005;438:512–5.
6. Balasanyan V, Arnold DB. Actin and Myosin-Dependent Localization of mRNA to Dendrites. *Plos One.* 2014;9:e92349.
7. Femino AM, Fay FS, Fogarty K, Singer RH. Visualization of single RNA transcripts in situ. *Science.* 1998;280:585–90.
8. Song T, Zheng Y, Wang Y, Katz Z, Liu X, Chen S, et al. Specific interaction of KIF11 with ZBP1 regulates the transport of β -actin mRNA and cell motility. *Journal of Cell Science* [Internet]. 2015;128:1001 LP – 1010. Available from: <http://jcs.biologists.org/content/128/5/1001.abstract>
9. Goering R, Hudish LI, Guzman BB, Raj N, Bassell GJ, Russ HA, et al. FMRP promotes RNA localization to neuronal projections through interactions between its RGG domain and G-quadruplex RNA sequences. *Elife.* 2020;9:e52621.
10. Rebagliati MR, Weeks DL, Harvey RP, Melton DA. Identification and cloning of localized maternal RNAs from xenopus eggs. *Cell* [Internet]. 1985;42:769–77. Available from: <https://www.sciencedirect.com/science/article/pii/0092867485902739>
11. Lehmann R, Nüsslein-Volhard C. Abdominal segmentation, pole cell formation, and embryonic polarity require the localized activity of oskar, a maternal gene in drosophila. *Cell* [Internet]. 1986;47:141–52. Available from: <https://www.sciencedirect.com/science/article/pii/0092867486903752>

12. Tian L, Chou H-L, Fukuda M, Kumamaru T, Okita TW. mRNA Localization in Plant Cells. *Plant Physiol* [Internet]. 2020;182:97–109. Available from: <https://pubmed.ncbi.nlm.nih.gov/31611420>
<https://www.ncbi.nlm.nih.gov/pmc/articles/PMC6945871/>
13. Knowles RB, Sabry JH, Martone ME, Deerinck TJ, Ellisman MH, Bassell GJ, et al. Translocation of RNA Granules in Living Neurons. *J Neurosci* [Internet]. 1996;16:7812–20. Available from: <https://pubmed.ncbi.nlm.nih.gov/8987809>
14. Long RM, Singer RH, Meng X, Gonzalez I, Nasmyth K, Jansen R-P. Mating Type Switching in Yeast Controlled by Asymmetric Localization of ASH1 mRNA. *Science* [Internet]. 1997;277:383–7. Available from: <https://doi.org/10.1126/science.277.5324.383>
15. Nevo-Dinur K, Nussbaum-Shochat A, Ben-Yehuda S, Amster-Choder O. Translation-Independent Localization of mRNA in *E. coli*. *Science* [Internet]. 2011;331:1081 LP – 1084. Available from: <http://science.sciencemag.org/content/331/6020/1081.abstract>
16. Wilk R, Hu J, Blotsky D, Krause HM. Diverse and pervasive subcellular distributions for both coding and long noncoding RNAs. *Gene Dev*. 2016;30:594–609.
17. Lécuyer E, Yoshida H, Parthasarathy N, Alm C, Babak T, Cerovina T, et al. Global Analysis of mRNA Localization Reveals a Prominent Role in Organizing Cellular Architecture and Function. *Cell* [Internet]. 2007;131:174–87. Available from: <https://www.sciencedirect.com/science/article/pii/S0092867407010227?via%3Dihub>
18. Taliaferro JM, Wang ET, Burge CB. Genomic analysis of RNA localization. *RNA Biology* [Internet]. 2014;11:1040–50. Available from: <http://www.ncbi.nlm.nih.gov/pmc/articles/PMC4615561/>
19. Fazal FM, Han S, Parker KR, Kaewsapsak P, Xu J, Boettiger AN, et al. Atlas of Subcellular RNA Localization Revealed by APEX-Seq. *Cell* [Internet]. 2019;178:473-490.e26. Available from: [https://www.cell.com/cell/pdf/S0092-8674\(19\)30555-0.pdf](https://www.cell.com/cell/pdf/S0092-8674(19)30555-0.pdf)
20. Chouaib R, Safieddine A, Pichon X, Imbert A, Kwon OS, Samacoits A, et al. A Dual Protein-mRNA Localization Screen Reveals Compartmentalized Translation and Widespread Co-translational RNA Targeting. *Dev Cell* [Internet]. 2020;54:773-791.e5. Available from: <http://www.sciencedirect.com/science/article/pii/S1534580720305840>
21. Khong A, Matheny T, Jain S, Mitchell SF, Wheeler JR, Parker R. The Stress Granule Transcriptome Reveals Principles of mRNA Accumulation in Stress Granules. *Molecular Cell* [Internet]. 2017;68:808-820.e5. Available from: <https://www.sciencedirect.com/science/article/pii/S1097276517307906?via%3Dihub>
22. Padrón A, Iwasaki S, Ingolia NT. Proximity RNA Labeling by APEX-Seq Reveals the Organization of Translation Initiation Complexes and Repressive RNA Granules. *Molecular Cell*

- [Internet]. 2019;75:875-887.e5. Available from:
<https://www.sciencedirect.com/science/article/abs/pii/S1097276519305854>
23. Cui T, Dou Y, Tan P, Ni Z, Liu T, Wang D, et al. RNALocate v2.0: an updated resource for RNA subcellular localization with increased coverage and annotation. *Nucleic Acids Res.* 2021;50:gkab825-.
24. Kedersha N, Cho MR, Li W, Yacono PW, Chen S, Gilks N, et al. Dynamic Shuttling of Tia-1 Accompanies the Recruitment of mRNA to Mammalian Stress Granules. *The Journal of Cell Biology* [Internet]. 2000;151:1257–68. Available from: <http://jcb.rupress.org/content/151/6/1257>
25. Buchan JR, Parker R. Eukaryotic Stress Granules: The Ins and Outs of Translation. *Molecular Cell* [Internet]. 2009;36:932–41. Available from:
<https://www.sciencedirect.com/science/article/pii/S1097276509008612?via%3Dihub>
26. Bruckenstein DA, Lein PJ, Higgins D, Fremeau RT. Distinct spatial localization of specific mRNAs in cultured sympathetic neurons. *Neuron* [Internet]. 1990;5:809–19. Available from:
<http://www.sciencedirect.com/science/article/pii/089662739090340L>
27. Zappulo A, Bruck D van den, Mattioli CC, Franke V, Imami K, McShane E, et al. RNA localization is a key determinant of neurite-enriched proteome. *Nat Commun.* 2017;8:583.
28. Holt CE, Martin KC, Schuman EM. Local translation in neurons: visualization and function. *Nature structural & molecular biology.* 2019;26:557–66.
29. Besse F, Ephrussi A. Translational control of localized mRNAs: restricting protein synthesis in space and time. *Nat Rev Mol Cell Bio* [Internet]. 2008;9:971–80. Available from:
<https://doi.org/10.1038/nrm2548>
30. Ryder PV, Lerit DA. RNA localization regulates diverse and dynamic cellular processes. *Traffic* [Internet]. 2018;19:496–502. Available from: <https://pubmed.ncbi.nlm.nih.gov/29653028>
31. Johnston DS. Moving messages: the intracellular localization of mRNAs. *Nat Rev Mol Cell Bio.* 2005;6:363–75.
32. Lasko P. mRNA localization and translational control in *Drosophila* oogenesis. *Cold Spring Harbor perspectives in biology.* 2012;4.
33. Fernandes N, Buchan JR. RPS28B mRNA acts as a scaffold promoting cis-translational interaction of proteins driving P-body assembly. *Nucleic Acids Res.* 2020;48:6265–79.
34. Eddy EM. Germ Plasm and the Differentiation of the Germ Cell Line. *Int Rev Cytol.* 1976;43:229–80.
35. Voronina E, Seydoux G, Sassone-Corsi P, Nagamori I. RNA Granules in Germ Cells. *Csh Perspect Biol* [Internet]. 2011;3:a002774. Available from:

<http://cshperspectives.cshlp.org/cgi/doi/10.1101/cshperspect.a002774%5Cnhttp://cshperspectives.cshlp.org/site/misc/subscribe.xhtml>

36. Okada M, Kleinman IA, Schneiderman HA. Restoration of fertility in sterilized *Drosophila* eggs by transplantation of polar cytoplasm. *Dev Biol.* 1974;37:43–54.
37. Illmensee K, Mahowald AP. Transplantation of Posterior Polar Plasm in *Drosophila*. Induction of Germ Cells at the Anterior Pole of the Egg. *Proc National Acad Sci.* 1974;71:1016–20.
38. Barbee SA, Lublin AL, Evans TC. A Novel Function for the Sm Proteins in Germ Granule Localization during *C. elegans* Embryogenesis. *Curr Biol.* 2002;12:1502–6.
39. Shimada M, Yokosawa H, Kawahara H. OMA-1 is a P granules-associated protein that is required for germline specification in *Caenorhabditis elegans* embryos. *Genes to Cells.* 2006;11:383–96.
40. Ogura K, Kishimoto N, Mitani S, Gengyo-Ando K, Kohara Y. Translational control of maternal *glp-1* mRNA by POS-1 and its interacting protein SPN-4 in *Caenorhabditis elegans*. *Development.* 2003;130:2495–503.
41. Kawasaki I, Amiri A, Fan Y, Meyer N, Dunkelbarger S, Motohashi T, et al. The PGL family proteins associate with germ granules and function redundantly in *Caenorhabditis elegans* germline development. *Genetics.* 2004;167:645–61.
42. Batista PJ, Ruby JG, Claycomb JM, Chiang R, Fahlgren N, Kasschau KD, et al. PRG-1 and 21U-RNAs Interact to Form the piRNA Complex Required for Fertility in *C. elegans*. *Mol Cell.* 2008;31:67–78.
43. Gallo CM, Munro E, Rasoloson D, Merritt C, Seydoux G. Processing bodies and germ granules are distinct RNA granules that interact in *C. elegans* embryos. *Developmental Biology* [Internet]. 2008;323:76–87. Available from: <http://www.sciencedirect.com/science/article/pii/S0012160608010555>
44. Spike C, Meyer N, Racen E, Orsborn A, Kirchner J, Kuznicki K, et al. Genetic Analysis of the *Caenorhabditis elegans* GLH Family of P-Granule Proteins. *Genetics* [Internet]. 2008;178:1973–87. Available from: <http://www.ncbi.nlm.nih.gov/pmc/articles/PMC2323790/>
45. Seydoux G, Fire A. Soma-germline asymmetry in the distributions of embryonic RNAs in *Caenorhabditis elegans*. *Development.* 1994;120:2823–34.
46. Schisa JA, Pitt JN, Priess JR. Analysis of RNA associated with P granules in germ cells of *C. elegans* adults. *Development (Cambridge, England)* [Internet]. 2001;128:1287–98. Available from: <http://www.ncbi.nlm.nih.gov/pubmed/11262230>

47. Lee C-YS, Putnam A, Lu T, He S, Ouyang JPT, Seydoux G. Recruitment of mRNAs to P granules by condensation with intrinsically-disordered proteins. *Elife* [Internet]. 2020;9:e52896. Available from: <https://elifesciences.org/articles/52896>
48. Parker DM, Winkenbach LP, Boyson S, Saxton MN, Daidone C, Al-Mazaydeh ZA, et al. mRNA localization is linked to translation regulation in the *Caenorhabditis elegans* germ lineage. *Dev Camb Engl*. 2020;147:dev186817.
49. Subramaniam K, Seydoux G. *nos-1* and *nos-2*, two genes related to *Drosophila nanos*, regulate primordial germ cell development and survival in *Caenorhabditis elegans*. *Development* (Cambridge, England). 1999;126:4861–71.
50. Jadhav S, Rana M, Subramaniam K. Multiple maternal proteins coordinate to restrict the translation of *C. elegans nanos-2* to primordial germ cells. *Development* [Internet]. 2008;135:1803–12. Available from: <http://www.ncbi.nlm.nih.gov/pmc/articles/PMC2573031/>
51. Nover L, Scharf KD, Neumann D. Formation of cytoplasmic heat shock granules in tomato cell cultures and leaves. *Mol Cell Biol*. 1983;3:1648–55.
52. Collier NC, Schlesinger MJ. The dynamic state of heat shock proteins in chicken embryo fibroblasts. *J Cell Biology*. 1986;103:1495–507.
53. Kedersha NL, Gupta M, Li W, Miller I, Anderson P. RNA-Binding Proteins Tia-1 and Tiar Link the Phosphorylation of Eif-2 α to the Assembly of Mammalian Stress Granules. *J Cell Biology*. 1999;147:1431–42.
54. Jain S, Wheeler JR, Walters RW, Agrawal A, Barsic A, Parker R. ATPase-Modulated Stress Granules Contain a Diverse Proteome and Substructure. *Cell*. 2016;164:487–98.
55. Zhang K, Daigle JG, Cunningham KM, Coyne AN, Ruan K, Grima JC, et al. Stress Granule Assembly Disrupts Nucleocytoplasmic Transport. *Cell*. 2018;173:958-971.e17.
56. Yang X, Shen Y, Garre E, Hao X, Krumlinde D, Cvijović M, et al. Stress Granule-Defective Mutants Deregulate Stress Responsive Transcripts. *Plos Genet*. 2014;10:e1004763.
57. Zhang G, Wang Z, Du Z, Zhang H. mTOR Regulates Phase Separation of PGL Granules to Modulate Their Autophagic Degradation. *Cell* [Internet]. 2018;174:1492-1506.e22. Available from: <https://www.sciencedirect.com/science/article/pii/S0092867418310225>
58. Youn J-Y, Dyakov BJA, Zhang J, Knight JDR, Vernon RM, Forman-Kay JD, et al. Properties of Stress Granule and P-Body Proteomes. *Mol Cell*. 2019;76:286–94.
59. Riggs CL, Kedersha N, Ivanov P, Anderson P. Mammalian stress granules and P bodies at a glance. *J Cell Sci*. 2020;133:jcs242487.

60. Bashkirov VI, Scherthan H, Solinger JA, Buerstedde J-M, Heyer W-D. A Mouse Cytoplasmic Exoribonuclease (mXRN1p) with Preference for G4 Tetraplex Substrates. *J Cell Biology*. 1997;136:761–73.
61. Fenger-Grøn M, Fillman C, Norrild B, Lykke-Andersen J. Multiple Processing Body Factors and the ARE Binding Protein TTP Activate mRNA Decapping. *Mol Cell*. 2005;20:905–15.
62. Toombs JA, Sytnikova YA, Chirn G, Ang I, Lau NC, Blower MD. Xenopus Piwi proteins interact with a broad proportion of the oocyte transcriptome. *Rna*. 2017;23:504–20.
63. Suen KM, Braukmann F, Butler R, Bensaddek D, Akay A, Lin C-C, et al. DEPS-1 is required for piRNA-dependent silencing and PIWI condensate organisation in *Caenorhabditis elegans*. *Nat Commun*. 2020;11:4242.
64. Szostak E, Gebauer F. Translational control by 3'-UTR-binding proteins. *Brief Funct Genomics* [Internet]. 2013;12:58–65. Available from: <http://www.ncbi.nlm.nih.gov/pmc/articles/PMC3548161/>
65. Sepulveda G, Antkowiak M, Brust-Mascher I, Mahe K, Ou T, Castro NM, et al. Co-translational protein targeting facilitates centrosomal recruitment of PCNT during centrosome maturation in vertebrates. *Elife* [Internet]. 2018;7:e34959. Available from: <https://elifesciences.org/articles/34959>
66. Mason N, Ciufo LF, Brown JD. Elongation arrest is a physiologically important function of signal recognition particle. *Embo J*. 2000;19:4164–74.
67. Palacios IM, Johnston DS. Getting the message across: the intracellular localization of mRNAs in higher eukaryotes. *Annual review of cell and developmental biology*. 2001;17:569–614.
68. Parton RM, Davidson A, Davis I, Weil TT. Subcellular mRNA localisation at a glance. *Journal of Cell Science* [Internet]. 2014;127:2127 LP – 2133. Available from: <http://jcs.biologists.org/content/127/10/2127.abstract>
69. Martin KC, Ephrussi A. mRNA Localization: Gene Expression in the Spatial Dimension. *Cell* [Internet]. 2009;136:719. Available from: <http://www.ncbi.nlm.nih.gov/pmc/articles/PMC2819924/>
70. Lu W, Lakonishok M, Liu R, Billington N, Rich A, Glotzer M, et al. Competition between kinesin-1 and myosin-V defines *Drosophila* posterior determination. [Yamashita, M] Yukiko, editors. *eLife* [Internet]. 2020;9:e54216. Available from: <https://doi.org/10.7554/eLife.54216>
71. Mukherjee J, Hermesh O, Eliscovich C, Nalpas N, Franz-Wachtel M, Mäcek B, et al. β -Actin mRNA interactome mapping by proximity biotinylation. *Proceedings of the National Academy of Sciences of the United States of America*. 2019;116:12863–72.

72. Steward O, Levy WB. Preferential localization of polyribosomes under the base of dendritic spines in granule cells of the dentate gyrus. *J Neurosci Official J Soc Neurosci*. 1982;2:284–91.
73. Garner CC, Tucker RP, Matus A. Selective localization of messenger RNA for cytoskeletal protein MAP2 in dendrites. *Nature*. 1988;336.
74. Wang ET, Taliaferro JM, Lee J-A, Sudhakaran IP, Rossoll W, Gross C, et al. Dysregulation of mRNA Localization and Translation in Genetic Disease. *J Neurosci* [Internet]. 2016;36:11418–26. Available from: <http://www.jneurosci.org/lookup/doi/10.1523/JNEUROSCI.2352-16.2016>
75. Muddashetty RS, Kelić S, Gross C, Xu M, Bassell GJ. Dysregulated metabotropic glutamate receptor-dependent translation of AMPA receptor and postsynaptic density-95 mRNAs at synapses in a mouse model of fragile X syndrome. *J Neurosci Official J Soc Neurosci*. 2007;27:5338–48.
76. Yoon BC, Zivraj KH, Holt CE. Cell Biology of the Axon. *Results Problems Cell Differ*. 2009;48:108–38.
77. Trcek T, Douglas TE, Grosch M, Yin Y, Eagle WVI, Gavis ER, et al. Sequence-Independent Self-Assembly of Germ Granule mRNAs into Homotypic Clusters. *Mol Cell*. 2020;
78. Irion U, Johnston DS. bicoid RNA localization requires specific binding of an endosomal sorting complex. *Nature* [Internet]. 2007;445:554–8. Available from: <https://pubmed.ncbi.nlm.nih.gov/17268469>
<https://www.ncbi.nlm.nih.gov/pmc/articles/PMC1997307/>
79. Frohnhöfer HG, Nüsslein-Volhard C. Organization of anterior pattern in the *Drosophila* embryo by the maternal gene bicoid. *Nature* [Internet]. 1986;324:120–5. Available from: <https://doi.org/10.1038/324120a0>
80. Gavis ER, Lehmann R. Localization of nanos RNA controls embryonic polarity. *Cell*. 1992;71:301–13.
81. Kugler J-M, Lasko P. Localization, anchoring and translational control of oskar, gurken, bicoid and nanos mRNA during *Drosophila* oogenesis. *Fly*. 2009;3:15–28.
82. Hughes SC, Simmonds AJ. *Drosophila* mRNA Localization During Later Development: Past, Present, and Future. *Frontiers Genetics*. 2019;10:135.
83. Ali-Murthy Z, Kornberg TB. Bicoid gradient formation and function in the *Drosophila* pre-syncytial blastoderm. *Elife*. 2016;5:e13222.
84. Shepard KA, Gerber AP, Jambhekar A, Takizawa PA, Brown PO, Herschlag D, et al. Widespread cytoplasmic mRNA transport in yeast: Identification of 22 bud-localized transcripts using DNA microarray analysis. *Proc National Acad Sci*. 2003;100:11429–34.

85. Tutucci E, Vera M, Biswas J, Garcia J, Parker R, Singer RH. An improved MS2 system for accurate reporting of the mRNA life cycle. *Nature methods* [Internet]. 2018;15:81–9. Available from: <http://www.ncbi.nlm.nih.gov/pmc/articles/PMC5843578/>
86. Bertrand E, Chartrand P, Schaefer M, Shenoy SM, Singer RH, Long RM. Localization of ASH1 mRNA Particles in Living Yeast. *Mol Cell*. 1998;2:437–45.
87. Long RM, Elliott DJ, Stutz F, Rosbash M, Singer RH. Spatial consequences of defective processing of specific yeast mRNAs revealed by fluorescent in situ hybridization. *Rna New York N Y*. 1995;1:1071–8.
88. Gu W, Deng Y, Zenklusen D, Singer RH. A new yeast PUF family protein, Puf6p, represses ASH1 mRNA translation and is required for its localization. *Gene Dev*. 2004;18:1452–65.
89. Paquin N, Chartrand P. Local regulation of mRNA translation: new insights from the bud. *Trends in cell biology*. 2008;18:105–11.
90. Ma W, Mayr C. A Membraneless Organelle Associated with the Endoplasmic Reticulum Enables 3'UTR-Mediated Protein-Protein Interactions. *Cell* [Internet]. 2018;175:1492-1506.e19. Available from: <https://doi.org/10.1016/j.cell.2018.10.007>
91. Pizzinga M, Bates C, Lui J, Forte G, Morales-Polanco F, Linney E, et al. Translation factor mRNA granules direct protein synthetic capacity to regions of polarized growth. *J Cell Biol*. 2019;218:1564–81.
92. Morales-Polanco F, Bates C, Lui J, Casson J, Solari CA, Pizzinga M, et al. Core Fermentation (CoFe) granules focus coordinated glycolytic mRNA localization and translation to fuel glucose fermentation. *Iscience*. 2021;24:102069.
93. Huizar RL, Lee C, Boulgakov AA, Horani A, Tu F, Marcotte EM, et al. A liquid-like organelle at the root of motile ciliopathy. *Elife*. 2018;7:e38497.
94. Aprea I, Raidt J, Höben IM, Loges NT, Nöthe-Menchen T, Pennekamp P, et al. Defects in the cytoplasmic assembly of axonemal dynein arms cause morphological abnormalities and dysmotility in sperm cells leading to male infertility. *Plos Genet*. 2021;17:e1009306.
95. Mardakheh FK, Paul A, Kümper S, Sadok A, Paterson H, Mccarthy A, et al. Global Analysis of mRNA, Translation, and Protein Localization: Local Translation Is a Key Regulator of Cell Protrusions. *Dev Cell*. 2015;35:344–57.
96. Costa AR, Sousa SC, Pinto-Costa R, Mateus JC, Lopes CD, Costa AC, et al. The membrane periodic skeleton is an actomyosin network that regulates axonal diameter and conduction. *Elife*. 2020;9:e55471.

97. Moissoglu K, Stueland M, Gasparski AN, Wang T, Jenkins LM, Hastings ML, et al. RNA localization and co-translational interactions control RAB13 GTPase function and cell migration. *Embo J*. 2020;39:e104958.
98. Wang T, Hamilla S, Cam M, Aranda-Espinoza H, Mili S. Extracellular matrix stiffness and cell contractility control RNA localization to promote cell migration. *Nat Commun*. 2017;8:896.
99. Pichon X, Moissoglu K, Coleno E, Wang T, Imbert A, Robert M-C, et al. The kinesin KIF1C transports APC-dependent mRNAs to cell protrusions. *Rna*. 2021;27:rna.078576.120.
100. Goering R, Arora A, Taliaferro JM. RNA localization mechanisms transcend cell morphology. *Biorxiv*. 2022;2022.04.14.488401.
101. Blobel G, Walter P, Chang CN, Goldman BM, Erickson AH, Lingappa VR. Translocation of proteins across membranes: the signal hypothesis and beyond. *Symposia of the Society for Experimental Biology* [Internet]. 1979;33:9–36. Available from: <http://europepmc.org/abstract/MED/524275>
102. Walter P, Blobel G. Translocation of proteins across the endoplasmic reticulum III. Signal recognition protein (SRP) causes signal sequence-dependent and site-specific arrest of chain elongation that is released by microsomal membranes. *J Cell Biology*. 1981;91:557–61.
103. Ast T, Cohen G, Schuldiner M. A network of cytosolic factors targets SRP-independent proteins to the endoplasmic reticulum. *Cell* [Internet]. 2013;152:1134–45. Available from: <https://doi.org/10.1016/j.cell.2013.02.003>
104. Jan CH, Williams CC, Weissman JS. Principles of ER cotranslational translocation revealed by proximity-specific ribosome profiling. *Science* [Internet]. 2014;346:1257521. Available from: <https://pubmed.ncbi.nlm.nih.gov/25378630>
<https://www.ncbi.nlm.nih.gov/pmc/articles/PMC4285348/>
105. Siegel V, Walter P. Removal of the Alu structural domain from signal recognition particle leaves its protein translocation activity intact. *Nature*. 1986;320:81–4.
106. Cohen-Zontag O, Baez C, Lim LQJ, Olender T, Schirman D, Dahary D, et al. A secretion-enhancing cis regulatory targeting element (SECRETE) involved in mRNA localization and protein synthesis. *Plos Genet*. 2019;15:e1008248.
107. Chartron JW, Hunt KCL, Frydman J. Cotranslational signal-independent SRP preloading during membrane targeting. *Nature* [Internet]. 2016;536:224–8. Available from: <https://doi.org/10.1038/nature19309>
108. Jagannathan S, Reid DW, Cox AH, Nicchitta CV. De novo translation initiation on membrane-bound ribosomes as a mechanism for localization of cytosolic protein mRNAs to the endoplasmic reticulum. *RNA (New York, NY)*. 2014;20:1489–98.

109. Wu B, Eliscovich C, Yoon YJ, Singer RH. Translation dynamics of single mRNAs in live cells and neurons. *Science*. 2016;352:1430–5.
110. Gadir N, Haim-Vilmovsky L, Kraut-Cohen J, Gerst JE. Localization of mRNAs coding for mitochondrial proteins in the yeast *Saccharomyces cerevisiae*. *Rna*. 2011;17:1551–65.
111. Williams CC, Jan CH, Weissman JS. Targeting and plasticity of mitochondrial proteins revealed by proximity-specific ribosome profiling. *Science*. 2014;346:748–51.
112. Lesnik C, Cohen Y, Atir-Lande A, Schuldiner M, Arava Y. OM14 is a mitochondrial receptor for cytosolic ribosomes that supports co-translational import into mitochondria. *Nat Commun*. 2014;5:5711.
113. Gold VA, Chroscicki P, Bragoszewski P, Chacinska A. Visualization of cytosolic ribosomes on the surface of mitochondria by electron cryo-tomography. *Embo Rep*. 2017;18:1786–800.
114. Gamerding M, Hanebuth MA, Frickey T, Deuerling E. The principle of antagonism ensures protein targeting specificity at the endoplasmic reticulum. *Science*. 2015;348:201–7.
115. Field CM, Alberts BM. Anillin, a contractile ring protein that cycles from the nucleus to the cell cortex. *The Journal of cell biology*. 1995;131:165–78.
116. Hirashima T, Tanaka R, Yamaguchi M, Yoshida H. The ABD on the nascent polypeptide and PH domain are required for the precise Anillin localization in *Drosophila* syncytial blastoderm. *Sci Rep-uk [Internet]*. 2018;8:12910. Available from: <https://doi.org/10.1038/s41598-018-31106-0>
117. Tocchini C, Rohner M, Guerard L, Ray P, Stetina SEV, Mango SE. Translation-dependent mRNA localization to *Caenorhabditis elegans* adherens junctions. *Dev Camb Engl [Internet]*. 2021;148:dev200027. Available from: <https://doi.org/10.1242/dev.200027>
118. Potapova T, Gorbsky GJ. The Consequences of Chromosome Segregation Errors in Mitosis and Meiosis. *Biology [Internet]*. 2017;6:12. Available from: <https://pubmed.ncbi.nlm.nih.gov/28208750>
<https://www.ncbi.nlm.nih.gov/pmc/articles/PMC5372005/>
119. Kim S, Rhee K. Importance of the CEP215-pericentrin interaction for centrosome maturation during mitosis. *PloS one [Internet]*. 2014;9:e87016–e87016. Available from: <https://pubmed.ncbi.nlm.nih.gov/24466316>
<https://www.ncbi.nlm.nih.gov/pmc/articles/PMC3899370/>
120. Safieddine A, Coleno E, Salloum S, Imbert A, Traboulsi A-M, Kwon OS, et al. A choreography of centrosomal mRNAs reveals a conserved localization mechanism involving active polysome transport. *Nat Commun [Internet]*. 2021;12:1352. Available from: <https://doi.org/10.1038/s41467-021-21585-7>

121. Moor AE, Golan M, Massasa EE, Lemze D, Weizman T, Shenhav R, et al. Global mRNA polarization regulates translation efficiency in the intestinal epithelium. *Science* [Internet]. 2017;357:1299 LP – 1303. Available from: <http://science.sciencemag.org/content/357/6357/1299.abstract>
122. Llopis PM, Jackson AF, Sliusarenko O, Surovtsev I, Heinritz J, Emonet T, et al. Spatial organization of the flow of genetic information in bacteria. *Nature* [Internet]. 2010;466:77–81. Available from: <https://pubmed.ncbi.nlm.nih.gov/20562858>
123. Broadus J, Fuerstenberg S, Doe CQ. Staufer-dependent localization of prospero mRNA contributes to neuroblast daughter-cell fate. *Nature* [Internet]. 1998;391:792–5. Available from: <https://doi.org/10.1038/35861>
124. Ephrussi A, Dickinson LK, Lehmann R. oskar organizes the germ plasm and directs localization of the posterior determinant nanos. *Cell* [Internet]. 1991;66:37–50. Available from: <https://www.sciencedirect.com/science/article/pii/009286749190137N>
125. Aoki ST, Lynch TR, Crittenden SL, Bingman CA, Wickens M, Kimble J. C. elegans germ granules require both assembly and localized regulators for mRNA repression. *Nat Commun* [Internet]. 2021;12:996. Available from: <https://doi.org/10.1038/s41467-021-21278-1>
126. Nishimura EO, Zhang JC, Werts AD, Goldstein B, Lieb JD. Asymmetric Transcript Discovery by RNA-seq in *C. elegans* Blastomeres Identifies neg-1, a Gene Important for Anterior Morphogenesis. ["Mango, E"] Susan, editors. *Plos Genet* [Internet]. 2015;11:e1005117. Available from: <http://www.ncbi.nlm.nih.gov/pmc/articles/PMC4395330/>
127. Updike D, Strome S. P Granule Assembly and Function in *Caenorhabditis elegans* Germ Cells. 2010;31:53–60.
128. Engel KL, Arora A, Goering R, Lo HG, Taliaferro JM. Mechanisms and consequences of subcellular RNA localization across diverse cell types. *Traffic* [Internet]. 2020;21:404–18. Available from: <https://pubmed.ncbi.nlm.nih.gov/32291836>
129. Walter P, Johnson AE. Signal sequence recognition and protein targeting to the endoplasmic reticulum membrane. *Annu Rev Cell Biol* [Internet]. 1994;10:87–119. Available from: <http://www.annualreviews.org/doi/10.1146/annurev.cb.10.110194.000511>
130. Tintori SC, Nishimura EO, Golden P, Lieb JD, Goldstein B. A Transcriptional Lineage of the Early *C. elegans* Embryo. *Dev Cell* [Internet]. 2016;38:430–44. Available from: <http://www.ncbi.nlm.nih.gov/pmc/articles/PMC4999266/>
131. Furden D van, Johnson K, Segbert C, Bossinger O. The *C. elegans* ezrin-radixin-moesin protein ERM-1 is necessary for apical junction remodelling and tubulogenesis in the intestine. *Dev Biol* [Internet]. 2004;272:262–76. Available from: <http://www.sciencedirect.com/science/article/pii/S0012160604003562>

132. Göbel V, Barrett PL, Hall DH, Fleming JT. Lumen Morphogenesis in *C. elegans* Requires the Membrane-Cytoskeleton Linker erm-1. *Dev Cell* [Internet]. 2004;6:865–73. Available from: <https://www.sciencedirect.com/science/article/pii/S1534580704001716>
133. Parker DM, Winkenbach LP, Boyson SP, Saxton MN, Daidone C, Al-Mazaydeh ZA, et al. mRNA localization is linked to translation regulation in the *Caenorhabditis elegans* germ lineage. *Development* [Internet]. 2020;2020.01.09.900498. Available from: <http://biorxiv.org/content/early/2020/01/09/2020.01.09.900498.abstract>
134. Fehon RG, McClatchey AI, Bretscher A. Organizing the cell cortex: the role of ERM proteins. *Nat Rev Mol Cell Bio* [Internet]. 2010;11:276–87. Available from: <https://doi.org/10.1038/nrm2866>
135. McClatchey AI. ERM proteins at a glance. *J Cell Sci* [Internet]. 2014;127:3199–204. Available from: <https://doi.org/10.1242/jcs.098343>
136. Ramalho JJ, Sepers JJ, Nicolle O, Schmidt R, Cravo J, Michaux G, et al. C-terminal phosphorylation modulates ERM-1 localization and dynamics to control cortical actin organization and support lumen formation during *Caenorhabditis elegans* development. *Development* [Internet]. 2020;147:dev188011. Available from: <http://dev.biologists.org/content/147/14/dev188011.abstract>
137. Berset C, Trachsel H, Altmann M. The TOR (target of rapamycin) signal transduction pathway regulates the stability of translation initiation factor eIF4G in the yeast *Saccharomyces cerevisiae*. *Proc National Acad Sci* [Internet]. 1998;95:4264–9. Available from: <http://www.pnas.org/content/95/8/4264.abstract>
138. Kim W, Underwood RS, Greenwald I, Shaye DD. OrthoList 2: A New Comparative Genomic Analysis of Human and *Caenorhabditis elegans* Genes. *Genetics* [Internet]. 2018;210:445–61. Available from: <https://pubmed.ncbi.nlm.nih.gov/30120140>
139. Ramírez-Valle F, Braunstein S, Zavadil J, Formenti SC, Schneider RJ. eIF4GI links nutrient sensing by mTOR to cell proliferation and inhibition of autophagy. *J Cell Biology* [Internet]. 2008;181:293–307. Available from: <https://doi.org/10.1083/jcb.200710215>
140. Rogers AN, Chen D, McColl G, Czerwieńiec G, Felkey K, Gibson BW, et al. Life span extension via eIF4G inhibition is mediated by posttranscriptional remodeling of stress response gene expression in *C. elegans*. *Cell Metab* [Internet]. 2011;14:55–66. Available from: <https://www.ncbi.nlm.nih.gov/pubmed/21723504>
<https://www.ncbi.nlm.nih.gov/pmc/PMC3220185/>
141. Corish P, Tyler-Smith C. Attenuation of green fluorescent protein half-life in mammalian cells. *Protein Eng Des Sel* [Internet]. 1999;12:1035–40. Available from: <https://doi.org/10.1093/protein/12.12.1035>

142. Kaymak E, Farley BM, Hay SA, Li C, Ho S, Hartman DJ, et al. Efficient generation of transgenic reporter strains and analysis of expression patterns in *Caenorhabditis elegans* using library MosSCI. *Dev Dynam*. 2016;245:925–36.
143. Li X, Zhao X, Fang Y, Jiang X, Duong T, Fan C, et al. Generation of destabilized green fluorescent protein as a transcription reporter. *J Biol Chem*. 1998;273:34970–5.
144. Cuesta R, Laroia G, Schneider RJ. Chaperone hsp27 inhibits translation during heat shock by binding eIF4G and facilitating dissociation of cap-initiation complexes. *Genes & development* [Internet]. 2000;14:1460–70. Available from: <https://www.ncbi.nlm.nih.gov/pubmed/10859165>
<https://www.ncbi.nlm.nih.gov/pmc/articles/PMC316692/>
145. Duncan R, Hershey JW. Heat shock-induced translational alterations in HeLa cells. Initiation factor modifications and the inhibition of translation. *J Biological Chem*. 1984;259:11882–9.
146. Duncan RF, Hershey JW. Protein synthesis and protein phosphorylation during heat stress, recovery, and adaptation. *The Journal of cell biology*. 1989;109:1467–81.
147. Shalgi R, Hurt JA, Krykbaeva I, Taipale M, Lindquist S, Burge CB. Widespread Regulation of Translation by Elongation Pausing in Heat Shock. *Mol Cell*. 2013;49:439–52.
148. Azzam ME, Algranati ID. Mechanism of Puromycin Action: Fate of Ribosomes after Release of Nascent Protein Chains from Polysomes. *Proceedings of the National Academy of Sciences of the United States of America* [Internet]. 1973;70:3866–9. Available from: <http://www.ncbi.nlm.nih.gov/pmc/articles/PMC427346/>
149. Schneider-Poetsch T, Ju J, Eyler DE, Dang Y, Bhat S, Merrick WC, et al. Inhibition of Eukaryotic Translation Elongation by Cycloheximide and Lactimidomycin. *Nat Chem Biol* [Internet]. 2010;6:209–17. Available from: <http://www.ncbi.nlm.nih.gov/pmc/articles/PMC2831214/>
150. Olson SK, Greenan G, Desai A, Müller-Reichert T, Oegema K. Hierarchical assembly of the eggshell and permeability barrier in *C. elegans*. *J Cell Biology* [Internet]. 2012;198:731–48. Available from: <http://www.ncbi.nlm.nih.gov/pmc/articles/PMC3514041/>
151. Stein KK, Golden A. The *C. elegans* eggshell. *Wormbook* [Internet]. 2015;1–35. Available from: <http://www.ncbi.nlm.nih.gov/pmc/articles/PMC5603424/>
152. Carvalho A, Olson SK, Gutierrez E, Zhang K, Noble LB, Zanin E, et al. Acute Drug Treatment in the Early *C. elegans* Embryo. [“Lehner, Ben”], editors. *Plos One* [Internet]. 2011;6:e24656. Available from: <http://www.ncbi.nlm.nih.gov/pmc/articles/PMC3173474/>

153. Bretscher A. Purification of an 80,000-dalton protein that is a component of the isolated microvillus cytoskeleton, and its localization in nonmuscle cells. *The Journal of cell biology*. 1983;97:425–32.
154. Lankes WT, Furthmayr H. Moesin: a member of the protein 4.1-talin-ezrin family of proteins. *Proceedings of the National Academy of Sciences* [Internet]. 1991;88:8297–301. Available from: <https://doi.org/10.1073/pnas.88.19.8297>
155. Tsukita S, Hieda Y, Tsukita S. A new 82-kD barbed end-capping protein (radixin) localized in the cell-to-cell adherens junction: purification and characterization. *J Cell Biology*. 1989;108:2369–82.
156. Barret C, Roy C, Montcourrier P, Mangeat P, Niggli V. Mutagenesis of the Phosphatidylinositol 4,5-Bisphosphate (Pip2) Binding Site in the Nh2-Terminal Domain of Ezrin Correlates with Its Altered Cellular Distribution. *J Cell Biology* [Internet]. 2000;151:1067–80. Available from: <https://pubmed.ncbi.nlm.nih.gov/11086008>
<https://www.ncbi.nlm.nih.gov/pmc/articles/PMC2174347/>
157. Roch F, Polesello C, Roubinet C, Martin M, Roy C, Valenti P, et al. Differential roles of PtdIns(4,5)P2 and phosphorylation in moesin activation during *Drosophila* development. *J Cell Sci* [Internet]. 2010;123:2058–67. Available from: <https://doi.org/10.1242/jcs.064550>
158. Li Q, Nance MR, Kulikauskas R, Nyberg K, Fehon R, Karplus PA, et al. Self-masking in an intact ERM-merlin protein: an active role for the central alpha-helical domain. *J Mol Biol*. 2007;365:1446–59.
159. Pearson MA, Reczek D, Bretscher A, Karplus PA. Structure of the ERM protein moesin reveals the FERM domain fold masked by an extended actin binding tail domain. *Cell*. 2000;101:259–70.
160. Carreno S, Kouranti I, Glusman ES, Fuller MT, Echard A, Payre F. Moesin and its activating kinase Slik are required for cortical stability and microtubule organization in mitotic cells. *J Cell Biology* [Internet]. 2008;180:739–46. Available from: <https://pubmed.ncbi.nlm.nih.gov/18283112>
<https://www.ncbi.nlm.nih.gov/pmc/articles/PMC2265583/>
161. Zhang X, Flores LR, Keeling MC, Sliogeryte K, Gavara N. Ezrin Phosphorylation at T567 Modulates Cell Migration, Mechanical Properties, and Cytoskeletal Organization. *Int J Mol Sci*. 2020;21:435.
162. Senju Y, Kalimeri M, Koskela EV, Somerharju P, Zhao H, Vattulainen I, et al. Mechanistic principles underlying regulation of the actin cytoskeleton by phosphoinositides. *Proc National Acad Sci* [Internet]. 2017;114:E8977–86. Available from: <https://www.pnas.org/content/114/43/E8977>

163. Maddox AS, Habermann B, Desai A, Oegema K. Distinct roles for two *C. elegans* anillins in the gonad and early embryo. *Development* [Internet]. 2005;132:2837–48. Available from: <https://doi.org/10.1242/dev.01828>
164. Rogalski TM, Mullen GP, Gilbert MM, Williams BD, Moerman DG. The UNC-112 Gene in *Caenorhabditis elegans* Encodes a Novel Component of Cell–Matrix Adhesion Structures Required for Integrin Localization in the Muscle Cell Membrane. *J Cell Biology* [Internet]. 2000;150:253–64. Available from: <https://pubmed.ncbi.nlm.nih.gov/10893272>
165. Piekny AJ, Johnson J-LF, Cham GD, Mains PE. The *Caenorhabditis elegans* nonmuscle myosin genes *nmy-1* and *nmy-2* function as redundant components of the *let-502*/Rho-binding kinase and *mel-11*/myosin phosphatase pathway during embryonic morphogenesis. *Development* [Internet]. 2003;130:5695–704. Available from: <https://doi.org/10.1242/dev.00807>
166. Hunt-Newbury R, Viveiros R, Johnsen R, Mah A, Anastas D, Fang L, et al. High-Throughput In Vivo Analysis of Gene Expression in *Caenorhabditis elegans*. *Plos Biol* [Internet]. 2007;5:e237. Available from: <https://pubmed.ncbi.nlm.nih.gov/17850180>
167. Josephson MP, Aliani R, Norris ML, Ochs ME, Gujar M, Lundquist EA. The *Caenorhabditis elegans* NF2/Merlin Molecule NFM-1 Nonautonomously Regulates Neuroblast Migration and Interacts Genetically with the Guidance Cue SLT-1/Slit. *Genetics* [Internet]. 2017;205:737–48. Available from: <https://pubmed.ncbi.nlm.nih.gov/27913619>
168. Thompson HM, Skop AR, Euteneuer U, Meyer BJ, McNiven MA. The Large GTPase Dynamin Associates with the Spindle Midzone and Is Required for Cytokinesis. *Curr Biol* [Internet]. 2002;12:2111–7. Available from: <https://pubmed.ncbi.nlm.nih.gov/12498685>
169. Uchida Y, Ogata M, Mori Y, Oh-hora M, Hatano N, Hamaoka T. Localization of PTP-FERM in Nerve Processes through Its FERM Domain. *Biochem Bioph Res Co* [Internet]. 2002;292:13–9. Available from: <https://www.sciencedirect.com/science/article/pii/S0006291X02966131>
170. Zou W, Lu Q, Zhao D, Li W, Mapes J, Xie Y, et al. *Caenorhabditis elegans* Myotubularin MTM-1 Negatively Regulates the Engulfment of Apoptotic Cells. *Plos Genet* [Internet]. 2009;5:e1000679. Available from: <https://pubmed.ncbi.nlm.nih.gov/19816564>
171. Li Z, Zhang P, Zhang R, Wang X, Tse YC, Zhang H. A collection of toolkit strains reveals distinct localization and dynamics of membrane-associated transcripts in epithelia. *Cell Reports* [Internet]. 2021;35:109072. Available from: <https://www.sciencedirect.com/science/article/pii/S2211124721004034>
172. Kobori T, Tameishi M, Tanaka C, Urashima Y, Obata T. Subcellular distribution of ezrin/radixin/moesin and their roles in the cell surface localization and transport function of P-glycoprotein in human colon adenocarcinoma LS180 cells. *Plos One* [Internet]. 2021;16:e0250889. Available from: <https://pubmed.ncbi.nlm.nih.gov/33974673>

173. McClatchey AI. Merlin and ERM proteins: unappreciated roles in cancer development? *Nat Rev Cancer* [Internet]. 2003;3:877–83. Available from: <https://doi.org/10.1038/nrc1213>
174. Das S, Vera M, Gandin V, Singer RH, Tutucci E. Intracellular mRNA transport and localized translation. *Nat Rev Mol Cell Bio* [Internet]. 2021;22:483–504. Available from: <https://doi.org/10.1038/s41580-021-00356-8>
175. Cohen MJ, Chirico WJ, Lipke PN. Through the back door: Unconventional protein secretion. *Cell Surf* [Internet]. 2020;6:100045. Available from: <https://www.sciencedirect.com/science/article/pii/S2468233020300128>
176. Keenan RJ, Freymann DM, Stroud RM, Walter P. THE SIGNAL RECOGNITION PARTICLE. *Annu Rev Biochem*. 2001;70:755–75.
177. Brenner S. THE GENETICS OF CAENORHABDITIS ELEGANS. *Genetics* [Internet]. 1974;77:71–94. Available from: <https://pubmed.ncbi.nlm.nih.gov/4366476>
178. Fraser AG, Kamath RS, Zipperlen P, Martinez-Campos M, Sohrmann M, Ahringer J. Functional genomic analysis of *C. elegans* chromosome I by systematic RNA interference. *Nature* [Internet]. 2000;408:325–30. Available from: <https://doi.org/10.1038/35042517>
179. Parker DM, Winkenbach LP, Parker A, Boyson S, Nishimura EO. Improved Methods for Single-Molecule Fluorescence In Situ Hybridization and Immunofluorescence in *Caenorhabditis elegans* Embryos. *Curr Protoc* [Internet]. 2021;1:e299. Available from: <https://doi.org/10.1002/cpz1.299>
180. Schindelin J, Arganda-Carreras I, Frise E, Kaynig V, Longair M, Pietzsch T, et al. Fiji: An open-source platform for biological-image analysis. *Nat Methods*. 2012;9:676–82.
181. Tsanov N, Samacoits A, Chouaib R, Traboulsi A-M, Gostan T, Weber C, et al. smiFISH and FISH-quant – a flexible single RNA detection approach with super-resolution capability. *Nucleic Acids Res*. 2016;44:e165–e165.
182. Ouyang W, Mueller F, Hjelmare M, Lundberg E, Zimmer C. ImJoy: an open-source computational platform for the deep learning era. *Nat Methods*. 2019;16:1199–200.
183. Mueller F, Senecal A, Tantale K, Marie-Nelly H, Ly N, Collin O, et al. FISH-quant: automatic counting of transcripts in 3D FISH images. *Nat Methods* [Internet]. 2013;10:277–8. Available from: <http://www.nature.com/doifinder/10.1038/nmeth.2406>
184. Macara IG. Transport into and out of the Nucleus. *Microbiol Mol Biol R*. 2001;65:570–94.
185. Dworetzky SI, Feldherr CM. Translocation of RNA-coated gold particles through the nuclear pores of oocytes. *J Cell Biology*. 1988;106:575–84.

186. Twyffels L, Gueydan C, Kruijs V. Transportin-1 and Transportin-2: Protein nuclear import and beyond. *Febs Lett.* 2014;588:1857–68.
187. Quan Y, Ji Z-L, Wang X, Tartakoff AM, Tao T. Evolutionary and Transcriptional Analysis of Karyopherin β Superfamily Proteins. *Mol Cell Proteomics.* 2008;7:1254–69.
188. Putker M, Madl T, Vos HR, Ruiter H de, Visscher M, Berg MCW van den, et al. Redox-dependent control of FOXO/DAF-16 by transportin-1. *Molecular cell.* 2013;49:730–42.
189. Kamath RS, Fraser AG, Dong Y, Poulin G, Durbin R, Gotta M, et al. Systematic functional analysis of the *Caenorhabditis elegans* genome using RNAi. *Nature.* 2003;421:231–7.
190. Rual J-F, Ceron J, Koreth J, Hao T, Nicot A-S, Hirozane-Kishikawa T, et al. Toward Improving *Caenorhabditis elegans* Phenome Mapping With an ORFeome-Based RNAi Library. *Genome Res.* 2004;14:2162–8.
191. Sönnichsen B, Koski LB, Walsh A, Marschall P, Neumann B, Brehm M, et al. Full-genome RNAi profiling of early embryogenesis in *Caenorhabditis elegans*. *Nature.* 2005;434:462–9.
192. Alqadah A, Hsieh Y-W, Xiong R, Lesch BJ, Chang C, Chuang C-F. A universal transportin protein drives stochastic choice of olfactory neurons via specific nuclear import of a sox-2-activating factor. *Proc National Acad Sci.* 2019;116:25137–46.
193. Pyhtila B, Zheng T, Lager PJ, Keene JD, Reedy MC, Nicchitta CV. Signal sequence- and translation-independent mRNA localization to the endoplasmic reticulum. *RNA (New York, NY)* [Internet]. 2008;14:445–53. Available from: <https://pubmed.ncbi.nlm.nih.gov/18192611>
<https://www.ncbi.nlm.nih.gov/pmc/articles/PMC2248262/>
194. Jagannathan S, Nwosu C, Nicchitta CV. Analyzing mRNA localization to the endoplasmic reticulum via cell fractionation. *Methods in molecular biology (Clifton, NJ)* [Internet]. 2011;714:301–21. Available from: <https://pubmed.ncbi.nlm.nih.gov/21431749>
<https://www.ncbi.nlm.nih.gov/pmc/articles/PMC3718476/>
195. Stein KK, Golden A. The *C. elegans* eggshell. *Wormbook.* 2018;1–36.
196. Cao Y, Cui Y, Liao J, Gao C, Zhao Z, Zhang J. Sevoflurane Preconditioning Increases Stress Resistance via IMB-2/DAF-16 in *Caenorhabditis Elegans*. Dose-response. 2022;20:15593258221082886.
197. Rodriguez M, Snoek LB, Bono MD, Kammenga JE. Worms under stress: *C. elegans* stress response and its relevance to complex human disease and aging. *Trends Genet.* 2013;29:367–74.
198. Duncan R, Hershey JW. Heat shock-induced translational alterations in HeLa cells. Initiation factor modifications and the inhibition of translation. *J Biol Chem.* 1984;259:11882–9.

199. Calissi G, Lam EW-F, Link W. Therapeutic strategies targeting FOXO transcription factors. *Nat Rev Drug Discov.* 2021;20:21–38.
200. Mahboubi H, Seganathy E, Kong D, Stochaj U. Identification of Novel Stress Granule Components That Are Involved in Nuclear Transport. *Plos One.* 2013;8:e68356.
201. Chang W-L, Tarn W-Y. A role for transportin in deposition of TTP to cytoplasmic RNA granules and mRNA decay. *Nucleic Acids Res.* 2009;37:6600–12.
202. Kim JH, Dhanasekaran SM, Prensner JR, Cao X, Robinson D, Kalyana-Sundaram S. Deep sequencing reveals distinct patterns of DNA methylation in prostate cancer. *Genome Res* [Internet]. 2011;21. Available from: <https://doi.org/10.1101/gr.119347.110>
203. Huelgas-Morales G, Silva-García CG, Salinas LS, Greenstein D, Navarro RE. The Stress Granule RNA-Binding Protein TIAR-1 Protects Female Germ Cells from Heat Shock in *Caenorhabditis elegans*. *G3 Genes Genomes Genetics.* 2016;6:1031–47.
204. Gaudet P, Livstone MS, Lewis SE, Thomas PD. Phylogenetic-based propagation of functional annotations within the Gene Ontology consortium. *Brief Bioinform.* 2011;12:449–62.
205. Vetter IR, Arndt A, Kutay U, Görlich D, Wittinghofer A. Structural view of the Ran-Importin beta interaction at 2.3 Å resolution. *Cell.* 1999;97:635–46.
206. Henderson ST, Johnson TE. *daf-16* integrates developmental and environmental inputs to mediate aging in the nematode *Caenorhabditis elegans*. *Curr Biol.* 2005;15:690.
207. Lee RYN, Hench J, Ruvkun G. Regulation of *C. elegans* DAF-16 and its human ortholog FKHRL1 by the *daf-2* insulin-like signaling pathway. *Curr Biol.* 2001;11:1950–7.
208. Folick A, Oakley HD, Yu Y, Armstrong EH, Kumari M, Sanor L, et al. Aging. Lysosomal signaling molecules regulate longevity in *Caenorhabditis elegans*. *Sci New York N Y.* 2015;347:83–6.
209. Ezak MJ, Ferkey DM. A Functional Nuclear Localization Sequence in the *C. elegans* TRPV Channel OCR-2. *Plos One.* 2011;6:e25047.
210. Duffy J, Zhang Q, Jung SY, Wang MC. Lipid chaperone LBP-8 coordinates with nuclear factors to promote longevity in *Caenorhabditis elegans*. *Biorxiv.* 2021;2021.09.09.459489.
211. Mboukou A, Rajendra V, Kleinova R, Tisné C, Jantsch MF, Barraud P. Transportin-1: A Nuclear Import Receptor with Moonlighting Functions. *Frontiers Mol Biosci.* 2021;8:638149.
212. Khong A, Parker R. mRNP architecture in translating and stress conditions reveals an ordered pathway of mRNP compaction. *J Cell Biol* [Internet]. 2018;217:4124–40. Available from: <http://jcb.rupress.org/content/217/12/4124>

213. Dormann D, Rodde R, Edbauer D, Bentmann E, Fischer I, Hruscha A, et al. ALS-associated fused in sarcoma (FUS) mutations disrupt Transportin-mediated nuclear import. *Embo J*. 2010;29:2841–57.
214. Berleth T, Burri M, Thoma G, Bopp D, Richstein S, Frigerio G, et al. The role of localization of bicoid RNA in organizing the anterior pattern of the *Drosophila* embryo. *The EMBO journal*. 1988;7:1749–56.
215. Kronja I, Yuan B, Eichhorn SW, Dzek K, Krijgsveld J, Bartel DP, et al. Widespread Changes in the Posttranscriptional Landscape at the *Drosophila* Oocyte-to-Embryo Transition. *Cell Reports*. 2014;7:1495–508.
216. Eichhorn SW, Subtelny AO, Kronja I, Kwasnieski JC, Orr-Weaver TL, Bartel DP. mRNA poly(A)-tail changes specified by deadenylation broadly reshape translation in *Drosophila* oocytes and early embryos. *Elife*. 2016;5:e16955.
217. Subtelny AO, Eichhorn SW, Chen GR, Sive H, Bartel DP. Poly(A)-tail profiling reveals an embryonic switch in translational control. *Nature*. 2014;508:66–71.
218. Wang QT, Piotrowska K, Ciemerych MA, Milenkovic L, Scott MP, Davis RW, et al. A Genome-Wide Study of Gene Activity Reveals Developmental Signaling Pathways in the Preimplantation Mouse Embryo. *Dev Cell*. 2004;6:133–44.
219. Baugh LR, Hill AA, Slonim DK, Brown EL, Hunter CP. Composition and dynamics of the *Caenorhabditis elegans* early embryonic transcriptome. *Development*. 2003;130:889–900.
220. Stoeckius M, Grün D, Kirchner M, Ayoub S, Torti F, Piano F, et al. Global characterization of the oocyte-to-embryo transition in *Caenorhabditis elegans* uncovers a novel mRNA clearance mechanism. *Embo J*. 2014;33:1751–66.
221. Thomsen S, Anders S, Janga SC, Huber W, Alonso CR. Genome-wide analysis of mRNA decay patterns during early *Drosophila* development. *Genome Biol*. 2010;11:R93–R93.
222. Wei Z, Angerer RC, Angerer LM. A database of mRNA expression patterns for the sea urchin embryo. *Dev Biol*. 2006;300:476–84.
223. Harvey SA, Sealy I, Kettleborough R, Fenyes F, White R, Stemple D, et al. Identification of the zebrafish maternal and paternal transcriptomes. *Dev Camb Engl*. 2013;140:2703–10.
224. Mishima Y, Tomari Y. Codon Usage and 3' UTR Length Determine Maternal mRNA Stability in Zebrafish. *Mol Cell*. 2016;61:874–85.
225. Vastenhouw NL, Zhang Y, Woods IG, Imam F, Regev A, Liu XS, et al. Chromatin signature of embryonic pluripotency is established during genome activation. *Nature*. 2010;464:922–6.

226. Cao WX, Kabelitz S, Gupta M, Yeung E, Lin S, Rammelt C, et al. Precise Temporal Regulation of Post-transcriptional Repressors Is Required for an Orderly Drosophila Maternal-to-Zygotic Transition. *Cell Reports*. 2020;31:107783–107783.
227. Burke KS, Antilla KA, Tirrell DA. A Fluorescence in Situ Hybridization Method To Quantify mRNA Translation by Visualizing Ribosome–mRNA Interactions in Single Cells. *ACS Central Sci*. 2017;3:425–33.
228. Buxbaum AR, Wu B, Singer RH. Single β -Actin mRNA Detection in Neurons Reveals a Mechanism for Regulating Its Translatability. *Science*. 2014;343:419–22.
229. Xia C, Babcock HP, Moffitt JR, Zhuang X. Multiplexed detection of RNA using MERFISH and branched DNA amplification. *Sci Rep-uk*. 2019;9:7721.
230. Eng C-HL, Shah S, Thomassie J, Cai L. Profiling the transcriptome by RNA SPOTs. *Nat Methods*. 2017;14:1153–5.
231. Lubeck E, Coskun AF, Zhiyentayev T, Ahmad M, Cai L. Single-cell in situ RNA profiling by sequential hybridization. *Nat Methods*. 2014;11:360–1.
232. Farris S, Wang Y, Ward JM, Dudek SM. Optimized Method for Robust Transcriptome Profiling of Minute Tissues Using Laser Capture Microdissection and Low-Input RNA-Seq. *Front Mol Neurosci*. 2017;10:185.
233. Lo HG, Engel KL, Goering R, Li Y, Spitale RC, Taliaferro JM. Halo-seq: An RNA Proximity Labeling Method for the Isolation and Analysis of Subcellular RNA Populations. *Curr Protoc*. 2022;2:e424.
234. Ingolia NT, Brar GA, Rouskin S, McGeachy AM, Weissman JS. The ribosome profiling strategy for monitoring translation in vivo by deep sequencing of ribosome-protected mRNA fragments. *Nat Protoc*. 2012;7:1534–50.
235. Halstead JM, Lionnet T, Wilbertz JH, Wippich F, Ephrussi A, Singer RH, et al. An RNA biosensor for imaging the first round of translation from single cells to living animals. *Science*. 2015;347:1367–671.
236. Pichon X, Bastide A, Safieddine A, Chouaib R, Samacoits A, Basyuk E, et al. Visualization of single endogenous polysomes reveals the dynamics of translation in live human cells. *J Cell Biol*. 2016;214:769–81.
237. Morisaki T, Lyon K, DeLuca KF, DeLuca JG, English BP, Zhang Z, et al. Real-time quantification of single RNA translation dynamics in living cells. *Science* [Internet]. 2016;352:1425 LP – 1429. Available from: <http://science.sciencemag.org/content/352/6292/1425.abstract>

Appendix A

FISH probes

Table A.1: smFISH and smiFISH probes used in this dissertation

Transcript_name	Sequence_ID	Wormbase_ID	Probe_sequence	FLAP/ FLUOROPHORE
<i>erm-1 synonymous</i>	N/A	N/A	tccatgtgaaggacatcgtaatcggtgacgg cctcctaagtttcgagctggactcagtg	FLAP-X
<i>erm-1 synonymous</i>	N/A	N/A	cgctcaacctctcgcgcatagagaacctcc taagtttcgagctggactcagtg	FLAP-X
<i>erm-1 synonymous</i>	N/A	N/A	agagcttgcttggaagttgaagttgcttaag cctcctaagtttcgagctggactcagtg	FLAP-X
<i>erm-1 synonymous</i>	N/A	N/A	agttaactccgtacattcaaggtctgagcg cctcctaagtttcgagctggactcagtg	FLAP-X
<i>erm-1 synonymous</i>	N/A	N/A	tctggggcagtagatttcgtcagaagga tctcctaagtttcgagctggactcagtg	FLAP-X
<i>erm-1 synonymous</i>	N/A	N/A	tcagcaacgtcctctgggtagaacttagccct cctaagtttcgagctggactcagtg	FLAP-X
<i>erm-1 synonymous</i>	N/A	N/A	gaaccttctgttaagcttaagccaagttggg cctcctaagtttcgagctggactcagtg	FLAP-X
<i>erm-1 synonymous</i>	N/A	N/A	catgttctcgtattggtcgatgcggcgcctc ctaagtttcgagctggactcagtg	FLAP-X
<i>erm-1 synonymous</i>	N/A	N/A	agtgttctcctccgagattggcgaaggcctc ctaagtttcgagctggactcagtg	FLAP-X
<i>erm-1 synonymous</i>	N/A	N/A	ctgtactatcacgtccagccttctgtctcc taagtttcgagctggactcagtg	FLAP-X
<i>erm-1 synonymous</i>	N/A	N/A	tttggctctgacggaatcgagctcagcct cctaagtttcgagctggactcagtg	FLAP-X
<i>erm-1 synonymous</i>	N/A	N/A	ttcagcagcggtagacacgtcaagttccctc ctaagtttcgagctggactcagtg	FLAP-X
<i>erm-1 synonymous</i>	N/A	N/A	gttgggaacgttttgctggcatcgttgta cctcctaagtttcgagctggactcagtg	FLAP-X
<i>erm-1 synonymous</i>	N/A	N/A	aatggattgagtttgagttggcgggtgac gcctcctaagtttcgagctggactcagtg	FLAP-X
<i>erm-1 synonymous</i>	N/A	N/A	tagccttctcagatggagttggcgggtacctc ctaagtttcgagctggactcagtg	FLAP-X
<i>erm-1 synonymous</i>	N/A	N/A	ctcgcggagctcgtactcctttgctcctcta agtttcgagctggactcagtg	FLAP-X
<i>erm-1 synonymous</i>	N/A	N/A	ggcctcaaggagtgatgtgttgag cctcctaagtttcgagctggactcagtg	FLAP-X
<i>erm-1 synonymous</i>	N/A	N/A	catgccttctcagcatcacgttgccctcct aagtttcgagctggactcagtg	FLAP-X
<i>erm-1 synonymous</i>	N/A	N/A	ttctctgttcagcgatcttgagggcacctcc taagtttcgagctggactcagtg	FLAP-X
<i>erm-1 synonymous</i>	N/A	N/A	cgcattgagttctggttcccatgcacct cctaagtttcgagctggactcagtg	FLAP-X
<i>erm-1 synonymous</i>	N/A	N/A	ggcggagatagccttggatgcaaggc ctcctaagtttcgagctggactcagtg	FLAP-X

<i>erm-1 synonymous</i>	N/A	N/A	gtcgtagatgtaagtccgagggcgtcgacc ctcctaagtttcgagctggactcagtg	FLAP-X
<i>erm-1 synonymous</i>	N/A	N/A	cgaggtaaaggctcggtccctcttgttacgc ctcctaagtttcgagctggactcagtg	FLAP-X
<i>erm-1 synonymous</i>	N/A	N/A	cttaaggfactcgagcatggcttgctcgcctc ctaagtttcgagctggactcagtg	FLAP-X
<i>nemamatrix gfp</i>	N/A	N/A	attccaatttgtccaagaatgttccatctcc tctaagtttcgagctggactcagtg	FLAP-X
<i>nemamatrix gfp</i>	N/A	N/A	aatatagtcttctgtacataacctcgggc ctcctaagtttcgagctggactcagtg	FLAP-X
<i>nemamatrix gfp</i>	N/A	N/A	ttgtatagttcatccatgccatgtgtaatcccc tctaagtttcgagctggactcagtg	FLAP-X
<i>nemamatrix gfp</i>	N/A	N/A	ctctctttcgttgggatcttccgaaggccc tctaagtttcgagctggactcagtg	FLAP-X
<i>nemamatrix gfp</i>	N/A	N/A	ttgtgataatggctcgtctagtgaacgctcc ctcctaagtttcgagctggactcagtg	FLAP-X
<i>nemamatrix gfp</i>	N/A	N/A	caacttgattcattctttgttctgcccct cctaagtttcgagctggactcagtg	FLAP-X
<i>nemamatrix gfp</i>	N/A	N/A	itaaacttacgtgtctgtagttcccgtcatccc tctaagtttcgagctggactcagtg	FLAP-X
<i>nemamatrix gfp</i>	N/A	N/A	taagggtaaagtttccgtatgttgcacacctc ctcctaagtttcgagctggactcagtg	FLAP-X
<i>nemamatrix gfp</i>	N/A	N/A	gcagctgttacaactcaagaaggaccatgt cctcctaagtttcgagctggactcagtg	FLAP-X
<i>nemamatrix gfp</i>	N/A	N/A	aactcgattctattaacaagggtatcacctcc ctcctaagtttcgagctggactcagtg	FLAP-X
<i>nemamatrix gfp</i>	N/A	N/A	atctgggtatctcgagaagcattgaacaccc ctcctaagtttcgagctggactcagtg	FLAP-X
<i>nemamatrix gfp</i>	N/A	N/A	aaacttaccatggaacaggtagtttccagt cctcctaagtttcgagctggactcagtg	FLAP-X
<i>nemamatrix gfp</i>	N/A	N/A	acatccatctaatcaacaagaattgggac cctcctaagtttcgagctggactcagtg	FLAP-X
<i>frm-7</i>	C51F7.1	WBGene00001 493	agtcgccattatgttctcattctagcaaaagt tacactcggacctcgtcgacatgcatt	FLAP-Y
<i>frm-7</i>	C51F7.1	WBGene00001 493	atttctgcaggaagcggctcagttgaagctta cactcggacctcgtcgacatgcatt	FLAP-Y
<i>frm-7</i>	C51F7.1	WBGene00001 493	tgcactcatcgagagaagtcgacgtttattgt tacactcggacctcgtcgacatgcatt	FLAP-Y
<i>frm-7</i>	C51F7.1	WBGene00001 493	tcgtgtcaggatgataagtttgatggcgaa cttacactcggacctcgtcgacatgcatt	FLAP-Y
<i>frm-7</i>	C51F7.1	WBGene00001 493	cgagtcgagaccgttcaatttcactactgtt acactcggacctcgtcgacatgcatt	FLAP-Y
<i>frm-7</i>	C51F7.1	WBGene00001 493	tcggatgatccaattccatcttctcgatttac actcggacctcgtcgacatgcatt	FLAP-Y
<i>frm-7</i>	C51F7.1	WBGene00001 493	tcgaatccattttgattcctaagacggagcttct acactcggacctcgtcgacatgcatt	FLAP-Y
<i>frm-7</i>	C51F7.1	WBGene00001 493	agacattgagccatggcaccgatctcttaca ctcggacctcgtcgacatgcatt	FLAP-Y
<i>frm-7</i>	C51F7.1	WBGene00001 493	caatgtcgcacatctcaatgcccttggttaca ctcggacctcgtcgacatgcatt	FLAP-Y
<i>frm-7</i>	C51F7.1	WBGene00001 493	ttataagggcaggtgcagccatgtaccagtt acactcggacctcgtcgacatgcatt	FLAP-Y
<i>frm-7</i>	C51F7.1	WBGene00001 493	gagcatactcataatttggccgctggattta cactcggacctcgtcgacatgcatt	FLAP-Y

<i>frm-7</i>	C51F7.1	WBGene00001 493	ccgcattccagagaacatcgtgtactttctta cactcggacctcgtcgacatgcatt	FLAP-Y
<i>frm-7</i>	C51F7.1	WBGene00001 493	actcgatgatgatggctgttagatggactt acactcggacctcgtcgacatgcatt	FLAP-Y
<i>frm-7</i>	C51F7.1	WBGene00001 493	ccggcagtgccatttagtgagaaagegga ttacactcggacctcgtcgacatgcatt	FLAP-Y
<i>frm-7</i>	C51F7.1	WBGene00001 493	atgatgatgtctgaactgtgagctttgtgctt acactcggacctcgtcgacatgcatt	FLAP-Y
<i>frm-7</i>	C51F7.1	WBGene00001 493	tgaccaactgtgtggtgtgataggagat tacctcggacctcgtcgacatgcatt	FLAP-Y
<i>frm-2</i>	T04C9.6	WBGene00001 489	aaagtctgtgacaattctccgtgatgttgc tacctcggacctcgtcgacatgcatt	FLAP-Y
<i>frm-2</i>	T04C9.6	WBGene00001 489	atctactccgtacattcaatccatcgtttaca ctcggacctcgtcgacatgcatt	FLAP-Y
<i>frm-2</i>	T04C9.6	WBGene00001 489	ttattcaagttagtcaactccgttgagccgtt acactcggacctcgtcgacatgcatt	FLAP-Y
<i>frm-2</i>	T04C9.6	WBGene00001 489	tgtggacattgcagacgtcctgaggagattta cactcggacctcgtcgacatgcatt	FLAP-Y
<i>frm-2</i>	T04C9.6	WBGene00001 489	aacattgaatggatctgttactgcaggcctt acactcggacctcgtcgacatgcatt	FLAP-Y
<i>frm-2</i>	T04C9.6	WBGene00001 489	ttctcggcagacaatatttaaatgtgctcctt acactcggacctcgtcgacatgcatt	FLAP-Y
<i>frm-2</i>	T04C9.6	WBGene00001 489	tcgaacagctggttggaggtgtgagctt acactcggacctcgtcgacatgcatt	FLAP-Y
<i>frm-2</i>	T04C9.6	WBGene00001 489	ctccgatgactgctcattctgggaattacac tcggacctcgtcgacatgcatt	FLAP-Y
<i>frm-2</i>	T04C9.6	WBGene00001 489	ttcgaattgactgatgagctggaagtgtgg ttacactcggacctcgtcgacatgcatt	FLAP-Y
<i>frm-2</i>	T04C9.6	WBGene00001 489	atgtggagaagttggatctgatttgcattgg ttacactcggacctcgtcgacatgcatt	FLAP-Y
<i>frm-2</i>	T04C9.6	WBGene00001 489	cgctgttgatcattggctcttctgctcttaca ctcggacctcgtcgacatgcatt	FLAP-Y
<i>frm-2</i>	T04C9.6	WBGene00001 489	ccgtggaccatactctgactaggcttttaca ctcggacctcgtcgacatgcatt	FLAP-Y
<i>frm-2</i>	T04C9.6	WBGene00001 489	ttccagaatgtttgccgcttttcagacgtt acactcggacctcgtcgacatgcatt	FLAP-Y
<i>frm-2</i>	T04C9.6	WBGene00001 489	ttgttcgattgatcagcatcctcctcgattaca ctcggacctcgtcgacatgcatt	FLAP-Y
<i>frm-2</i>	T04C9.6	WBGene00001 489	tctgtgctgtgacgattccgtgagaatcttta cactcggacctcgtcgacatgcatt	FLAP-Y
<i>frm-2</i>	T04C9.6	WBGene00001 489	tttgctctcttgagagttctcatctccttaca ctcggacctcgtcgacatgcatt	FLAP-Y
<i>frm-4</i>	C24A11.8	WBGene00001 491	tcgacaacgtagtggcgagttggctcatagtt acactcggacctcgtcgacatgcatt	FLAP-Y
<i>frm-4</i>	C24A11.8	WBGene00001 491	acgttgatgatgatgacgttgcaactcctta cactcggacctcgtcgacatgcatt	FLAP-Y
<i>frm-4</i>	C24A11.8	WBGene00001 491	attggcacaggagatgctgatgggatgat tacctcggacctcgtcgacatgcatt	FLAP-Y
<i>frm-4</i>	C24A11.8	WBGene00001 491	tggaagtcgtagtttcattcataactccgact tacctcggacctcgtcgacatgcatt	FLAP-Y
<i>frm-4</i>	C24A11.8	WBGene00001 491	tcagtttgacatcctgagcagaagtttcattgt tacctcggacctcgtcgacatgcatt	FLAP-Y
<i>frm-4</i>	C24A11.8	WBGene00001 491	tgtttcggaattgaccgatggacaagtgtt tacctcggacctcgtcgacatgcatt	FLAP-Y

<i>frm-4</i>	C24A11.8	WBGene00001 491	aatacttggatcctggaccatgtccattac actcggacctcgtcgacatgcatt	FLAP-Y
<i>frm-4</i>	C24A11.8	WBGene00001 491	aactggcaatgtgtcgtgggttcctaatatt acactcggacctcgtcgacatgcatt	FLAP-Y
<i>frm-4</i>	C24A11.8	WBGene00001 491	gtatggatcaaatgogtacctatcgagctggt tacctcggacctcgtcgacatgcatt	FLAP-Y
<i>frm-4</i>	C24A11.8	WBGene00001 491	gcctctccagaaactccaattcgcttacac tcggacctcgtcgacatgcatt	FLAP-Y
<i>frm-4</i>	C24A11.8	WBGene00001 491	gacgtgctggatccgatggataatatcgatt acactcggacctcgtcgacatgcatt	FLAP-Y
<i>frm-4</i>	C24A11.8	WBGene00001 491	gtaacgatgcttatggtgatcctgatatcggt acactcggacctcgtcgacatgcatt	FLAP-Y
<i>frm-4</i>	C24A11.8	WBGene00001 491	atgaacgttgaccggacatccttagcttac actcggacctcgtcgacatgcatt	FLAP-Y
<i>frm-4</i>	C24A11.8	WBGene00001 491	catgaagctcgatcttctcgaagtcgtaagtc ttacctcggacctcgtcgacatgcatt	FLAP-Y
<i>frm-4</i>	C24A11.8	WBGene00001 491	attgttctgagttccgaattgtccggagatgt acactcggacctcgtcgacatgcatt	FLAP-Y
<i>frm-4</i>	C24A11.8	WBGene00001 491	ccgagaacgacgacgacgtgtgtttgcg gttacctcggacctcgtcgacatgcatt	FLAP-Y
<i>let-502</i>	C10H11.9	WBGene00002 694	tagattgtggaagagtttgacgatcctggag cttacctcggacctcgtcgacatgcatt	FLAP-Y
<i>let-502</i>	C10H11.9	WBGene00002 694	tgttgatcgacattggcaacgatccttita cactcggacctcgtcgacatgcatt	FLAP-Y
<i>let-502</i>	C10H11.9	WBGene00002 694	acgtcgtatgtgataggagagctcttgatt acactcggacctcgtcgacatgcatt	FLAP-Y
<i>let-502</i>	C10H11.9	WBGene00002 694	agcgatagccagccttcatttgaatagtta cactcggacctcgtcgacatgcatt	FLAP-Y
<i>let-502</i>	C10H11.9	WBGene00002 694	gactttccagagctcatcctgacagattaca ctcggacctcgtcgacatgcatt	FLAP-Y
<i>let-502</i>	C10H11.9	WBGene00002 694	tcattctgcagcagctcataatcgtttacac tcggacctcgtcgacatgcatt	FLAP-Y
<i>let-502</i>	C10H11.9	WBGene00002 694	cacacttgtcccgaactgtcattcgttac actcggacctcgtcgacatgcatt	FLAP-Y
<i>let-502</i>	C10H11.9	WBGene00002 694	ccgaatcagcgccatgctcagttatttaca ctcggacctcgtcgacatgcatt	FLAP-Y
<i>let-502</i>	C10H11.9	WBGene00002 694	ccgttaaagtcttcggcaattgaaagtcct tacctcggacctcgtcgacatgcatt	FLAP-Y
<i>let-502</i>	C10H11.9	WBGene00002 694	gacgatctggagccgagagggaatttita cactcggacctcgtcgacatgcatt	FLAP-Y
<i>let-502</i>	C10H11.9	WBGene00002 694	gcatcgcacaactccattggcattcattacac tcggacctcgtcgacatgcatt	FLAP-Y
<i>let-502</i>	C10H11.9	WBGene00002 694	tgatcatgattcacgagatccacctttaca ctcggacctcgtcgacatgcatt	FLAP-Y
<i>let-502</i>	C10H11.9	WBGene00002 694	ccattcgtattcgtgagccataatatttac actcggacctcgtcgacatgcatt	FLAP-Y
<i>let-502</i>	C10H11.9	WBGene00002 694	ttttgcattcgaatgcagcgtcggtcgttac actcggacctcgtcgacatgcatt	FLAP-Y
<i>let-502</i>	C10H11.9	WBGene00002 694	ttgacgagcgtgtgatggtgtcgagcatta cactcggacctcgtcgacatgcatt	FLAP-Y
<i>let-502</i>	C10H11.9	WBGene00002 694	ctttcgtatttatcgggattttgatccactt acactcggacctcgtcgacatgcatt	FLAP-Y
<i>mrck-1</i>	K08B12.5	WBGene00006 437	ggaacttctattgaatcttgatctggagcact tacctcggacctcgtcgacatgcatt	FLAP-Y

<i>mrck-1</i>	K08B12.5	WBGene00006 437	tgtttgaaccattcagcaagggtcacattgtt acactcggacctcgtcgacatgcatt	FLAP-Y
<i>mrck-1</i>	K08B12.6	WBGene00006 438	aatacggctcgtgtaggcgaaatatttggct tacctcggacctcgtcgacatgcatt	FLAP-Y
<i>mrck-1</i>	K08B12.7	WBGene00006 439	gtgggagaatccaacgtatagacggccgttt tacctcggacctcgtcgacatgcatt	FLAP-Y
<i>mrck-1</i>	K08B12.8	WBGene00006 440	tctgaccgatctatttgaagatggtgacactt acactcggacctcgtcgacatgcatt	FLAP-Y
<i>mrck-1</i>	K08B12.9	WBGene00006 441	tcagcaattggcgactaatctcgatgcagtta cactcggacctcgtcgacatgcatt	FLAP-Y
<i>mrck-1</i>	K08B12.10	WBGene00006 442	gtctcacaagaccttctgaagctgttcatta cactcggacctcgtcgacatgcatt	FLAP-Y
<i>mrck-1</i>	K08B12.11	WBGene00006 443	ctctgcacatgacacgtggcatgcatttacac tcggacctcgtcgacatgcatt	FLAP-Y
<i>mrck-1</i>	K08B12.12	WBGene00006 444	tcacgcatcagagaagccattcgttttcagtt acactcggacctcgtcgacatgcatt	FLAP-Y
<i>mrck-1</i>	K08B12.13	WBGene00006 445	tggaagagcggccatttgttgagagactttt acactcggacctcgtcgacatgcatt	FLAP-Y
<i>mrck-1</i>	K08B12.14	WBGene00006 446	tcagcgacatgttgcaataattgtttgagct tacctcggacctcgtcgacatgcatt	FLAP-Y
<i>mrck-1</i>	K08B12.15	WBGene00006 447	actcgaggaggttgtttctgaagacaag gttacactcggacctcgtcgacatgcatt	FLAP-Y
<i>mrck-1</i>	K08B12.16	WBGene00006 448	ggaagtcgacatgcttctgatggctcataatt tacctcggacctcgtcgacatgcatt	FLAP-Y
<i>mrck-1</i>	K08B12.17	WBGene00006 449	aggcttcacgtccgatgcacatatcttacac tcggacctcgtcgacatgcatt	FLAP-Y
<i>mrck-1</i>	K08B12.18	WBGene00006 450	gcattcttacgacggcaacttctccgaattac actcggacctcgtcgacatgcatt	FLAP-Y
<i>mrck-1</i>	K08B12.19	WBGene00006 451	aatatttcaagggtttgaggcgaaccggcg ttacctcggacctcgtcgacatgcatt	FLAP-Y
<i>mtm-1</i>	Y110A7A.5	WBGene00003 475	attgtcgcataattgccataggcagtcactta cactcggacctcgtcgacatgcatt	FLAP-Y
<i>mtm-1</i>	Y110A7A.5	WBGene00003 475	gacgtcagctgtgacgttcgatcccaattaca ctcggacctcgtcgacatgcatt	FLAP-Y
<i>mtm-1</i>	Y110A7A.5	WBGene00003 475	agcattggcattcataatgttcgtgagatgtct tacctcggacctcgtcgacatgcatt	FLAP-Y
<i>mtm-1</i>	Y110A7A.5	WBGene00003 475	gtcattggctgtgagcatcgtgaaattgaagc ttacctcggacctcgtcgacatgcatt	FLAP-Y
<i>mtm-1</i>	Y110A7A.5	WBGene00003 475	ttctatccgagacactgtccgagtgaatatt acactcggacctcgtcgacatgcatt	FLAP-Y
<i>mtm-1</i>	Y110A7A.5	WBGene00003 475	ctaggcggtaatttttgagcagcgtcgtctt acactcggacctcgtcgacatgcatt	FLAP-Y
<i>mtm-1</i>	Y110A7A.5	WBGene00003 475	tcategcatttctatcctcagccggttacact cggacctcgtcgacatgcatt	FLAP-Y
<i>mtm-1</i>	Y110A7A.5	WBGene00003 475	gtagttatcgtcgcctgaccgattctctttac actcggacctcgtcgacatgcatt	FLAP-Y
<i>mtm-1</i>	Y110A7A.5	WBGene00003 475	ttcgattcgttaacgctttgtagtatccctta cactcggacctcgtcgacatgcatt	FLAP-Y
<i>mtm-1</i>	Y110A7A.5	WBGene00003 475	tcgtcctcagcacttctttccagaaattctta cactcggacctcgtcgacatgcatt	FLAP-Y
<i>mtm-1</i>	Y110A7A.5	WBGene00003 475	tctttctttgcttctaaactcggagcttacac tcggacctcgtcgacatgcatt	FLAP-Y
<i>mtm-1</i>	Y110A7A.5	WBGene00003 475	ggcaacactcgtcgttcttctaccaactttaca ctcggacctcgtcgacatgcatt	FLAP-Y

<i>mtm-1</i>	Y110A7A.5	WBGene00003 475	gagctccattgctcatacattttccacttaca ctcggacctcgtcgacatgcatt	FLAP-Y
<i>nfm-1</i>	F42A10.2	WBGene00003 593	gtttcaggccgcaaatcgcacgtaattta cactcggacctcgtcgacatgcatt	FLAP-Y
<i>nfm-1</i>	F42A10.2	WBGene00003 593	attgcagttgatgaaatgatcctgttgatggct tactcggacctcgtcgacatgcatt	FLAP-Y
<i>nfm-1</i>	F42A10.2	WBGene00003 593	gtcaaggcttacatctgctagtgcattgatta cactcggacctcgtcgacatgcatt	FLAP-Y
<i>nfm-1</i>	F42A10.2	WBGene00003 593	aacatcaaagttcatgttactgtgtcgtgctt acactcggacctcgtcgacatgcatt	FLAP-Y
<i>nfm-1</i>	F42A10.2	WBGene00003 593	cgttttattcgatctctccacatcagcattac actcggacctcgtcgacatgcatt	FLAP-Y
<i>nfm-1</i>	F42A10.2	WBGene00003 593	tcaaatgtcagcttctgccattcagtggtaca ctcggacctcgtcgacatgcatt	FLAP-Y
<i>nfm-1</i>	F42A10.2	WBGene00003 593	gtcccgccacatgtctagcgacagtattaca ctcggacctcgtcgacatgcatt	FLAP-Y
<i>nfm-1</i>	F42A10.2	WBGene00003 593	cattttgtgatgaaccgcatcatgctttaca ctcggacctcgtcgacatgcatt	FLAP-Y
<i>nfm-1</i>	F42A10.2	WBGene00003 593	ttccaggtgctccttgagattcgcgcttaca ctcggacctcgtcgacatgcatt	FLAP-Y
<i>nfm-1</i>	F42A10.2	WBGene00003 593	actgactcgaatactgtgctatttccgattctt acactcggacctcgtcgacatgcatt	FLAP-Y
<i>nfm-1</i>	F42A10.2	WBGene00003 593	gcttttcgtccattctcaacagagcttctttac actcggacctcgtcgacatgcatt	FLAP-Y
<i>nfm-1</i>	F42A10.2	WBGene00003 593	tgtgatctcattgttgaaccttaacgtgtctt acactcggacctcgtcgacatgcatt	FLAP-Y
<i>nfm-1</i>	F42A10.2	WBGene00003 593	ggtgttattcgattcactcccttatagattcctt acactcggacctcgtcgacatgcatt	FLAP-Y
<i>nfm-1</i>	F42A10.2	WBGene00003 593	tgattgtcctgattccgtgaccaccttacact cggacctcgtcgacatgcatt	FLAP-Y
<i>nfm-1</i>	F42A10.2	WBGene00003 593	tgtacagtcgcatgcattgctgaactttaca ctcggacctcgtcgacatgcatt	FLAP-Y
<i>nfm-1</i>	F42A10.2	WBGene00003 593	attgtgctcacttttgcgtaaatggcttcttac actcggacctcgtcgacatgcatt	FLAP-Y
<i>ani-1</i>	Y49E10.19	WBGene00013 038	tactgattaacaatcggatttctccacgtgctt acactcggacctcgtcgacatgcatt	FLAP-Y
<i>ani-1</i>	Y49E10.19	WBGene00013 038	atgtcttcaactaccgatgcaccttctgtacac tcggacctcgtcgacatgcatt	FLAP-Y
<i>ani-1</i>	Y49E10.19	WBGene00013 038	ttccgagcaaattgaagttggatgtggtcgac ttacactcggacctcgtcgacatgcatt	FLAP-Y
<i>ani-1</i>	Y49E10.19	WBGene00013 038	aataggctctggttctgatgaagttgatctt acactcggacctcgtcgacatgcatt	FLAP-Y
<i>ani-1</i>	Y49E10.19	WBGene00013 038	agaagacttcacggatttctgcttgacgctt acactcggacctcgtcgacatgcatt	FLAP-Y
<i>ani-1</i>	Y49E10.19	WBGene00013 038	gctttccacatgacgaagcattgcccttaca ctcggacctcgtcgacatgcatt	FLAP-Y
<i>ani-1</i>	Y49E10.19	WBGene00013 038	gaaacttgcttatcccggccaatatcttac actcggacctcgtcgacatgcatt	FLAP-Y
<i>ani-1</i>	Y49E10.19	WBGene00013 038	gagcatccttagccgactcgacaattcgttac actcggacctcgtcgacatgcatt	FLAP-Y
<i>ani-1</i>	Y49E10.19	WBGene00013 038	cgacttcaaattctcagcttccaactccttac actcggacctcgtcgacatgcatt	FLAP-Y
<i>ani-1</i>	Y49E10.19	WBGene00013 038	tcttcaattctcctcaactgaagccgtcttac actcggacctcgtcgacatgcatt	FLAP-Y

<i>ani-1</i>	Y49E10.19	WBGene00013038	ggagcattcgatattccagacgtttagagct tacctcggacctcgtcgacatgcatt	FLAP-Y
<i>ani-1</i>	Y49E10.19	WBGene00013038	agtgcctcgtatcgtttacagatgatccggatta cactcggacctcgtcgacatgcatt	FLAP-Y
<i>ani-1</i>	Y49E10.19	WBGene00013038	atgcggcgcgagcttccaatccgacattcttac actcggacctcgtcgacatgcatt	FLAP-Y
<i>ani-1</i>	Y49E10.19	WBGene00013038	cacagatgtaattttgaggtcactggccatt acactcggacctcgtcgacatgcatt	FLAP-Y
<i>ani-1</i>	Y49E10.19	WBGene00013038	catcaatgtggaagctattcgggaatggcctt acactcggacctcgtcgacatgcatt	FLAP-Y
<i>ani-1</i>	Y49E10.19	WBGene00013038	tagttcacattcacaattggctgggcgaat acactcggacctcgtcgacatgcatt	FLAP-Y
<i>ani-2</i>	K10B2.5	WBGene00019608	cacaactcgtctttctcgagaagactgggtt acactcggacctcgtcgacatgcatt	FLAP-Y
<i>ani-2</i>	K10B2.5	WBGene00019608	tcaatgagcagttcgatggaattcgtgct ttacctcggacctcgtcgacatgcatt	FLAP-Y
<i>ani-2</i>	K10B2.5	WBGene00019608	agtcgcgatcaagtgtcagctttccacattac actcggacctcgtcgacatgcatt	FLAP-Y
<i>ani-2</i>	K10B2.5	WBGene00019608	cctggcatcgagagaactgttcgattgacat tacctcggacctcgtcgacatgcatt	FLAP-Y
<i>ani-2</i>	K10B2.5	WBGene00019608	ccaatactcgtcgacatgctttcaggattac actcggacctcgtcgacatgcatt	FLAP-Y
<i>ani-2</i>	K10B2.5	WBGene00019608	ctgtactcgggaacacgcatcatgtacatta cactcggacctcgtcgacatgcatt	FLAP-Y
<i>ani-2</i>	K10B2.5	WBGene00019608	tgaatgacatgcattctgtctggaatgagct tacctcggacctcgtcgacatgcatt	FLAP-Y
<i>ani-2</i>	K10B2.5	WBGene00019608	caaccattgggctcttttagcatcgatgatt acactcggacctcgtcgacatgcatt	FLAP-Y
<i>ani-2</i>	K10B2.5	WBGene00019608	tgatctatcagctgcagagaagtgtgctgatt acactcggacctcgtcgacatgcatt	FLAP-Y
<i>ani-2</i>	K10B2.5	WBGene00019608	tcctgtcagagacagatattccgaactta cactcggacctcgtcgacatgcatt	FLAP-Y
<i>ani-2</i>	K10B2.5	WBGene00019608	attggccagcgtgaggtgtaacgagagtg ttacctcggacctcgtcgacatgcatt	FLAP-Y
<i>ani-2</i>	K10B2.5	WBGene00019608	ctataacctgtaccatctctcaactccttac actcggacctcgtcgacatgcatt	FLAP-Y
<i>ani-2</i>	K10B2.5	WBGene00019608	ttccatgtgaacttggatgcatttctattac actcggacctcgtcgacatgcatt	FLAP-Y
<i>ani-2</i>	K10B2.5	WBGene00019608	tgactgattctaggaacgaagtcgttgcatt acactcggacctcgtcgacatgcatt	FLAP-Y
<i>ani-2</i>	K10B2.5	WBGene00019608	cacgtccgtcattagcgaatccgaattgggt acactcggacctcgtcgacatgcatt	FLAP-Y
<i>ani-2</i>	K10B2.5	WBGene00019608	ttaatgacgtccagcgtaaacctgtggat tacctcggacctcgtcgacatgcatt	FLAP-Y
<i>dyn-1</i>	C02C6.1	WBGene00001130	cttcagagataatgcggagcgcctccttaca ctcggacctcgtcgacatgcatt	FLAP-Y
<i>dyn-1</i>	C02C6.1	WBGene00001130	caagcatgttacattcggagcatctcctttac actcggacctcgtcgacatgcatt	FLAP-Y
<i>dyn-1</i>	C02C6.1	WBGene00001130	atgagagcatcagttcgcgcgattggttac actcggacctcgtcgacatgcatt	FLAP-Y
<i>dyn-1</i>	C02C6.1	WBGene00001130	tgaaccaggtccttaattgtcttggaatgat tacctcggacctcgtcgacatgcatt	FLAP-Y
<i>dyn-1</i>	C02C6.1	WBGene00001130	atttctccaattgggtcatccaactcttac actcggacctcgtcgacatgcatt	FLAP-Y

<i>dyn-1</i>	C02C6.1	WBGene00001 130	gcatatgcgagacgacgattctttccagctta cactcggacctcgtcgacatgcatt	FLAP-Y
<i>dyn-1</i>	C02C6.1	WBGene00001 130	ccagctttgcagaggaaaccttcaatggagtt acactcggacctcgtcgacatgcatt	FLAP-Y
<i>dyn-1</i>	C02C6.1	WBGene00001 130	aagagtgtgtgaaggtgactgttcccaacc ttacactcggacctcgtcgacatgcatt	FLAP-Y
<i>dyn-1</i>	C02C6.1	WBGene00001 130	tgaagaactttctcggcgtccaagcagtt acactcggacctcgtcgacatgcatt	FLAP-Y
<i>dyn-1</i>	C02C6.1	WBGene00001 130	ctaataccttgcgaccgacaataccttctta cactcggacctcgtcgacatgcatt	FLAP-Y
<i>dyn-1</i>	C02C6.1	WBGene00001 130	gacgaagtgtgaacagcttgtctcgaggat cttactcggacctcgtcgacatgcatt	FLAP-Y
<i>dyn-1</i>	C02C6.1	WBGene00001 130	cactttgtgagaccggcgaatcgatgagtt tactcggacctcgtcgacatgcatt	FLAP-Y
<i>dyn-1</i>	C02C6.1	WBGene00001 130	aatccacaagcgatgacccttctgtgttac actcggacctcgtcgacatgcatt	FLAP-Y
<i>dyn-1</i>	C02C6.1	WBGene00001 130	gaactcggcgtactcattgcatcttgaattta cactcggacctcgtcgacatgcatt	FLAP-Y
<i>dyn-1</i>	C02C6.1	WBGene00001 130	ccgacgacggcgtctgtggaagtgcgaatt acactcggacctcgtcgacatgcatt	FLAP-Y
<i>dyn-1</i>	C02C6.1	WBGene00001 130	tgacagatgtcccagctgggagaaggta cactcggacctcgtcgacatgcatt	FLAP-Y
<i>efa-6</i>	Y55D9A.1	WBGene00013 223	atcataatgttattgtggtgctgaagacgct tactcggacctcgtcgacatgcatt	FLAP-Y
<i>efa-6</i>	Y55D9A.1	WBGene00013 223	atataggtactgtagcgtctttctcgaactt tactcggacctcgtcgacatgcatt	FLAP-Y
<i>efa-6</i>	Y55D9A.1	WBGene00013 223	atggaagtgtggcgatgagaatgcggcgtt acactcggacctcgtcgacatgcatt	FLAP-Y
<i>efa-6</i>	Y55D9A.1	WBGene00013 223	gacgagcgtataaccattctccaactgcttaca ctcggacctcgtcgacatgcatt	FLAP-Y
<i>efa-6</i>	Y55D9A.1	WBGene00013 223	tggtgaagcaactgaaccatttgcgctgatt acactcggacctcgtcgacatgcatt	FLAP-Y
<i>efa-6</i>	Y55D9A.1	WBGene00013 223	ctgatgattaccacggagctctactcttaca ctcggacctcgtcgacatgcatt	FLAP-Y
<i>efa-6</i>	Y55D9A.1	WBGene00013 223	attactgctcggcggatcgaagtatatta cactcggacctcgtcgacatgcatt	FLAP-Y
<i>efa-6</i>	Y55D9A.1	WBGene00013 223	gcgtcaatgatccattcaggtcatcattaca ctcggacctcgtcgacatgcatt	FLAP-Y
<i>efa-6</i>	Y55D9A.1	WBGene00013 223	tctcattcgatcgaagatgtggtgaaagtgt ttactcggacctcgtcgacatgcatt	FLAP-Y
<i>efa-6</i>	Y55D9A.1	WBGene00013 223	gcattcgaatagctgttgggtgaagactctt acactcggacctcgtcgacatgcatt	FLAP-Y
<i>efa-6</i>	Y55D9A.1	WBGene00013 223	tggtgtgaaactggaactggaagtcttga ttactcggacctcgtcgacatgcatt	FLAP-Y
<i>efa-6</i>	Y55D9A.1	WBGene00013 223	acgttttctgccaactaccagcttcttcta cactcggacctcgtcgacatgcatt	FLAP-Y
<i>efa-6</i>	Y55D9A.1	WBGene00013 223	ttgacagctgatgtgggtgaatgctcgattta cactcggacctcgtcgacatgcatt	FLAP-Y
<i>efa-6</i>	Y55D9A.1	WBGene00013 223	aactgtggtactcggagcagttggtcgta cactcggacctcgtcgacatgcatt	FLAP-Y
<i>efa-6</i>	Y55D9A.1	WBGene00013 223	agcctcggacttttgacattccggcgttaca ctcggacctcgtcgacatgcatt	FLAP-Y
<i>efa-6</i>	Y55D9A.1	WBGene00013 223	catcaatggtggccagtgcctctctgttacac tcggacctcgtcgacatgcatt	FLAP-Y

<i>exoc-8</i>	Y105E8B.2	WBGene00013 687	ccaggctggggaattgatcaatcaggcggtta cactcggacctcgtcgacatgcatt	FLAP-Y
<i>exoc-8</i>	Y105E8B.2	WBGene00013 687	tctcgaaacattcaacgagcttctcgatttta cactcggacctcgtcgacatgcatt	FLAP-Y
<i>exoc-8</i>	Y105E8B.2	WBGene00013 687	tcatttcagaaatcgccattccacattttac actcggacctcgtcgacatgcatt	FLAP-Y
<i>exoc-8</i>	Y105E8B.2	WBGene00013 687	cgattcagtcgagattccgattccagcattac actcggacctcgtcgacatgcatt	FLAP-Y
<i>exoc-8</i>	Y105E8B.2	WBGene00013 687	cttaaatagacatctgttcgtaggtccacgt tacctcggacctcgtcgacatgcatt	FLAP-Y
<i>exoc-8</i>	Y105E8B.2	WBGene00013 687	tcgatgagcaatgcaatcgtccagttctgta cactcggacctcgtcgacatgcatt	FLAP-Y
<i>exoc-8</i>	Y105E8B.2	WBGene00013 687	ggataaccaggaaatgcattgtcgtttctctt tacctcggacctcgtcgacatgcatt	FLAP-Y
<i>exoc-8</i>	Y105E8B.2	WBGene00013 687	tctctcatcagatgggtctcgtacggttaca ctcggacctcgtcgacatgcatt	FLAP-Y
<i>exoc-8</i>	Y105E8B.2	WBGene00013 687	tgcacttcgttcattgcacttctccttacactc ggacctcgtcgacatgcatt	FLAP-Y
<i>exoc-8</i>	Y105E8B.2	WBGene00013 687	tggttagaagagttcggctttttcatggct tacctcggacctcgtcgacatgcatt	FLAP-Y
<i>exoc-8</i>	Y105E8B.2	WBGene00013 687	ccggcttacatcgtcgtgagcagttgttaca ctcggacctcgtcgacatgcatt	FLAP-Y
<i>exoc-8</i>	Y105E8B.2	WBGene00013 687	aattacagcatcttctcgtggcactgtttttac actcggacctcgtcgacatgcatt	FLAP-Y
<i>exoc-8</i>	Y105E8B.2	WBGene00013 687	tttctcgaatagttgcctgtctcacgagttac actcggacctcgtcgacatgcatt	FLAP-Y
<i>exoc-8</i>	Y105E8B.2	WBGene00013 687	ttccctatgtagaatctctcgtttcgccttaca ctcggacctcgtcgacatgcatt	FLAP-Y
<i>exoc-8</i>	Y105E8B.2	WBGene00013 687	gcggcgctgattcacgatcttaacgttaca ctcggacctcgtcgacatgcatt	FLAP-Y
<i>exoc-8</i>	Y105E8B.2	WBGene00013 687	gactggggcaactgagtttagtgagagggtt gttacctcggacctcgtcgacatgcatt	FLAP-Y
<i>F07C6.4</i>	F07C6.4	WBGene00008 555	ggaggtggtgaaatcgaggagttctgatg cttacctcggacctcgtcgacatgcatt	FLAP-Y
<i>F07C6.4</i>	F07C6.4	WBGene00008 555	taaggtttccggataagattacggtagccgc ttacctcggacctcgtcgacatgcatt	FLAP-Y
<i>F07C6.4</i>	F07C6.4	WBGene00008 555	acgatgtggaacggtagccgacgtttctgat tacctcggacctcgtcgacatgcatt	FLAP-Y
<i>F07C6.4</i>	F07C6.4	WBGene00008 555	ccatttctcaaatctggcaccgatccattaca ctcggacctcgtcgacatgcatt	FLAP-Y
<i>F07C6.4</i>	F07C6.4	WBGene00008 555	tgtaaggctactaatatccggtttactcgtta cactcggacctcgtcgacatgcatt	FLAP-Y
<i>F07C6.4</i>	F07C6.4	WBGene00008 555	gggagcacaacgtcgttaatttcgacaggct tacctcggacctcgtcgacatgcatt	FLAP-Y
<i>F07C6.4</i>	F07C6.4	WBGene00008 555	cattgtgccgatcagcagttcgagtgaaga gttacctcggacctcgtcgacatgcatt	FLAP-Y
<i>F07C6.4</i>	F07C6.4	WBGene00008 555	ccaactgttcggcacacgagaggatttg gttacctcggacctcgtcgacatgcatt	FLAP-Y
<i>F07C6.4</i>	F07C6.4	WBGene00008 555	tgccggtcattgatcaggatcacatcatttac actcggacctcgtcgacatgcatt	FLAP-Y
<i>F07C6.4</i>	F07C6.4	WBGene00008 555	aggtacggtgtgatcaaatctgatgtcgact ttacctcggacctcgtcgacatgcatt	FLAP-Y
<i>F07C6.4</i>	F07C6.4	WBGene00008 555	atcattccagtacctacaggcagtcgtcttac actcggacctcgtcgacatgcatt	FLAP-Y

<i>F07C6.4</i>	F07C6.4	WBGene00008 555	ccagttcaagtagtcttcgctggtcactagtt acactcggacctcgtcgacatgcatt	FLAP-Y
<i>F07C6.4</i>	F07C6.4	WBGene00008 555	atcgacaaggtcaatgtgcctttggatttt acactcggacctcgtcgacatgcatt	FLAP-Y
<i>F07C6.4</i>	F07C6.4	WBGene00008 555	atcaatgctttggcctacgcgaggettaca ctcggacctcgtcgacatgcatt	FLAP-Y
<i>F07C6.4</i>	F07C6.4	WBGene00008 555	aatgtctcattgttgaagtcctgctgattac actcggacctcgtcgacatgcatt	FLAP-Y
<i>F07C6.4</i>	F07C6.4	WBGene00008 555	tcctctgccgtcttctcactgattacactc ggacctcgtcgacatgcatt	FLAP-Y
<i>ptp-1</i>	C48D5.2	WBGene00004 213	acatctcggatcgttttggccaaatcgtta cactcggacctcgtcgacatgcatt	FLAP-Y
<i>ptp-1</i>	C48D5.2	WBGene00004 213	gtaagcctcatatattcatcgacattccttac actcggacctcgtcgacatgcatt	FLAP-Y
<i>ptp-1</i>	C48D5.2	WBGene00004 213	agagcttctggtgccacacgggatattaca ctcggacctcgtcgacatgcatt	FLAP-Y
<i>ptp-1</i>	C48D5.2	WBGene00004 213	tgcaacggaattcgggactcgaagtgtat ttactcggacctcgtcgacatgcatt	FLAP-Y
<i>ptp-1</i>	C48D5.2	WBGene00004 213	agaggtacatgcatgctcggagtccttaca ctcggacctcgtcgacatgcatt	FLAP-Y
<i>ptp-1</i>	C48D5.2	WBGene00004 213	aacgggatgaatcaattgattgtgttccg ttactcggacctcgtcgacatgcatt	FLAP-Y
<i>ptp-1</i>	C48D5.2	WBGene00004 213	ctcgatcgacattccagagaagtttgatt acactcggacctcgtcgacatgcatt	FLAP-Y
<i>ptp-1</i>	C48D5.2	WBGene00004 213	ttcgcggacatgatgttgaagatcatgattgt tacactcggacctcgtcgacatgcatt	FLAP-Y
<i>ptp-1</i>	C48D5.2	WBGene00004 213	taattccaactgctcactccaatttcttaca ctcggacctcgtcgacatgcatt	FLAP-Y
<i>ptp-1</i>	C48D5.2	WBGene00004 213	acatccattccgtacatttcgagacgccttac actcggacctcgtcgacatgcatt	FLAP-Y
<i>ptp-1</i>	C48D5.2	WBGene00004 213	gacattccatgagtttctcctcaagtcctta cactcggacctcgtcgacatgcatt	FLAP-Y
<i>ptp-1</i>	C48D5.2	WBGene00004 213	acttcgctgtaccacataactagccttaca ctcggacctcgtcgacatgcatt	FLAP-Y
<i>ptp-1</i>	C48D5.2	WBGene00004 213	acgattcgggtcccgtacgtagaatttgacat tacactcggacctcgtcgacatgcatt	FLAP-Y
<i>ptp-1</i>	C48D5.2	WBGene00004 213	atgatacgggtggcaaatcattgttttcgcat tacactcggacctcgtcgacatgcatt	FLAP-Y
<i>ptp-1</i>	C48D5.2	WBGene00004 213	ttcgaatattcagcaagcggtttgatggtcct tacactcggacctcgtcgacatgcatt	FLAP-Y
<i>ptp-1</i>	C48D5.2	WBGene00004 213	tgtgtattggcccgggtctgaataagcattta cactcggacctcgtcgacatgcatt	FLAP-Y
<i>unc-112</i>	C47E8.7	WBGene00006 836	atcttgagatgctgaatttcccagttgacatgt tacactcggacctcgtcgacatgcatt	FLAP-Y
<i>unc-112</i>	C47E8.7	WBGene00006 836	aataatgaattccgtgttcgggaagtgcctgc ttactcggacctcgtcgacatgcatt	FLAP-Y
<i>unc-112</i>	C47E8.7	WBGene00006 836	gtgagttgctgaacatttccatgagcatctgt acactcggacctcgtcgacatgcatt	FLAP-Y
<i>unc-112</i>	C47E8.7	WBGene00006 836	cgaatcagccattgacttccctctggattaca ctcggacctcgtcgacatgcatt	FLAP-Y
<i>unc-112</i>	C47E8.7	WBGene00006 836	atcgtctgtaagagcagctcgtcaagggtta cactcggacctcgtcgacatgcatt	FLAP-Y
<i>unc-112</i>	C47E8.7	WBGene00006 836	acccaatcacggcacaatttcttgttctta cactcggacctcgtcgacatgcatt	FLAP-Y

<i>unc-112</i>	C47E8.7	WBGene00006 836	tgtaattccattctggccaagagtcgatcgagt tacctcggacctcgtcgacatgcatt	FLAP-Y
<i>unc-112</i>	C47E8.7	WBGene00006 836	tcgttcaacatcgcatcgcctaacaagttcgtt acctcggacctcgtcgacatgcatt	FLAP-Y
<i>unc-112</i>	C47E8.7	WBGene00006 836	ttgagaatgttctttgcttcgacatgacaggatt acctcggacctcgtcgacatgcatt	FLAP-Y
<i>unc-112</i>	C47E8.7	WBGene00006 836	ttgaaatcatttggtagttttacagcggcggt tacctcggacctcgtcgacatgcatt	FLAP-Y
<i>unc-112</i>	C47E8.7	WBGene00006 836	tcgtatcgttatatgctcctggcgatggttaca ctcggacctcgtcgacatgcatt	FLAP-Y
<i>unc-112</i>	C47E8.7	WBGene00006 836	tggtccaactgattcttctcctggacgttacac tcggacctcgtcgacatgcatt	FLAP-Y
<i>unc-112</i>	C47E8.7	WBGene00006 836	tgctcggatattgaagtttcgcttcggttgtt acctcggacctcgtcgacatgcatt	FLAP-Y
<i>unc-112</i>	C47E8.7	WBGene00006 836	actcgtcttgaatttgttcttctgctttacac tcggacctcgtcgacatgcatt	FLAP-Y
<i>unc-112</i>	C47E8.7	WBGene00006 836	gctcgtctacgtatttcgacgatgtacttt acctcggacctcgtcgacatgcatt	FLAP-Y
<i>unc-112</i>	C47E8.7	WBGene00006 836	gatgtccacgtcgaagatcctcgtgttac actcggacctcgtcgacatgcatt	FLAP-Y
<i>wsp-1</i>	C07G1.4	WBGene00006 957	ccattccagcggctccagaagtcgtattaca ctcggacctcgtcgacatgcatt	FLAP-Y
<i>wsp-1</i>	C07G1.4	WBGene00006 957	gcaaattcgaatcctccatcctgagcaggttac actcggacctcgtcgacatgcatt	FLAP-Y
<i>wsp-1</i>	C07G1.4	WBGene00006 957	tatcggagccattccaaatgattggtggttt acctcggacctcgtcgacatgcatt	FLAP-Y
<i>wsp-1</i>	C07G1.4	WBGene00006 957	ttgaggtaaagttcttgatggtgcaattccac ttacctcggacctcgtcgacatgcatt	FLAP-Y
<i>wsp-1</i>	C07G1.4	WBGene00006 957	atgatgggaatgatggtttgattgacgcatt tacctcggacctcgtcgacatgcatt	FLAP-Y
<i>wsp-1</i>	C07G1.4	WBGene00006 957	tgctgaattggtggtggaagaggtgatgaga ttacctcggacctcgtcgacatgcatt	FLAP-Y
<i>wsp-1</i>	C07G1.4	WBGene00006 957	tctgtactactatcacttctccagaacattac actcggacctcgtcgacatgcatt	FLAP-Y
<i>wsp-1</i>	C07G1.4	WBGene00006 957	gtcaccgaagtcacgtatgtaatacgtgtc ttacctcggacctcgtcgacatgcatt	FLAP-Y
<i>wsp-1</i>	C07G1.4	WBGene00006 957	ttggtagagtatgactccgatgggtagtagc attacctcggacctcgtcgacatgcatt	FLAP-Y
<i>wsp-1</i>	C07G1.4	WBGene00006 957	ctcggagctctatgctgacgaggttctgtta cactcggacctcgtcgacatgcatt	FLAP-Y
<i>wsp-1</i>	C07G1.4	WBGene00006 957	tagctgctgttctgctgctgatgatgttacac tcggacctcgtcgacatgcatt	FLAP-Y
<i>wsp-1</i>	C07G1.4	WBGene00006 957	atcttggtattctgcagatgagcttgtgagtta cactcggacctcgtcgacatgcatt	FLAP-Y
<i>wsp-1</i>	C07G1.4	WBGene00006 957	aacggttgacggttattggacgacggattg gttacctcggacctcgtcgacatgcatt	FLAP-Y
<i>wsp-1</i>	C07G1.4	WBGene00006 957	ctgctagcattccatctgtatgtatgtttac actcggacctcgtcgacatgcatt	FLAP-Y
<i>wsp-1</i>	C07G1.4	WBGene00006 957	ttgtggtgcagcagccatagtccattacac tcggacctcgtcgacatgcatt	FLAP-Y
<i>wsp-1</i>	C07G1.4	WBGene00006 957	tactgctggcaatccatcgggtgtttacac tcggacctcgtcgacatgcatt	FLAP-Y
<i>Y41E3.7</i>	Y41E3.7	WBGene00012 765	gataacgatgacttcccgcatacttctttac actcggacctcgtcgacatgcatt	FLAP-Y

Y41E3.7	Y41E3.7	WBGene00012 765	caccgaaactgattactgtcggctacggtt acactcggacctcgtcgacatgcatt	FLAP-Y
Y41E3.7	Y41E3.7	WBGene00012 765	taatctcctgccgattccagagtggccttac actcggacctcgtcgacatgcatt	FLAP-Y
Y41E3.7	Y41E3.7	WBGene00012 765	tcatcacgacgaatctgatgttgatgcgact acactcggacctcgtcgacatgcatt	FLAP-Y
Y41E3.7	Y41E3.7	WBGene00012 765	attgctcctgagcgtaggctgagaattgatta cactcggacctcgtcgacatgcatt	FLAP-Y
Y41E3.7	Y41E3.7	WBGene00012 765	tgtaaattcatcgaaatctctccatgttggt acactcggacctcgtcgacatgcatt	FLAP-Y
Y41E3.7	Y41E3.7	WBGene00012 765	tctcctcatcatcgattcactaacgttacac tcggacctcgtcgacatgcatt	FLAP-Y
Y41E3.7	Y41E3.7	WBGene00012 765	cgccgtgccaaacttaataattccctcgttac actcggacctcgtcgacatgcatt	FLAP-Y
Y41E3.7	Y41E3.7	WBGene00012 765	tccgtcttctgatattgccttgactcttaca ctcggacctcgtcgacatgcatt	FLAP-Y
Y41E3.7	Y41E3.7	WBGene00012 765	tctggattcatttctgcaccgttcggcttacact cggacctcgtcgacatgcatt	FLAP-Y
Y41E3.7	Y41E3.7	WBGene00012 765	tggtgatagtgtgctcttgagctgtcgaatt acactcggacctcgtcgacatgcatt	FLAP-Y
Y41E3.7	Y41E3.7	WBGene00012 765	agtgtcgtctgttccgggtgctcctggttac actcggacctcgtcgacatgcatt	FLAP-Y
Y41E3.7	Y41E3.7	WBGene00012 765	tgttcagtgacctgtggcggaattcttttac actcggacctcgtcgacatgcatt	FLAP-Y
Y41E3.7	Y41E3.7	WBGene00012 765	gttcgcgctctttatagccttctatcggttac actcggacctcgtcgacatgcatt	FLAP-Y
Y41E3.7	Y41E3.7	WBGene00012 765	cgtttcagtgatatctagccatccagcttaca ctcggacctcgtcgacatgcatt	FLAP-Y
Y41E3.7	Y41E3.7	WBGene00012 765	catatccaacaggctcctgtttcccgttacact cggacctcgtcgacatgcatt	FLAP-Y
<i>imb-2 synonymous</i>	N/A	N/A	aatgaattgctcatagctggcccactcctc ctaagtctcagctggactcagtg	FLAP-X
<i>imb-2 synonymous</i>	N/A	N/A	caagtgggtccatgtgctctggaagagacc ctcctaagtctcagctggactcagtg	FLAP-X
<i>imb-2 synonymous</i>	N/A	N/A	tgatgaaatcagctctcggggcctcaaccctc ctaagtctcagctggactcagtg	FLAP-X
<i>imb-2 synonymous</i>	N/A	N/A	ctggacgcacttctcgataagagagcagcc ctcctaagtctcagctggactcagtg	FLAP-X
<i>imb-2 synonymous</i>	N/A	N/A	ggacgtccttgaagaattgctggcgaagtc ctcctaagtctcagctggactcagtg	FLAP-X
<i>imb-2 synonymous</i>	N/A	N/A	caggtgatagagcggacaagtggctttttac ctcctaagtctcagctggactcagtg	FLAP-X
<i>imb-2 synonymous</i>	N/A	N/A	ttccgactccttaacaagccagtatcgct cctaagtctcagctggactcagtg	FLAP-X
<i>imb-2 synonymous</i>	N/A	N/A	cggcagatgcagagttctcggcgaatagac ctcctaagtctcagctggactcagtg	FLAP-X
<i>imb-2 synonymous</i>	N/A	N/A	tgtactcaataacgttggaaagtgtggcacc ctcctaagtctcagctggactcagtg	FLAP-X
<i>imb-2 synonymous</i>	N/A	N/A	gaggaattggtcgaatagcgaagtcgattgg gtcctcctaagtctcagctggactcagtg	FLAP-X
<i>imb-2 synonymous</i>	N/A	N/A	tcgtagaagacgaggagcttggcatgattg gcctcctaagtctcagctggactcagtg	FLAP-X
<i>imb-2 synonymous</i>	N/A	N/A	ggaggaactcagactcgtaacggtcagcgc ctcctaagtctcagctggactcagtg	FLAP-X

<i>imb-2 synonymous</i>	N/A	N/A	ataagtggctcttggtccgatagacttaac ctcctaagtttcgagctggactcagtg	FLAP-X
<i>imb-2 synonymous</i>	N/A	N/A	agttgtccaattgaagtctcaactgttgcc ctcctaagtttcgagctggactcagtg	FLAP-X
<i>imb-2 synonymous</i>	N/A	N/A	ctcagcgttgctcttgatgttacggagagagc ctcctaagtttcgagctggactcagtg	FLAP-X
<i>imb-2 synonymous</i>	N/A	N/A	gggcaagttctctccgagcattgtctctct aagtttcgagctggactcagtg	FLAP-X
<i>imb-2 synonymous</i>	N/A	N/A	aaggcgtccgatggtgatacggtgttcct cctaagtttcgagctggactcagtg	FLAP-X
<i>imb-2 synonymous</i>	N/A	N/A	ggtctggggccatgatatgtgtgttcctc ctaagtttcgagctggactcagtg	FLAP-X
<i>imb-2 synonymous</i>	N/A	N/A	ctcatcgaaagacgctcccactttcccctc ctaagtttcgagctggactcagtg	FLAP-X
<i>imb-2 synonymous</i>	N/A	N/A	atttctccgaggaatgggataagttgttccc ctcctaagtttcgagctggactcagtg	FLAP-X
<i>imb-2 synonymous</i>	N/A	N/A	gcaagcggcctcttgacccttctgtctctc aagtttcgagctggactcagtg	FLAP-X
<i>imb-2 synonymous</i>	N/A	N/A	ctccgagtcctgttgcttagactgtggcct cctaagtttcgagctggactcagtg	FLAP-X
<i>imb-2 synonymous</i>	N/A	N/A	ggactcgtgtggctcctgggtcttctgcctc taagtttcgagctggactcagtg	FLAP-X
<i>imb-2 synonymous</i>	N/A	N/A	gtcgttatcgttgtagcggcggaagagga gcctcctaagtttcgagctggactcagtg	FLAP-X
<i>erm-1</i>	C01G8.5	WBGene00001 333	gtttgaactgctggaccaat	Cal Fluor 610
<i>erm-1</i>	C01G8.5	WBGene00001 333	ccgcaaccattttctattt	Cal Fluor 610
<i>erm-1</i>	C01G8.5	WBGene00001 333	gacacgcacattgatatgc	Cal Fluor 610
<i>erm-1</i>	C01G8.5	WBGene00001 333	aaaagttgcttctctgtgt	Cal Fluor 610
<i>erm-1</i>	C01G8.5	WBGene00001 333	cggagaccaatggtttgac	Cal Fluor 610
<i>erm-1</i>	C01G8.5	WBGene00001 333	gtcagtgactgaagtcaa	Cal Fluor 610
<i>erm-1</i>	C01G8.5	WBGene00001 333	ttctgttcaattcagcca	Cal Fluor 610
<i>erm-1</i>	C01G8.5	WBGene00001 333	cttctaactctctgagaca	Cal Fluor 610
<i>erm-1</i>	C01G8.5	WBGene00001 333	ggatagaattggcgcggaa	Cal Fluor 610
<i>erm-1</i>	C01G8.5	WBGene00001 333	attccatcttcactggag	Cal Fluor 610
<i>erm-1</i>	C01G8.5	WBGene00001 333	aagaacagaggttccggtg	Cal Fluor 610
<i>erm-1</i>	C01G8.5	WBGene00001 333	atttagctgcatcgcgtaa	Cal Fluor 610
<i>erm-1</i>	C01G8.5	WBGene00001 333	gtgtctctggaacatagtct	Cal Fluor 610
<i>erm-1</i>	C01G8.5	WBGene00001 333	gatcagcagtaagacatccg	Cal Fluor 610
<i>erm-1</i>	C01G8.5	WBGene00001 333	agaacgcgttgaggaagcag	Cal Fluor 610

<i>erm-1</i>	C01G8.5	WBGene00001 333	acgtgtagtgcacgatgat	Cal Fluor 610
<i>erm-1</i>	C01G8.5	WBGene00001 333	gactccatacatctcgagat	Cal Fluor 610
<i>erm-1</i>	C01G8.5	WBGene00001 333	tagagatcagttccctttt	Cal Fluor 610
<i>erm-1</i>	C01G8.5	WBGene00001 333	cgactttcggcgaaagacga	Cal Fluor 610
<i>erm-1</i>	C01G8.5	WBGene00001 333	gccttctatcaattggtt	Cal Fluor 610
<i>erm-1</i>	C01G8.5	WBGene00001 333	cgtttggtgatacggagtcg	Cal Fluor 610
<i>erm-1</i>	C01G8.5	WBGene00001 333	tcgtgattccatacacia	Cal Fluor 610
<i>erm-1</i>	C01G8.5	WBGene00001 333	caatggtatctggctttct	Cal Fluor 610
<i>erm-1</i>	C01G8.5	WBGene00001 333	cggcaatcttaagagcacga	Cal Fluor 610
<i>erm-1</i>	C01G8.5	WBGene00001 333	tgcttcagccaattcaagac	Cal Fluor 610
<i>erm-1</i>	C01G8.5	WBGene00001 333	tgcaattgctgagttgagc	Cal Fluor 610
<i>erm-1</i>	C01G8.5	WBGene00001 333	tctgtccaatgctgttta	Cal Fluor 610
<i>erm-1</i>	C01G8.5	WBGene00001 333	tgaagttgagcagtgagctc	Cal Fluor 610
<i>erm-1</i>	C01G8.5	WBGene00001 333	atcactcattgcttttcgg	Cal Fluor 610
<i>erm-1</i>	C01G8.5	WBGene00001 333	gtctctcaaatgacgtctct	Cal Fluor 610
<i>erm-1</i>	C01G8.5	WBGene00001 333	ttcaggttcacgagcatcaa	Cal Fluor 610
<i>erm-1</i>	C01G8.5	WBGene00001 333	cgacttcttctctcatcgaa	Cal Fluor 610
<i>erm-1</i>	C01G8.5	WBGene00001 333	tctgtgtctgaagttgctt	Cal Fluor 610
<i>erm-1</i>	C01G8.5	WBGene00001 333	gtagtggtgagtggtgtt	Cal Fluor 610
<i>erm-1</i>	C01G8.5	WBGene00001 333	gtgtccattggaacgtgat	Cal Fluor 610
<i>erm-1</i>	C01G8.5	WBGene00001 333	tatcttcatcatcagtgga	Cal Fluor 610
<i>erm-1</i>	C01G8.5	WBGene00001 333	catttgtagttcagttgct	Cal Fluor 610
<i>erm-1</i>	C01G8.5	WBGene00001 333	ttgtggcacattctgatcag	Cal Fluor 610
<i>erm-1</i>	C01G8.5	WBGene00001 333	atccagcttattctgatct	Cal Fluor 610
<i>erm-1</i>	C01G8.5	WBGene00001 333	ttaacactgtcaagctcgcg	Cal Fluor 610
<i>erm-1</i>	C01G8.5	WBGene00001 333	ccatatgcagaacgtcgtag	Cal Fluor 610
<i>erm-1</i>	C01G8.5	WBGene00001 333	cacggatttgacggagagtc	Cal Fluor 610

<i>erm-1</i>	C01G8.5	WBGene00001333	attctctgttttgtttcc	Cal Fluor 610
<i>erm-1</i>	C01G8.5	WBGene00001333	tttgaagttggtgggagac	Cal Fluor 610
<i>erm-1</i>	C01G8.5	WBGene00001333	gtaaaaggcactgatggggt	Cal Fluor 610
<i>erm-1</i>	C01G8.5	WBGene00001333	tttggcggcgatttaaca	Cal Fluor 610
<i>erm-1</i>	C01G8.5	WBGene00001333	gtctttgcgcgagaaattcg	Cal Fluor 610
<i>erm-1</i>	C01G8.5	WBGene00001333	gtttgatggggagagagagg	Cal Fluor 610
<i>egfp</i>	N/A	N/A	ccagtgaacaattcttctcc	Quasar 670
<i>egfp</i>	N/A	N/A	ctcgacgaggattgggacaa	Quasar 670
<i>egfp</i>	N/A	N/A	ggagacggagaacttgtgtc	Quasar 670
<i>egfp</i>	N/A	N/A	tgagggtgagctttccgtag	Quasar 670
<i>egfp</i>	N/A	N/A	ttccggtggtgcagatgaa	Quasar 670
<i>egfp</i>	N/A	N/A	gaaggtggtgacgagggttg	Quasar 670
<i>egfp</i>	N/A	N/A	agaagcattgactccgtag	Quasar 670
<i>egfp</i>	N/A	N/A	ttcatgtggtctgggtaacg	Quasar 670
<i>egfp</i>	N/A	N/A	tggcggactgaagaagtcg	Quasar 670
<i>egfp</i>	N/A	N/A	tggtacgctcttgacgtat	Quasar 670
<i>egfp</i>	N/A	N/A	ttccgctgccttgaagaa	Quasar 670
<i>egfp</i>	N/A	N/A	tcgaactgacctggcagc	Quasar 670
<i>egfp</i>	N/A	N/A	cgatacgggtgacgagggtg	Quasar 670
<i>egfp</i>	N/A	N/A	ttgaagtcgattccctgag	Quasar 670
<i>egfp</i>	N/A	N/A	cttgtgtccgaggatgttc	Quasar 670
<i>egfp</i>	N/A	N/A	tgggagttgtagtttactc	Quasar 670
<i>egfp</i>	N/A	N/A	ttgtcggccatgatgtagac	Quasar 670
<i>egfp</i>	N/A	N/A	aagttgaccttgattccgtt	Quasar 670
<i>egfp</i>	N/A	N/A	ctcgatgtgtgacggatct	Quasar 670
<i>egfp</i>	N/A	N/A	tgtttgttgtagtggtcg	Quasar 670
<i>egfp</i>	N/A	N/A	gttgtctgggaggaggactg	Quasar 670
<i>egfp</i>	N/A	N/A	cggattgggtggagaggtag	Quasar 670
<i>egfp</i>	N/A	N/A	gtgacgaactcaggaggac	Quasar 670
<i>imb-2</i>	R06A4.4	WBGene00002076	attcggcaaatgaggcatca	Quasar 670
<i>imb-2</i>	R06A4.4	WBGene00002076	actcgttgtgatcttgagtc	Quasar 670
<i>imb-2</i>	R06A4.4	WBGene00002076	aaaactcgcaggcctctaag	Quasar 670
<i>imb-2</i>	R06A4.4	WBGene00002076	gagatgtggaagcaccattg	Quasar 670
<i>imb-2</i>	R06A4.4	WBGene00002076	agcagaactggtatgagctt	Quasar 670

<i>imb-2</i>	R06A4.4	WBGene 00002076	ctcagaatatgcatggagc	Quasar 670
<i>imb-2</i>	R06A4.4	WBGene 00002076	cattagctttcaacgcagga	Quasar 670
<i>imb-2</i>	R06A4.4	WBGene 00002076	aaacctaggtgatatcct	Quasar 670
<i>imb-2</i>	R06A4.4	WBGene 00002076	gaacacctctgatattcca	Quasar 670
<i>imb-2</i>	R06A4.4	WBGene 00002076	tccaacagatccttccaaa	Quasar 670
<i>imb-2</i>	R06A4.4	WBGene 00002076	tcatcaatgtgtccttgagg	Quasar 670
<i>imb-2</i>	R06A4.4	WBGene 00002076	gcaagtattccagactcttt	Quasar 670
<i>imb-2</i>	R06A4.4	WBGene 00002076	catgaatggtatgagctcgc	Quasar 670
<i>imb-2</i>	R06A4.4	WBGene 00002076	gtggcttctgtcaaacatc	Quasar 670
<i>imb-2</i>	R06A4.4	WBGene 00002076	cagcacgtgatcgcgaac	Quasar 670
<i>imb-2</i>	R06A4.4	WBGene 00002076	cgtcggatgcaatatgcaa	Quasar 670
<i>imb-2</i>	R06A4.4	WBGene 00002076	aacagcggagaagattggcg	Quasar 670
<i>imb-2</i>	R06A4.4	WBGene 00002076	tgaacttctgtttccgctc	Quasar 670
<i>imb-2</i>	R06A4.4	WBGene 00002076	tcttctcgagagttgcaa	Quasar 670
<i>imb-2</i>	R06A4.4	WBGene 00002076	ttgaccagttgatcgaggat	Quasar 670
<i>imb-2</i>	R06A4.4	WBGene 00002076	gactacagcaccttgtgaat	Quasar 670
<i>imb-2</i>	R06A4.4	WBGene 00002076	gagccataatgtgtgtgg	Quasar 670
<i>imb-2</i>	R06A4.4	WBGene 00002076	tgataaagtccgttcggga	Quasar 670
<i>imb-2</i>	R06A4.4	WBGene 00002076	catatgttccgtaacgact	Quasar 670
<i>imb-2</i>	R06A4.4	WBGene 00002076	cgtcacatctaacgagcaga	Quasar 670
<i>imb-2</i>	R06A4.4	WBGene 00002076	gtaacggaagcagcattgt	Quasar 670
<i>imb-2</i>	R06A4.4	WBGene 00002076	ggacacgcttctgcaaatc	Quasar 670
<i>imb-2</i>	R06A4.4	WBGene 00002076	aatgcattgtgcacacac	Quasar 670
<i>imb-2</i>	R06A4.4	WBGene 00002076	cccgatgaactgttcattg	Quasar 670
<i>imb-2</i>	R06A4.4	WBGene 00002076	attctgctggctattgatga	Quasar 670
<i>imb-2</i>	R06A4.4	WBGene 00002076	tccgcgttatccttaatt	Quasar 670
<i>imb-2</i>	R06A4.4	WBGene 00002076	cgacgggattcatgtgatc	Quasar 670

<i>imb-2</i>	R06A4.4	WBGene 00002076	tactgtccacgaagcgatag	Quasar 670
<i>imb-2</i>	R06A4.4	WBGene 00002076	gccgacttggtttgaatg	Quasar 670
<i>imb-2</i>	R06A4.4	WBGene 00002076	agagagacgttcacgcaacg	Quasar 670

Appendix B

FISH probes

Table A.2: FERM, PH, and PH-like domain containing maternal transcripts

WBGeneID	gene_name	interpro_description	interpro_short_description	domain_count
WBGene00000102	akt-1	PH-like domain superfamily	PH-like_dom_sf	2
WBGene00000103	akt-2	PH-like domain superfamily	PH-like_dom_sf	1
WBGene00000149	apl-1	PH-like domain superfamily	PH-like_dom_sf	2
WBGene00000420	ced-6	PH-like domain superfamily	PH-like_dom_sf	1
WBGene00000426	ced-12	PH-like domain superfamily	PH-like_dom_sf	2
WBGene00000564	cnk-1	PH-like domain superfamily	PH-like_dom_sf	1
WBGene00000565	cnt-1	PH-like domain superfamily	PH-like_dom_sf	3
WBGene00000894	dab-1	PH-like domain superfamily	PH-like_dom_sf	2
WBGene00001093	drp-1	PH-like domain superfamily	PH-like_dom_sf	2
WBGene00001116	dyc-1	PH-like domain superfamily	PH-like_dom_sf	2
WBGene00001130	dyn-1	PH-like domain superfamily	PH-like_dom_sf	1
WBGene00001153	ech-4	FERM/acyl-CoA-binding protein superfamily	FERM/acyl-CoA-bd_prot_sf	1
WBGene00001330	eps-8	PH-like domain superfamily	PH-like_dom_sf	4
WBGene00001333	erm-1	Band 4.1 domain	Band_41_domain	10
WBGene00001333	erm-1	ERM family, FERM domain C-lobe	ERM_FERM_C	2
WBGene00001333	erm-1	Ezrin/radixin/moesin	ERM	2
WBGene00001333	erm-1	Ezrin/radixin/moesin-like	Ez/rad/moesin-like	16
WBGene00001333	erm-1	Ezrin/radixin/moesin, C-terminal	ERM_C_dom	2
WBGene00001333	erm-1	FERM central domain	FERM_central	4
WBGene00001333	erm-1	FERM conserved site	FERM_CS	4
WBGene00001333	erm-1	FERM domain	FERM_domain	2

WBGene00001333	erm-1	FERM superfamily, second domain	FERM_2	2
WBGene00001333	erm-1	FERM, C-terminal PH-like domain	FERM_PH-like_C	4
WBGene00001333	erm-1	FERM, N-terminal	FERM_N	2
WBGene00001333	erm-1	FERM/acyl-CoA-binding protein superfamily	FERM/acyl-CoA-bd_prot_sf	2
WBGene00001333	erm-1	Moesin tail domain superfamily	Moesin_tail_sf	4
WBGene00001333	erm-1	PH-like domain superfamily	PH-like_dom_sf	2
WBGene00001366	exc-5	PH-like domain superfamily	PH-like_dom_sf	6
WBGene00001410	feh-1	PH-like domain superfamily	PH-like_dom_sf	4
WBGene00001488	frm-1	Band 4.1 domain	Band_41_domain	10
WBGene00001488	frm-1	Ezrin/radixin/moesin-like	Ez/rad/moesin-like	9
WBGene00001488	frm-1	FERM central domain	FERM_central	4
WBGene00001488	frm-1	FERM conserved site	FERM_CS	2
WBGene00001488	frm-1	FERM domain	FERM_domain	2
WBGene00001488	frm-1	FERM superfamily, second domain	FERM_2	2
WBGene00001488	frm-1	FERM, C-terminal PH-like domain	FERM_PH-like_C	4
WBGene00001488	frm-1	FERM, N-terminal	FERM_N	2
WBGene00001488	frm-1	FERM/acyl-CoA-binding protein superfamily	FERM/acyl-CoA-bd_prot_sf	2
WBGene00001488	frm-1	PH-like domain superfamily	PH-like_dom_sf	2
WBGene00001489	frm-2	Band 4.1 domain	Band_41_domain	10
WBGene00001489	frm-2	Ezrin/radixin/moesin-like	Ez/rad/moesin-like	8
WBGene00001489	frm-2	FERM central domain	FERM_central	4
WBGene00001489	frm-2	FERM conserved site	FERM_CS	2
WBGene00001489	frm-2	FERM domain	FERM_domain	2
WBGene00001489	frm-2	FERM superfamily, second domain	FERM_2	2
WBGene00001489	frm-2	FERM, C-terminal PH-like domain	FERM_PH-like_C	4
WBGene00001489	frm-2	FERM, N-terminal	FERM_N	2

WBGene00001489	frm-2	FERM/acyl-CoA-binding protein superfamily	FERM/acyl-CoA-bd_prot_sf	2
WBGene00001489	frm-2	PH-like domain superfamily	PH-like_dom_sf	2
WBGene00001490	frm-3	Band 4.1 domain	Band_41_domain	10
WBGene00001490	frm-3	Ezrin/radixin/moesin-like	Ez/rad/moesin-like	8
WBGene00001490	frm-3	FERM central domain	FERM_central	4
WBGene00001490	frm-3	FERM conserved site	FERM_CS	2
WBGene00001490	frm-3	FERM domain	FERM_domain	2
WBGene00001490	frm-3	FERM superfamily, second domain	FERM_2	2
WBGene00001490	frm-3	FERM, C-terminal PH-like domain	FERM_PH-like_C	4
WBGene00001490	frm-3	FERM, N-terminal	FERM_N	2
WBGene00001490	frm-3	FERM/acyl-CoA-binding protein superfamily	FERM/acyl-CoA-bd_prot_sf	2
WBGene00001490	frm-3	PH-like domain superfamily	PH-like_dom_sf	6
WBGene00001491	frm-4	Band 4.1 domain	Band_41_domain	9
WBGene00001491	frm-4	FERM central domain	FERM_central	4
WBGene00001491	frm-4	FERM domain	FERM_domain	2
WBGene00001491	frm-4	FERM superfamily, second domain	FERM_2	2
WBGene00001491	frm-4	FERM, C-terminal PH-like domain	FERM_PH-like_C	4
WBGene00001491	frm-4	FERM, N-terminal	FERM_N	1
WBGene00001491	frm-4	FERM/acyl-CoA-binding protein superfamily	FERM/acyl-CoA-bd_prot_sf	2
WBGene00001491	frm-4	PH-like domain superfamily	PH-like_dom_sf	2
WBGene00001492	frm-5.1	Band 4.1 domain	Band_41_domain	5
WBGene00001492	frm-5.1	FERM central domain	FERM_central	2
WBGene00001492	frm-5.1	FERM domain	FERM_domain	2
WBGene00001492	frm-5.1	FERM superfamily, second domain	FERM_2	1
WBGene00001492	frm-5.1	FERM, C-terminal PH-like domain	FERM_PH-like_C	4
WBGene00001492	frm-5.1	FERM, N-terminal	FERM_N	1

WBGene0000149 2	frm-5.1	FERM/acyl-CoA-binding protein superfamily	FERM/acyl-CoA-bd_prot_sf	1
WBGene0000149 2	frm-5.1	PH-like domain superfamily	PH-like_dom_sf	2
WBGene0000149 3	frm-7	Band 4.1 domain	Band_41_domain	1
WBGene0000149 3	frm-7	FERM central domain	FERM_central	2
WBGene0000149 3	frm-7	FERM domain	FERM_domain	1
WBGene0000149 3	frm-7	FERM superfamily, second domain	FERM_2	1
WBGene0000149 3	frm-7	FERM, C-terminal PH-like domain	FERM_PH-like_C	2
WBGene0000149 3	frm-7	FERM, N-terminal	FERM_N	1
WBGene0000149 3	frm-7	PH-like domain superfamily	PH-like_dom_sf	1
WBGene0000149 4	frm-8	Band 4.1 domain	Band_41_domain	2
WBGene0000149 4	frm-8	FERM central domain	FERM_central	4
WBGene0000149 4	frm-8	FERM domain	FERM_domain	2
WBGene0000149 4	frm-8	FERM superfamily, second domain	FERM_2	2
WBGene0000149 4	frm-8	FERM/acyl-CoA-binding protein superfamily	FERM/acyl-CoA-bd_prot_sf	2
WBGene0000149 6	frm-10	Band 4.1 domain	Band_41_domain	1
WBGene0000149 6	frm-10	FERM domain	FERM_domain	2
WBGene0000149 6	frm-10	FERM superfamily, second domain	FERM_2	2
WBGene0000149 6	frm-10	FERM/acyl-CoA-binding protein superfamily	FERM/acyl-CoA-bd_prot_sf	2
WBGene0000151 5	gap-1	PH-like domain superfamily	PH-like_dom_sf	1
WBGene0000170 9	grk-2	PH-like domain superfamily	PH-like_dom_sf	1
WBGene0000174 3	grp-1	PH-like domain superfamily	PH-like_dom_sf	1
WBGene0000197 3	hmg-3	PH-like domain superfamily	PH-like_dom_sf	2
WBGene0000197 4	hmg-4	PH-like domain superfamily	PH-like_dom_sf	2
WBGene0000203 7	hum-4	Band 4.1 domain	Band_41_domain	8
WBGene0000203 7	hum-4	FERM central domain	FERM_central	8
WBGene0000203 7	hum-4	FERM domain	FERM_domain	8

WBGene0000203 7	hum-4	FERM superfamily, second domain	FERM_2	8
WBGene0000203 7	hum-4	PH-like domain superfamily	PH-like_dom_sf	8
WBGene0000203 9	hum-6	Band 4.1 domain	Band_41_domain	2
WBGene0000203 9	hum-6	FERM central domain	FERM_central	3
WBGene0000203 9	hum-6	FERM domain	FERM_domain	2
WBGene0000203 9	hum-6	FERM superfamily, second domain	FERM_2	2
WBGene0000203 9	hum-6	FERM/acyl-CoA- binding protein superfamily	FERM/acyl-CoA-bd_prot_sf	1
WBGene0000203 9	hum-6	PH-like domain superfamily	PH-like_dom_sf	2
WBGene0000204 6	icl-1	PH-like domain superfamily	PH-like_dom_sf	2
WBGene0000216 3	ist-1	PH-like domain superfamily	PH-like_dom_sf	2
WBGene0000217 6	jip-1	PH-like domain superfamily	PH-like_dom_sf	6
WBGene0000221 3	kin-32	Band 4.1 domain	Band_41_domain	1
WBGene0000221 3	kin-32	FERM domain	FERM_domain	2
WBGene0000221 3	kin-32	FERM superfamily, second domain	FERM_2	2
WBGene0000221 3	kin-32	FERM/acyl-CoA- binding protein superfamily	FERM/acyl-CoA-bd_prot_sf	2
WBGene0000221 3	kin-32	PH-like domain superfamily	PH-like_dom_sf	2
WBGene0000229 7	ect-2	PH-like domain superfamily	PH-like_dom_sf	1
WBGene0000269 4	let-502	PH-like domain superfamily	PH-like_dom_sf	1
WBGene0000299 9	lin-10	PH-like domain superfamily	PH-like_dom_sf	3
WBGene0000314 3	max-1	Band 4.1 domain	Band_41_domain	2
WBGene0000314 3	max-1	FERM central domain	FERM_central	4
WBGene0000314 3	max-1	FERM domain	FERM_domain	2
WBGene0000314 3	max-1	FERM superfamily, second domain	FERM_2	2
WBGene0000314 3	max-1	FERM/acyl-CoA- binding protein superfamily	FERM/acyl-CoA-bd_prot_sf	2
WBGene0000314 3	max-1	PH-like domain superfamily	PH-like_dom_sf	6
WBGene0000324 3	mig-10	PH-like domain superfamily	PH-like_dom_sf	3

WBGene00003475	mtm-1	PH-like domain superfamily	PH-like_dom_sf	1
WBGene00003477	mtm-5	PH-like domain superfamily	PH-like_dom_sf	1
WBGene00003478	mtm-6	PH-like domain superfamily	PH-like_dom_sf	2
WBGene00003479	mtm-9	PH-like domain superfamily	PH-like_dom_sf	2
WBGene00003593	nfm-1	Band 4.1 domain	Band_41_domain	5
WBGene00003593	nfm-1	ERM family, FERM domain C-lobe	ERM_FERM_C	1
WBGene00003593	nfm-1	Ezrin/radixin/moesin-like	Ez/rad/moesin-like	6
WBGene00003593	nfm-1	Ezrin/radixin/moesin, C-terminal	ERM_C_dom	4
WBGene00003593	nfm-1	FERM central domain	FERM_central	2
WBGene00003593	nfm-1	FERM domain	FERM_domain	1
WBGene00003593	nfm-1	FERM superfamily, second domain	FERM_2	1
WBGene00003593	nfm-1	FERM, C-terminal PH-like domain	FERM_PH-like_C	2
WBGene00003593	nfm-1	FERM, N-terminal	FERM_N	1
WBGene00003593	nfm-1	FERM/acyl-CoA-binding protein superfamily	FERM/acyl-CoA-bd_prot_sf	1
WBGene00003593	nfm-1	Moesin tail domain superfamily	Moesin_tail_sf	6
WBGene00003593	nfm-1	PH-like domain superfamily	PH-like_dom_sf	1
WBGene00003795	npp-9	PH-like domain superfamily	PH-like_dom_sf	4
WBGene00003802	npp-16	PH-like domain superfamily	PH-like_dom_sf	1
WBGene00003830	num-1	PH-like domain superfamily	PH-like_dom_sf	4
WBGene00003965	pdk-1	PH-like domain superfamily	PH-like_dom_sf	2
WBGene00004036	plc-1	Band 4.1 domain	Band_41_domain	7
WBGene00004036	plc-1	FERM central domain	FERM_central	7
WBGene00004039	plc-4	PH-like domain superfamily	PH-like_dom_sf	1
WBGene00004045	pll-1	PH-like domain superfamily	PH-like_dom_sf	2
WBGene00004213	ptp-1	Band 4.1 domain	Band_41_domain	5
WBGene00004213	ptp-1	FERM central domain	FERM_central	2
WBGene00004213	ptp-1	FERM conserved site	FERM_CS	2

WBGene0000421 3	ptp-1	FERM domain	FERM_domain	1
WBGene0000421 3	ptp-1	FERM superfamily, second domain	FERM_2	1
WBGene0000421 3	ptp-1	FERM, C-terminal PH-like domain	FERM_PH-like_C	2
WBGene0000421 3	ptp-1	FERM, N-terminal	FERM_N	1
WBGene0000421 3	ptp-1	FERM/acyl-CoA- binding protein superfamily	FERM/acyl-CoA-bd_prot_sf	1
WBGene0000421 3	ptp-1	PH-like domain superfamily	PH-like_dom_sf	1
WBGene0000430 6	ran-5	PH-like domain superfamily	PH-like_dom_sf	1
WBGene0000485 5	sma-1	PH-like domain superfamily	PH-like_dom_sf	3
WBGene0000492 8	soc-1	PH-like domain superfamily	PH-like_dom_sf	1
WBGene0000494 7	sos-1	PH-like domain superfamily	PH-like_dom_sf	1
WBGene0000606 2	stn-1	PH-like domain superfamily	PH-like_dom_sf	2
WBGene0000643 1	tag-52	PH-like domain superfamily	PH-like_dom_sf	1
WBGene0000643 7	mrck-1	PH-like domain superfamily	PH-like_dom_sf	5
WBGene0000645 0	tag-77	PH-like domain superfamily	PH-like_dom_sf	3
WBGene0000646 8	rhgf-1	PH-like domain superfamily	PH-like_dom_sf	1
WBGene0000647 6	rhgf-2	PH-like domain superfamily	PH-like_dom_sf	3
WBGene0000649 6	cgef-1	PH-like domain superfamily	PH-like_dom_sf	2
WBGene0000650 8	tns-1	PH-like domain superfamily	PH-like_dom_sf	7
WBGene0000676 7	unc-31	PH-like domain superfamily	PH-like_dom_sf	6
WBGene0000677 0	unc-34	PH-like domain superfamily	PH-like_dom_sf	3
WBGene0000677 1	tln-1	Band 4.1 domain	Band_41_domain	1
WBGene0000677 1	tln-1	FERM central domain	FERM_central	2
WBGene0000677 1	tln-1	FERM conserved site	FERM_CS	2
WBGene0000677 1	tln-1	FERM domain	FERM_domain	1
WBGene0000677 1	tln-1	FERM superfamily, second domain	FERM_2	1
WBGene0000677 1	tln-1	FERM/acyl-CoA- binding protein superfamily	FERM/acyl-CoA-bd_prot_sf	2

WBGene0000677 1	tln-1	PH-like domain superfamily	PH-like_dom_sf	2
WBGene0000680 3	unc-70	PH-like domain superfamily	PH-like_dom_sf	4
WBGene0000680 5	unc-73	PH-like domain superfamily	PH-like_dom_sf	6
WBGene0000682 0	unc-89	PH-like domain superfamily	PH-like_dom_sf	1
WBGene0000683 1	unc-104	PH-like domain superfamily	PH-like_dom_sf	2
WBGene0000683 6	unc-112	Band 4.1 domain	Band_41_domain	1
WBGene0000683 6	unc-112	FERM central domain	FERM_central	3
WBGene0000683 6	unc-112	FERM conserved site	FERM_CS	1
WBGene0000683 6	unc-112	FERM superfamily, second domain	FERM_2	1
WBGene0000683 6	unc-112	PH-like domain superfamily	PH-like_dom_sf	2
WBGene0000688 7	vav-1	PH-like domain superfamily	PH-like_dom_sf	3
WBGene0000695 7	wsp-1	PH-like domain superfamily	PH-like_dom_sf	1
WBGene0000752 0	C11E4.6	PH-like domain superfamily	PH-like_dom_sf	1
WBGene0000768 0	maa-1	FERM/acyl-CoA- binding protein superfamily	FERM/acyl-CoA-bd_prot_sf	1
WBGene0000784 0	C31C9.6	PH-like domain superfamily	PH-like_dom_sf	1
WBGene0000784 9	tbc-19	PH-like domain superfamily	PH-like_dom_sf	1
WBGene0000800 6	tag-325	PH-like domain superfamily	PH-like_dom_sf	2
WBGene0000840 4	wbp-2	PH-like domain superfamily	PH-like_dom_sf	1
WBGene0000855 5	F07C6.4	Band 4.1 domain	Band_41_domain	1
WBGene0000855 5	F07C6.4	FERM central domain	FERM_central	2
WBGene0000855 5	F07C6.4	FERM domain	FERM_domain	2
WBGene0000855 5	F07C6.4	FERM superfamily, second domain	FERM_2	1
WBGene0000855 5	F07C6.4	FERM, C-terminal PH-like domain	FERM_PH-like_C	2
WBGene0000855 5	F07C6.4	FERM/acyl-CoA- binding protein superfamily	FERM/acyl-CoA-bd_prot_sf	1
WBGene0000866 6	F10G8.8	PH-like domain superfamily	PH-like_dom_sf	2
WBGene0000891 9	vps-36	PH-like domain superfamily	PH-like_dom_sf	1

WBGene00008927	snx-17	PH-like domain superfamily	PH-like_dom_sf	2
WBGene00009065	F22G12.5	PH-like domain superfamily	PH-like_dom_sf	1
WBGene00009120	F25H2.6	PH-like domain superfamily	PH-like_dom_sf	1
WBGene00009292	F31D4.5	PH-like domain superfamily	PH-like_dom_sf	1
WBGene00009337	uig-1	PH-like domain superfamily	PH-like_dom_sf	6
WBGene00009534	F38B7.3	PH-like domain superfamily	PH-like_dom_sf	1
WBGene00009818	acbp-3	FERM/acyl-CoA-binding protein superfamily	FERM/acyl-CoA-bd_prot_sf	1
WBGene00009930	F52D10.2	PH-like domain superfamily	PH-like_dom_sf	1
WBGene00010641	crml-1	PH-like domain superfamily	PH-like_dom_sf	1
WBGene00010774	K11E4.2	PH-like domain superfamily	PH-like_dom_sf	1
WBGene00010907	M88.4	PH-like domain superfamily	PH-like_dom_sf	1
WBGene00011680	T10B10.3	PH-like domain superfamily	PH-like_dom_sf	1
WBGene00011731	acbp-5	FERM/acyl-CoA-binding protein superfamily	FERM/acyl-CoA-bd_prot_sf	1
WBGene00012019	dkf-2	PH-like domain superfamily	PH-like_dom_sf	5
WBGene00012198	W02B8.2	PH-like domain superfamily	PH-like_dom_sf	1
WBGene00012352	dkf-1	PH-like domain superfamily	PH-like_dom_sf	1
WBGene00012457	acbp-6	FERM/acyl-CoA-binding protein superfamily	FERM/acyl-CoA-bd_prot_sf	1
WBGene00012560	Y37D8A.25	PH-like domain superfamily	PH-like_dom_sf	1
WBGene00012765	Y41E3.7	FERM/acyl-CoA-binding protein superfamily	FERM/acyl-CoA-bd_prot_sf	1
WBGene00012835	ani-3	PH-like domain superfamily	PH-like_dom_sf	1
WBGene00012868	tbc-9	PH-like domain superfamily	PH-like_dom_sf	3
WBGene00012889	icap-1	PH-like domain superfamily	PH-like_dom_sf	2
WBGene00012930	obr-1	PH-like domain superfamily	PH-like_dom_sf	3
WBGene00013038	ani-1	PH-like domain superfamily	PH-like_dom_sf	1
WBGene00013135	rga-2	PH-like domain superfamily	PH-like_dom_sf	1

WBGene0001322 3	efa-6	PH-like domain superfamily	PH-like_dom_sf	4
WBGene0001368 2	Y105E8A.2 5	PH-like domain superfamily	PH-like_dom_sf	7
WBGene0001368 7	exoc-8	PH-like domain superfamily	PH-like_dom_sf	1
WBGene0001395 5	kri-1	FERM central domain	FERM_central	2
WBGene0001395 5	kri-1	FERM domain	FERM_domain	2
WBGene0001395 5	kri-1	PH-like domain superfamily	PH-like_dom_sf	1
WBGene0001401 9	ZK632.12	PH-like domain superfamily	PH-like_dom_sf	1
WBGene0001421 5	obr-3	PH-like domain superfamily	PH-like_dom_sf	2
WBGene0001510 0	B0280.2	PH-like domain superfamily	PH-like_dom_sf	1
WBGene0001510 7	viro-2	PH-like domain superfamily	PH-like_dom_sf	1
WBGene0001541 8	pac-1	PH-like domain superfamily	PH-like_dom_sf	4
WBGene0001595 5	C18B2.4	PH-like domain superfamily	PH-like_dom_sf	1
WBGene0001633 1	obr-4	PH-like domain superfamily	PH-like_dom_sf	1
WBGene0001665 5	acbp-1	FERM/acyl-CoA- binding protein superfamily	FERM/acyl-CoA-bd_prot_sf	1
WBGene0001746 3	F14D12.1	PH-like domain superfamily	PH-like_dom_sf	1
WBGene0001807 5	tbc-11	PH-like domain superfamily	PH-like_dom_sf	1
WBGene0001828 5	smk-1	PH-like domain superfamily	PH-like_dom_sf	2
WBGene0001878 8	shc-1	PH-like domain superfamily	PH-like_dom_sf	1
WBGene0001884 9	spt-16	PH-like domain superfamily	PH-like_dom_sf	1
WBGene0001894 9	acbp-4	FERM/acyl-CoA- binding protein superfamily	FERM/acyl-CoA-bd_prot_sf	1
WBGene0001908 7	F59A6.5	PH-like domain superfamily	PH-like_dom_sf	1
WBGene0001946 2	ccm-2	PH-like domain superfamily	PH-like_dom_sf	1
WBGene0001948 7	ephx-1	PH-like domain superfamily	PH-like_dom_sf	4
WBGene0001960 8	ani-2	PH-like domain superfamily	PH-like_dom_sf	1
WBGene0001961 5	K10B4.3	PH-like domain superfamily	PH-like_dom_sf	1
WBGene0001972 6	bris-1	PH-like domain superfamily	PH-like_dom_sf	4

WBGene00019749	M03A8.3	PH-like domain superfamily	PH-like_dom_sf	1
WBGene00019821	gtf-2H1	PH-like domain superfamily	PH-like_dom_sf	1
WBGene00020209	T04C9.1	PH-like domain superfamily	PH-like_dom_sf	1
WBGene00020867	shc-2	PH-like domain superfamily	PH-like_dom_sf	2
WBGene00021406	frm-5.2	Band 4.1 domain	Band_41_domain	10
WBGene00021406	frm-5.2	FERM central domain	FERM_central	4
WBGene00021406	frm-5.2	FERM domain	FERM_domain	4
WBGene00021406	frm-5.2	FERM superfamily, second domain	FERM_2	2
WBGene00021406	frm-5.2	FERM, C-terminal PH-like domain	FERM_PH-like_C	8
WBGene00021406	frm-5.2	FERM, N-terminal	FERM_N	2
WBGene00021406	frm-5.2	FERM/acyl-CoA-binding protein superfamily	FERM/acyl-CoA-bd_prot_sf	2
WBGene00021406	frm-5.2	PH-like domain superfamily	PH-like_dom_sf	4
WBGene00021929	dcap-1	PH-like domain superfamily	PH-like_dom_sf	1
WBGene00022391	prhg-1	PH-like domain superfamily	PH-like_dom_sf	6
WBGene00022453	ncap-1	PH-like domain superfamily	PH-like_dom_sf	2
WBGene00022593	ZC328.3	PH-like domain superfamily	PH-like_dom_sf	1
WBGene00022880	tbc-2	PH-like domain superfamily	PH-like_dom_sf	1
WBGene00044603	acbp-7	FERM/acyl-CoA-binding protein superfamily	FERM/acyl-CoA-bd_prot_sf	1